DIRECT MODEL REFERENCE ADAPTIVE CONTROL OF NUTRIENT REMOVAL AT ACTIVATED SLUDGE WASTEWATER TREATMENT PLANT

by

MAO LI

A thesis submitted to

The University of Birmingham

for the degree of

DOCTOR OF PHILOSOPHY

Department of Electronic, Electrical and System Engineering

University of Birmingham

2024

To my parents

ACKNOWLEDGEMENT

First of all, I would like to express my gratitude supervisor Prof. XiaoPing Zhang, for his support and encouragement throughout my doctoral studies, with his guidance, I successfully completed this research. Additionally, I extend my heartfelt thanks to my mentor, professor Mietek A.Brdys, who provided me with the opportunity to pursue a PhD. His patient guidance and invaluable advice were instrumental in navigating the initial stages of my project research and profoundly impacted my career development.

I would also like to extend my gratitude to my colleagues Dr. Suyang Zhou, Dr. Zhi Wu, Dr. Puyu Wang, Dr. Jing Li, Dr. Ying Xue, Mr. Hao Fu, Mr Xie MingYue and all the members of the Power and Control Group, for their thoughtful help and guidance. Collaborating with them has been a great privilege.

Finally, I must express my deepest gratitude to my parents. Their unending affection and unwavering support for me is priceless.

ABSTRACT

The population growth correlates with an increase in the volume of wastewater generated through daily activities, exacerbating environmental issues. Therefore, countries have proposed stricter wastewater purification and discharge standards. Consequently, the control community is increasingly interested in researching the efficacy and discharge standards of wastewater treatment plants. This thesis proposes designing different architectures for activated sludge wastewater treatments to address various wastewater requirements. Additionally, it suggests designing and applying advanced control systems to enhance the efficiency of wastewater treatment and ensure compliance with emission quality standards.

Various challenges are encountered during the design and operation of activated sludge wastewater treatment plants. The architecture of these plants must accommodate the required wastewater volume while considering space limitations for construction. Moreover, the designs must prioritize ease of maintenance and durability.

Due to the complexity of activated sludge wastewater treatment plants, which are highly nonlinear systems with many unknown and time-varying plant parameters, designing control systems that adjust global plant parameters using local constraints to achieve efficient wastewater purification is challenging.

For small wastewater treatment requirements, a single aeration system architecture for activated sludge treatment was designed. An advanced adaptive control system was developed and applied to this architecture. The simulation results of the wastewater purification process were satisfactory.

During the activated sludge wastewater treatment process, unexpected situations may arise that affect the quality of sewage purification and energy consumption. For instance, if the air supply exceeds the required amount in the aeration system, the discharged water quality may not meet the desired standard. To address this issue, a new adaptive control system was designed and applied in the sewage treatment of a single air aeration system. Experimental results demonstrated that the new adaptive control system is efficient in resolving this issue.

For large wastewater treatment requirements, an aeration system with three settlement tanks was designed for the activated sludge process. A supervised decentralized adaptive control system was developed and applied to this architecture. The simulation results were satisfactory.

The architecture of the activated sludge wastewater treatment plant was designed based on wastewater purification volume requirements. The activated sludge treatment mathematical model was based on mass balance and ion kinetic energy conservation.

The advanced adaptive control systems were designed using global plant parameters and local mathematical model limitations.

The designed architecture of the activated sludge wastewater treatment plant, along with the corresponding adaptive control system, effectively addressed the wastewater treatment challenges mentioned.

Table of Contents

List of Figure

Chapter 1 Introduction

1.1 Background

During the development of industrialization and urbanization, wastewater discharge and treatment have had an increasing impact on human life. Therefore, researchers are required to find the best ways to solve this issue. The activated sludge method for addressing wastewater discharges has garnered researchers' attention. Because the activated sludge wastewater treatment plant uses biological treatment approaches, it does not produce secondary pollutants and has a simple architecture. Moreover, a straightforward control system can be applied to achieve the goal of wastewater purification.

Wastewater contains a large volume of metals, toxic microorganisms, and bacteria. The activated sludge wastewater purification method removes these harmful substances through the growth and development of microorganisms. There are corresponding purification structures and control systems to eliminate different harmful substances.

The activated sludge wastewater treatment process involves the degradation of organic and inorganic matter by microorganisms, converting waste into carbon dioxide and biomass. The process is designed to purify wastewater. Organic matter is a compound

containing carbon and hydrogen, which provides energy and a carbon source for microorganisms. Nutrients such as nitrogen and phosphorus support the basic biomass of microorganisms and promote their degradation activity.

In previous activated sludge wastewater industries, individual components were used to perform specific purification functions, such as primary filtration, aeration systems, and sedimentation components. During the development of wastewater purification technology, modular components have replaced individual components to complete the wastewater purification process, which can save construction space and time. Technical issues will be encountered in the process of modular design and application. For example, the modular structure must effectively respond to changes in wastewater volume and chemical composition through standardized industrial units while saving construction space to achieve the standard for discharging clean water after wastewater purification.

The activated sludge wastewater treatment plant is widely used for city wastewater, domestic wastewater, and industrial wastewater. However, achieving a balance between saving building space, reducing energy consumption, and maintaining efficient purification without advanced control system applications remains a challenging issue. Therefore, the structural design of activated sludge wastewater treatment plants and the application of control systems continue to pose challenges.

1.1.1 Activated sludge wastewater treatment manufactory components

The activated sludge wastewater treatment manufactory can be divided into three components depending on the function of the purification wastewater. The first component is a primary treatment plant, the second component is a secondary treatment plant, and the last component is a tertiary treatment plant, as shown in Figure 1-1.

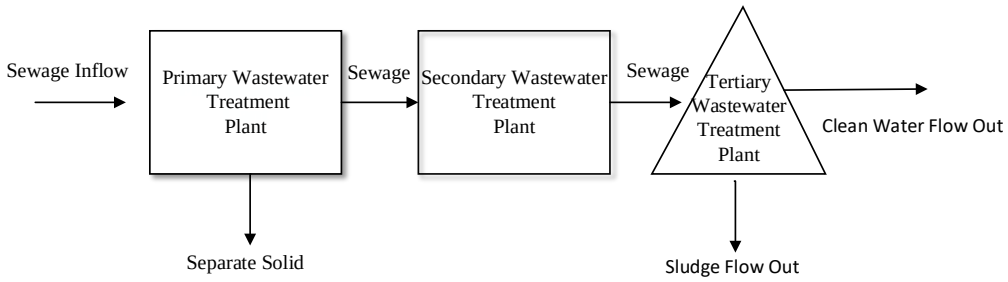

Figure 1- 1 The basic structure of activated sludge wastewater treatment plant

The primary wastewater treatment equipment includes collection tanks and primary filtration tanks. In this stage, sewage is collected, and larger particles are filtered out using pipes and hydraulic devices. The main function of primary wastewater treatment is to filter and initially physically precipitate large particles of impurities. After this process, the wastewater flows into secondary treatment.

The secondary treatment of activated sludge is to achieve the purpose of sewage purification by promoting the growth and degradation of microorganisms in sewage

through dissolved oxygen. The growth and degradation of organic microorganisms include microbial adsorption, oxygen ion replacement reactions, and oxidation reactions. Biochemical reactions within different microbial populations occur on varying time scales.

Tertiary wastewater treatment uses gravity to settle the harmful substances of the flocculent to the bottom of the sedimentation tank. This sedimentation process is the process of separating the clean water and the sludge. The clean water is either discharged or further settled, while the new sludge is recycled, and the old sludge is discharged.

Wastewater purification plants use integrated components and advanced control systems to address the constraints of construction area and purification efficiency. New components include miniaturized integrated aeration systems, variable frequency blowers, and integrated biochemical reaction tanks. The focus of this paper is integrated aeration systems and biochemical reaction tanks. In terms of control systems, advanced adaptive control systems will be used to adjust dissolved oxygen concentrations to solve efficient and stable sewage purification processes. Since the time scales of biochemical reactions are different and involve many unknown reaction parameters, merging or reorganizing these treatment stages poses challenges. Therefore, designing an efficient control system is a challenge.

1.1.2 Activated wastewater treatment purification advanced control system

The basic principle of the activated sludge sewage treatment purification method is to use the replacement and oxidation of dissolved oxygen to support the growth of organic microorganisms and remove harmful substances. The biochemical reactions during microbial growth occur on different time scales; therefore, the concentration of dissolved oxygen is crucial and directly affects the efficiency of sewage purification.

In earlier control systems, the concentration of dissolved oxygen was adjusted using only simple control logic due to the hardware constraints of the detection and purification systems. With advancements in automation and digitalization, modern control systems now integrate more advanced hardware and technologies. In this study, we introduce an adaptive control system based on artificial intelligence to enhance the efficiency of sewage treatment plants with various architectures while reducing energy consumption.

1.2 Motivations

Wastewater contains harmful microorganisms, including nitrogen compounds, phosphorus compounds, heavy metals, bacteria, and viruses. Therefore, the ability and efficiency of sewage purification are crucial.

Activated sludge wastewater treatment is an organic purification method that helps reduce secondary environmental pollution. Activated sludge wastewater purification removes harmful substances by utilizing the decomposition and degradation of microorganisms. Dissolved oxygen is an indispensable chemical substance in the growth of organic microorganisms. The concentration of dissolved oxygen serves not only as a criterion for assessing the efficiency of sewage purification but also as a measure of energy consumption.

When the dissolved oxygen concentration is extremely high, it can accelerate the growth of microorganisms, but it can also inhibit microbial degradation. On the contrary, when the dissolved oxygen concentration is low, it will lead to a decrease in the rate of microbial oxidation reactions, resulting in excessive growth of algae and bacteria, thereby changing the structure of microorganisms in the natural environment. Therefore, the regulation of dissolved oxygen concentration is crucial.

The structure and control system of the activated sludge wastewater treatment manufactory are both important factors that directly affect the efficiency of wastewater

purification. The size and number of aeration system components in a wastewater treatment plant can affect the distribution and transport efficiency of dissolved oxygen and even cause the collapse of the purification system.

In addition, advanced control systems are essential to improve the balance between purification efficiency and energy consumption. The application of unstable control systems during the operation of the wastewater purification factory will lead to an increase in energy consumption during the purification process and even cause the collapse of the purification process. Therefore, advanced dissolved oxygen concentration control systems have attracted attention from the control community.

Activated sludge wastewater treatment manufactories with typical architecture cannot efficiently purify various types and volumes of wastewater within a limited space. In this thesis, we integrate the second and third wastewater treatment components into one comprehensive purification functional component to solve the specific wastewater purification requirements.

It is crucial to design a suitable activated sludge sewage treatment plant structure and advanced control system according to the sewage treatment requirements of different scales and chemical characteristics. Advanced control systems can help improve wastewater purification efficiency. In the activated sludge sewage purification process, there are many unknown parameters. These uncertain system parameters increase the

difficulty and stability of designing advanced control systems. Maintaining a suitable dissolved oxygen concentration in the aeration tank is the only way to increase the efficiency of organic matter degradation and the rate of nitrification. In addition, the advantage control system can effectively dissolve and regulate, prevent the occurrence of anaerobic bacteria, and inhibit the growth of filamentous bacteria. It can also enhance the responsiveness of the purification system to load fluctuations, thereby achieving efficient, stable operation and the anti-interference capabilities of activated sludge sewage purification.

This study designs the structure and components of an activated sludge wastewater treatment plant based on different construction and wastewater volume constraints. Based on these constraints, an advanced adaptive control system is designed and implemented to achieve real-time adjustment of the blower. The control system ensures that the microorganisms receive the appropriate dissolved oxygen concentration during growth and degradation, thereby promoting an efficient and energy-saving wastewater purification process.

1.3 Aims and objectives

This study aims to address the requirements of building space limitations by designing the structure of a wastewater treatment facility and designing an advanced adaptive control system to achieve efficient and stable operation. The activated sludge

wastewater purification system must be able to cope with unpredictable external and internal disturbances while reducing energy consumption accordingly.

According to the constraints of the sewage treatment plant, an active sewage treatment plant was built, and an advanced control system was designed and implemented. This enables real-time monitoring and regulation of dissolved oxygen concentration in the biochemical reaction tank. The purpose of the dissolved oxygen control system is to increase the degradation rate of microorganisms and improve the adsorption capacity of oxygen atoms by optimizing the proportion of dissolved oxygen in the biochemical reaction process. To meet the efficient nutrient removal. In addition, energy-saving requirements are achieved by accurately controlling the oxygen supply system.

The objectives can be summarized as follows:

1) Under the constraints of purifying a small amount of sewage and limited building area in the sewage treatment plant, an activated sludge sewage treatment plant is designed, composed of a biochemical reaction unit, a sedimentation unit, and an aeration unit. The sewage purification plant operates under the ideal conditions of the blower. Based on this new structure and operating state, a direct model reference adaptive control system is designed to adjust the dissolved oxygen concentration in the biochemical reaction tank. This control system needs to keep the dissolved oxygen concentration in the

biochemical reaction tank at an optimal level to support the degradation, decomposition, and precipitation processes of organic microorganisms, thereby achieving stable and efficient operation of the activated sludge sewage purification process. At the same time, it aims to achieve a balance between purification efficiency and energy consumption.

2) According to the structure of the existing activated sludge sewage purification plant, we assume that the blower is working in an overloaded state, which leads to instability and even collapse of the sewage purification system. Therefore, it is necessary to design and implement a control system that can filter out excess air and adjust the dissolved oxygen concentration adaptively. When designing a new adaptive control system, its ability to filter out excess air and adjust the dissolved oxygen concentration must be considered to ensure that the decomposition, degradation, and precipitation of microorganisms remain in the best state. An adaptive control system should also have the ability to resist uncertain interference to achieve stable and efficient operation of the sewage purification process.

3) Assume that the wastewater treatment manufactory needs to purify a large amount of wastewater while meeting the constraint of a small building area. To satisfy these two constraints, the structure of the activated sludge wastewater treatment manufactory is designed to be segmented, including three aeration

units and one sedimentation unit. It will use an air supplier to provide an appropriate proportion of dissolved oxygen concentration to the three aeration units in series to smoothly complete the wastewater purification process. Based on the structure of the wastewater purification manufactory, a supervised fuzzy logic direct model reference adaptive control system is designed and applied to adjust the dissolved oxygen concentration during the biochemical reaction process to meet the air supply needs of each aeration unit. This ensures that the microorganisms are always in the best active state, thereby improving the stability, adaptability, and purification rate of the wastewater purification process.

1.4 Contributions

The architecture of the activated sludge wastewater treatment manufactory was designed according to the building area restrictions and the requirements for the volume of wastewater to be purified. Through a detailed analysis of the biochemical decomposition and degradation processes of wastewater by activated sludge, an adaptive control system was designed and applied to achieve stable operation of the wastewater purification process in both time and spatial dimensions.

The ASWWTP purification process is a complex system with many uncertain manufacturing parameters, multiple time-scale parameters, and unmeasurable parameters throughout the entire process. The mathematical model of the ASWWTP is established based on mass balance and ion conservation of kinetic energy to simulate the entire wastewater purification process using disciplines such as fluid mechanics, biology, chemical engineering, and gravity. This mathematical model is used to describe the wastewater purification process under different building structures and operating conditions. By considering more wastewater purification process parameters in two-dimensional space, the accuracy and predictive ability of the mathematical model can be improved. Therefore, we can design an accurate and stable control system according to different manufacturing architectures and operating conditions

According to the construction architecture and operating conditions of different wastewater purification manufactories, this study proposes an adaptive control system strategy based on real-time monitoring and prediction of wastewater purification process parameters, which are used to adjust the dissolved oxygen concentration in time and space as conditions vary. Different adaptive control systems are designed to adjust the dissolved oxygen concentration involved in biochemical reactions in two dimensions, thereby improving the stability and efficiency of wastewater purification. Since dissolved oxygen is the only catalyst that participates in chemical and biological reactions to remove pollutants from wastewater, the effectiveness, stability, and anti-

interference ability of the adaptive control system are confirmed by MATLAB simulation.

These adaptive control systems enable the detection and prediction of the wastewater purification process under different operating conditions in real time. Dynamic adjustment of the dissolved oxygen concentration in the aeration system allows microorganisms to grow in their optimal state, thereby improving the degradation rate of organic matter and achieving the stability, efficiency, and anti-interference capabilities of the wastewater purification manufactory while reducing the energy consumption of the wastewater purification plant's operation.

1.5 Thesis outlines

The content of each chapter can be summarized as follows:

Chapter 2: The components and functions of each wastewater purification unit, as well as the energy consumption required by these components, are reviewed. Next, the biochemical reactions involved in the growth of microorganisms under different wastewater purification operating conditions are examined in detail. The catalytic effect of dissolved oxygen in the ASWWTP purification process and the effects of different dissolved oxygen concentrations on the decomposition, degradation, and precipitation

processes of organic matter at various time points are discussed. The description of biochemical reactions and physical phenomena involved in the wastewater purification process through mathematics is also reviewed. These mathematical models are all based on mass balance and ion conservation of kinetic energy. Finally, this chapter reviews the basic theories of adaptive control and fuzzy control, along with their optimization methods.

Chapter 3: The architecture of the ASWWTP is designed based on the wastewater volume requirements, manufacturing area limitations, and stability. It is also necessary to consider the stability and purification efficiency of the control system, as well as the anti-interference requirements of its purification system. The manufactory architecture consists of a bioreactor unit, a blower, and a sedimentation unit. The blower is assumed to operate under ideal conditions. Subsequently, the mathematical model of the ASWWTP is established to describe the wastewater purification process. This mathematical model is based on the principles of mass balance and the conservation of ionic kinetic energy, and it is implemented by modifying the Activated Sludge Model 2D.

Based on the finite parameters derived from the mathematical model of the ASWWTP, a direct model reference adaptive control system for regulating dissolved oxygen concentration is designed. Subsequently, the global parameters of the ASWWTP are used to achieve a stable control state, and the adaptive controller parameters are

adjusted through MATLAB simulation to meet the design requirements of the control system. The simulation results confirm the stability, effectiveness, and anti-interference ability of the ASWWTP adaptive control system. The stability of the controller is further verified using the Lyapunov function.

Chapter 4: In the existing ASWWTP manufactory architectures, we assume that the blower is overproducing and delivering an excess volume of air, which can lead to excessive energy consumption and may even cause the purification system to collapse. Considering the specific operating status of the ASWWTP, a direct model reference adaptive control system with a filtering function is designed. The adaptive control parameters are derived from the finite parameters of the wastewater purification process. The adaptive control system is then applied to the global parameter mathematical model of the ASWWTP to achieve a stable wastewater purification process. The parameters of the adaptive filtering control system are adjusted and verified through MATLAB simulation. The simulation results demonstrate the adaptive control system's ability to filter excess air volume, as well as its stability and anti-interference capabilities. The stability of the adaptive control system is verified using the Lyapunov function.

Chapter 5: In this chapter, a different ASWWTP manufactory architecture is designed compared to those in Chapters 3 and 4 to meet the constraints of large-scale wastewater treatment while minimizing building area usage. The mathematical model describing

the operation of the ASWWTP is formed by modifying the Activated Sludge Model 2D based on the principles of mass balance and the conservation of ionic kinetic energy.

The supervised fuzzy logic - direct model reference adaptive controller design is based on the specific parameters of a limited ASWWTP. The control system is applied to the ASWWTP with global variable parameters. The adaptive control parameters are adjusted through MATLAB simulations to meet the controller design requirements, and the fuzzy logic is optimized through a genetic algorithm. The simulation results confirm that the control system can handle varying flows of wastewater, and it is stable, efficient, and possesses strong anti-interference capabilities. The stability of the two-layer control system is further confirmed by using the Lyapunov function.

Chapter 6: The research is summarized, and future research topics are anticipated.

Chapter 2 Literature Review

2.1 Overview of Activated Sludge Wastewater Treatment Plant and Application

2.1.1 History of the development of activated sludge wastewater treatment Plant

The activated sludge process is one of the wastewater purification methods. Its purification principle is to continuously introduce air into the wastewater so that microorganisms form sludge on suspended organic particles. The sludge contains microorganisms and bacteria. The activated sludge purification method was invented by Edward Arden and William Lockett in 1914 [1, 2]. With increasingly stringent wastewater purification and discharge standards, the sewage treatment method has evolved from a single method of continuously injecting air into wastewater to form flocs and then precipitating to form sludge to the current method of removing chemical pollutants. Now consider removing nutrients such as nitrogen and phosphorus to ensure that the discharged clean water will not be over eutrophic. Although the existing sludge treatment methods include the high negative pressure activated sludge method, delayed

gas explosion method, and activated sludge method, it is still a challenge for the design of control systems to maintain a stable and efficient purification process.

2.1.2 Basic working principles of ASWWTPs

Dissolved oxygen is an important factor that directly affects the efficiency and energy consumption of sewage purification. The concentration of dissolved oxygen determines the activity of microorganisms in the aeration tank. In addition, it is also the key to determining the degradation rate of organic microorganisms. The concentration of dissolved oxygen in the aeration tank should be maintained in a reasonable range of 2 mg/l to 4 mg/l [3]. The mixed liquid will separate the sludge and clean water in the sedimentation tank. The separation process may take several hours to several days, depending on the different chemical components of the wastewater [4].

In the sewage purification process, the time and proportion of dissolved oxygen injection into the aeration tank are crucial. Therefore, the accuracy, response time, and robustness of dissolved oxygen concentration control have received attention. The control system needs to be able to detect and adjust the dissolved oxygen concentration in the aeration tank in real time [5]. It is crucial to monitor the fusion rate of dissolved oxygen and organic microorganisms in real time because the fusion rate is the key factor in adjusting the blower power [6]. The growth of organic microorganisms in the

activated sludge purification plant is closely related to the concentration of dissolved oxygen, and dissolved oxygen can determine the growth process of organic microorganisms.

2.1.3 Types of ASWWTPs

In the development of activated sludge sewage purification technology, sewage purification methods can be divided into traditional activated sludge methods, delayed aeration methods, sequencing batch reactor methods, and membrane bioreactor methods [7].

The traditional activated sludge method has the characteristics of strong fluidity and short aeration time. Compared with other sewage purification methods, only the traditional activated sludge purification method uses young sludge return flow, which uses the organic microorganisms contained in young sludge to help the growth rate of biological populations [8]. This sewage purification method is often used for municipal sewage treatment and industrial sewage with high pollutant concentrations.

The delayed aeration sewage treatment method has the advantage of less sludge discharge. However, its aeration time is extremely long. Therefore, this sewage purification method is often used in small sewage purification projects in smaller communities [9].

The sequencing batch wastewater purification method uses a single container to carry out aeration, sedimentation, drainage, sludge removal, and other processes in sequence. Although it has the advantage of a small footprint, it has the disadvantage of a long purification cycle. Therefore, it is suitable for treating sewage containing highly sensitive pollutants.

The membrane bioreactor wastewater purification method adds membrane filtration to the traditional activated sludge method and uses biofilm to further filter the wastewater produced by the activated sludge method [10]. Because it can achieve higher water quality, but the purification cost is higher, it is usually used in treatment plants with strict purification standards.

For this study, the traditional activated sludge method was selected to solve some limitations of wastewater purification. Although this method has advantages such as simple maintenance and low energy consumption that other methods do not have, it relies heavily on an efficient dissolved oxygen control system. Therefore, the design and application of the dissolved oxygen control system must meet strict requirements.

2.1.4 Basic structure of ASWWTP

The process of decomposition and degradation of organic microorganisms that occurs during sewage purification is an important procedure for sewage purification. The

process involves various biochemical reaction units and physical components, each of which has a specific role and is essential to ensure that sewage is properly treated and meets the required discharge standards. Sewage undergoes oxidation and displacement. Clean water is produced in the combined process. An activated sludge wastewater treatment plant consists of three main treatment units: Primary treatment unit: sewage collection tank and primary sedimentation tank. Secondary treatment unit: bioreactor, aeration station, and secondary sedimentation tank. Tertiary treatment unit: secondary sedimentation tank, clean water outflow, and sludge treatment facility [11, 12]. These units are shown in Figure 2-1.

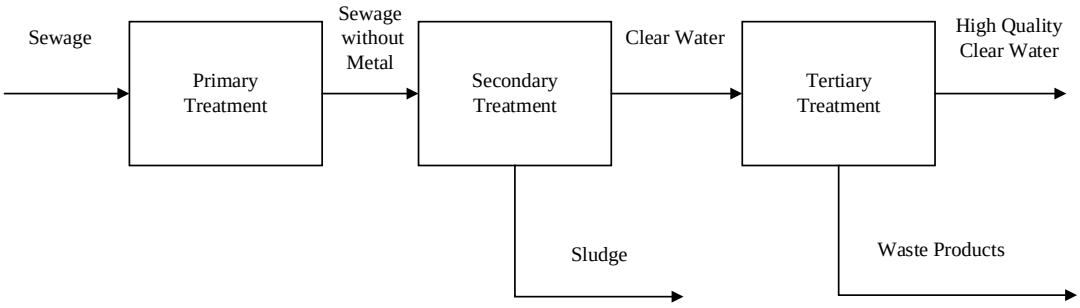

Figure 2- 1 The architecture structure of ASWWTP

The wastewater flows into the primary sedimentation tank. The primary sedimentation tank uses a screen to physically filter out impurities such as silt and oil. This step is to precipitate and remove large impurities, such as heavy metal particles. Next, the sewage

flows into the biochemical reaction tank. Next, organic microorganisms decompose harmful substances through redox reactions, thereby removing toxic and harmful substances from sewage. Finally, the clean water is separated from the sludge in the secondary sedimentation tank [13, 14].

The aeration station consists of a bioreactor and an air supply system. The bioreactor acts as a container for chemical reactions, while the air supply provides the necessary oxygen for biodegradation. In addition, the sedimentation tank uses gravity to separate clean water from sludge [15, 16]. Clean water is suspended above the tank, while sludge settles at the bottom of the tank. Afterwards, the clean water is discharged, while the sludge is concentrated, digested, and dried before being discharged into the environment. This thesis focuses on the working status of the aeration station to improve the purification efficiency of the ASWWTP.

2.1.5 Limitation and challenges in ASWWTP

There are some constraints in the construction and operation of sewage treatment plants. As described in [17], the increasing urban population and the reduction of available urban space limit the construction area of sewage treatment plants, which poses a challenge to the treatment capacity of sewage treatment plants. In addition, the composition of wastewater pollutants has become increasingly diverse, ranging from

single organic microorganisms to various chemical elements such as phosphorus and nitrogen, as described in [18]. Various internal and external interferences will be encountered in the sewage purification process, such as external temperature, humidity, and the coupling phenomenon of each microbial population inside, as described in the [19].

Traditional activated sludge wastewater treatment has the disadvantage of requiring a larger aeration system unit, unlike other activated sludge processes. This leads to high construction and maintenance costs, and in addition, it has special requirements for the control system [20]. The aeration system includes an aeration tank, a sedimentation tank, and a blower. This study aims to design an advanced adaptive control system for sewage treatment plants to enhance the efficiency and stability of the treatment process. In addition, building space limitations need to be considered when designing the structure of a sewage treatment plant. In addition, the design of the control system will consider energy consumption, focusing on the problem of balancing energy consumption and wastewater purification rate.

According to the characteristics of the activated sludge method, the blower needs to continuously supply air to the biochemical reaction tank. This is because dissolved oxygen is an essential element for the decomposition and degradation of organic microorganisms [21]. The continuous oxygen supply system consumes a lot of energy, accounting for 50% to 70% of the total energy consumption. Although the traditional

activated sludge method can effectively remove organic microorganisms, it is difficult to balance energy consumption and purification efficiency. The use of advanced adaptive controllers to dynamically adjust the power of the oxygen supply system to obtain the optimal purification efficiency is described in detail in Chapter 3.

In addition, the traditional sewage purification method also has the problem of sludge swelling, leading to a reduction in sedimentation rate when the dissolved oxygen concentration in the aeration tank is extremely low [22]. Moreover, if the dissolved oxygen concentration is extremely high, foaming problems will occur, resulting in the sludge not being able to settle quickly. Therefore, improving the dynamic adjustment ability of the dissolved oxygen control system is also a research focus. We will try to obtain the optimal online adjustment parameter capability by implementing monitoring and analysing system parameters.

2.2 Key Components of Aeration Station: Air Supplier Unit, Bioreaction Unit, and Sedimentation Unit

2.2.1 Air Supplier unit

The principle of sewage purification is to utilize the growth of aerobic microorganisms to achieve the degradation of organic pollutants. These microorganisms require adequate oxygen for respiration and metabolism [23, 24]. Therefore, maintaining an optimal dissolved oxygen concentration is essential for enhancing the efficiency of the activity sludge system operation and achieving the desired standards for effluent water quality [25].

The air supply station provides sufficient air for aerobic microorganisms, ensuring their metabolism and reproduction processes. These microorganisms utilize organic matter in wastewater as a carbon and energy source, thereby facilitating the decomposition of organic pollutants into harmless carbon dioxide and water [26, 27]. Moreover, the air supply process also prevents anaerobic conditions under specific circumstances. In addition, when the diffuser introduces air into the water, it creates a stirring effect, promoting the uniform distribution of activated sludge in the biochemical reaction tank [28, 29]. This process effectively prevents sludge settling and clumping.

Aeration methods can be divided into mechanical aeration, blower aeration, pure oxygen aeration, and surface aeration. Compared with other types, blower aeration can produce tiny bubbles through diffusers, thereby providing a larger gas-liquid contact surface area and promoting efficient oxygen transfer [30]. The blower can be controlled by an intelligent system to precisely adjust the air volume to meet different wastewater

treatment requirements and changes in wastewater capacity load, thereby reducing energy consumption [31].

2.2.2 Bioreaction unit

Microbial metabolism refers to the degradation of organic and inorganic matter in the bioreactor. The bioreactor must be carefully considered when designing and constructing an ASWWTP facility. It requires less space than traditional treatment methods, and its operating conditions (such as dissolved oxygen, pH, and temperature) are easier to accurately control. The bioreaction tank is capable of treating various types and concentrations of wastewater. In addition, the activated sludge wastewater purification method is less dependent on chemical catalysts than other treatment methods [32, 33].

In wastewater, the microorganisms use dissolved oxygen to decompose organic matter into carbon dioxide and water, as well as new biomass. The anaerobic zone of the bioreactor refers to the specific microorganisms that carry out denitrification and biological phosphorus removal [34-36]. The bioreaction tank is the most important component of the ASWWTP. Wastewater, oxygen, and young sludge flow into the biochemical reaction tank. After that, mix the water flow into the settlement tank.

There are four types of bioreactors: complete mixing reactor (CMR), plug flow reactor (PFR), sequencing batch reactor (SBR), and membrane bioreactor (MBR) [37-39]. The

SBR uses a staged approach to purify wastewater. Each stage of water inlet, biochemical reaction, and sedimentation operates independently. Precise control over the timing and operating conditions of each stage leads to efficient and accurate online updating of system parameters [40]. In our experiment, we chose SBR as the bioreactor. More details will be discussed later.

2.2.3 Sedimentation unit

Sedimentation systems are an integral component of the ASWWTP. The separation of liquids and solids takes hours or days, using gravity to concentrate the solid sludge. This process ensures that the clean water is free of toxic and hazardous substances. Depending on the clean water discharge requirements, secondary or tertiary sedimentation may be required [41].

According to the standards and process requirements for wastewater purification, there are four types of sedimentation systems: primary sedimentation tank, secondary sedimentation tank, final sedimentation tank, and advection sedimentation tank. In the sedimentation tank, the mixed liquid is separated into activated sludge and clear water by gravity [42]. Other sedimentation methods can be used according to different discharge requirements. In our study, a primary sedimentation device was used in Chapter 3.

Another function of the sedimentation tank is to separate new activated sludge from aged sludge. New activated sludge is circulated to the biochemical reaction tank to ensure that the biological treatment process is uninterrupted by the population of organic microorganisms. The speed of this cycle depends on various factors, as studied in [43]]. As described in [1, 2, 44], new sludge contains microbial populations that have adapted to the biochemical treatment environment, so increasing the return of young sludge can enhance the adaptability of the microbial community, accelerate microbial degradation, and improve the separation efficiency of liquids and solids. Finally, clean water and aged sludge are discharged, as shown in Figure 3.

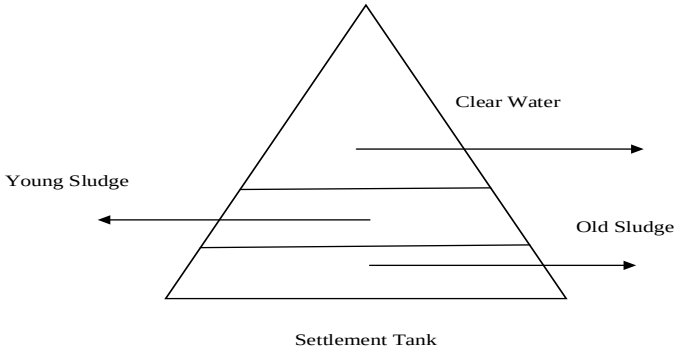

Figure 2- 2 The settler process in the ASWWTP

2.3 Challenges in Mathematical Modelling of ASWWTP

2.3.1 Nonlinear behaviour in biological and chemical processes

The activated sludge wastewater purification process is a very complex and nonlinear system. Since the metabolism of microorganisms is nonlinear, the chemical reactions are also nonlinear in the microbial metabolism process [45, 46]. Furthermore, the metabolism and chemical reactions of these microorganisms occur on different time scales and exist in different spatial dimensions.

As mentioned in [47], the growth rate of organic microorganisms in the metabolic process is nonlinear and will be affected by internal and external disturbances, including changes in dissolved oxygen concentration and temperature during microbial growth. As discussed in [48], the metabolic rate of microorganisms depends on the mixing rate of dissolved oxygen and organic microorganisms. In addition, there are coupled reactions between their parameters, so chemical reactions will also affect the growth of organic microorganisms in both temporal and spatial dimensions. Each microbial population has its own biological characteristics, resulting them to compete with each other during growth. This competition can either accelerate their growth or inhibit the growth of other populations in a short period of time, as mentioned in [49, 50]. When the external environment fluctuates greatly, the metabolic rate of microorganisms will fluctuate greatly. It is a nonlinear dynamic process, which is demonstrated in [51].

As mentioned in [52], the sewage purification process involves many chemical reactions. According to the characteristics of each chemical reaction, the process and results of these chemical reactions will be affected by factors such as temperature and pollutant concentration. Therefore, these chemical reactions are highly nonlinear. In addition, according to the characteristics of each chemical reaction, the biochemical reactions of pollutants in different environments will be saturated and inhibited, as studied in [53, 54].

In addition, since the growth of microorganisms and chemical reactions are nonlinear, the impact of changes in the external environment on the sewage purification system is also nonlinear, which is a challenge for describing the sewage purification process using mathematical models, as studied in [55].

2.3.2 Operation of coupled processes and multivariable interactions

There is a coupling phenomenon between the metabolism of organic microorganisms and biochemical reactions in the activated sludge purification process. As mentioned in [56], changes in any parameter between them will cause changes in other parameters, thereby directly changing and affecting the structure of microbial metabolic processes and chemical reactions through various pathways. Therefore, these coupling phenomena and the influence between parameters will lead to the enhancement of their

nonlinear characteristics and the complexity of dynamics. As demonstrated in [57], the activated sludge purification process cannot be described by a simple coupling method, and it is necessary to consider the influence of multiple factors on biochemical reactions.

The activated sludge purification process also involves the phenomenon of mutual constraints between physical processes and microbial growth processes. As studied in [58], when oxygen enters the biochemical pool and merges with wastewater, the connect aera and time between oxygen ions and pollutant ions during the fusion process need to be considered because these factors directly affect the activity of organic microorganisms. As studied in [59], the amount of oxygen supplied and the cycle in the aeration tank will directly affect whether the microorganisms have enough dissolved oxygen to promote biochemical reactions. Therefore, when using mathematical models to describe the activated sludge purification process, it is necessary to consider the effects of multiple time scales and multiple variables on its growth process.

Since the activated sludge purification system involves the growth and chemical reaction processes of various types of organic microorganisms, these processes are described by different time-scale parameters, growth state parameters, and required chemical reaction environment parameters, such as chemical, physical, biological, environmental, and mechanical parameters, as detailed in [60-62].

Therefore, in the complex microbial growth and chemical reaction process, it is impossible to describe it with a mathematical model of a single feedback mechanism. Multiple mechanisms such as positive feedback and negative feedback need to be described at the same time, otherwise the predictability and accuracy of the mathematical model will decrease, resulting in a decrease in the performance of the subsequent control system, as described in [63].

2.3.3 Challenges of external disturbances and uncertainties to mathematical models

The oxygen concentration and microbial concentration in organic matter in sewage affected by the pollution source and the external environment in the biochemical reaction tank. As described in [64, 65], when these parameters change, the concentration parameters of organic matter in the biochemical reaction tank will change nonlinearly, resulting in periodic changes in the organic load. In addition, these changes can also cause the microorganisms to become less active or anaerobic, resulting in a decrease in sewage purification capacity, as discussed in [66-68]. The changes in these parameters pose a challenge to the accuracy of the mathematical model.

The changes in chemical composition and concentration fluctuations in sewage are based on the source of sewage and external interference [69]. The fluctuations and

changes in oxygen concentration and microbial concentration are nonlinear or periodic. The composition of factory emissions determines the composition of wastewater. Changes in the external natural environment determine the concentration of wastewater [70]. For example, excessive rainfall will cause the concentration of pollutants in sewage to decrease while high temperatures will cause the concentration of pollutants in sewage to increase. Pollutants in sewage include toxic chemical components, organic microorganisms, and metal components. Chemical composition and pollutant concentrations affect the growth of organic microbial populations in wastewater, and these effects can lead to reduced wastewater purification efficiency. The growth process of microorganisms is nonlinear. Organic microbial populations compete with each other during growth. This relationship is nonlinear, as studied in [71, 72].

As external environmental disturbance factors change, the chemical composition and concentration of pollutants in wastewater change over time, and this change is nonlinear [73]. Chemical components in wastewater, such as nitrogen, phosphorus, potassium, can affect the activity of organic matter in a short period of time, which is difficult to predict. Therefore, the requirement for the dynamic adjustment capability of mathematical models poses a huge challenge, as described in [74, 75].

Fluctuations in wastewater flow affect the amount of gas supplied to the bioreactor and the rate at which dissolved oxygen combines with organic matter. In addition, these fluctuation affects the residence time of dissolved oxygen and wastewater mixing in the

sedimentation tank. Furthermore, the effect on microbial growth is nonlinear, as mentioned in [76-78]. For example, when the wastewater flow rate fluctuations greatly, the oxygen supply system needs to respond quickly to provide a large amount of air. such a phenomenon affects the stability of the wastewater purification system. In addition, if the oxygen supply system responds extremely slowly, the oxygen supply system needs to respond quick to provide a small amount of air. Such a phenomenon will cause the sewage purification rate to drop rapidly, as discussed in [79].

2.3.4 High-dimensional models and model validation

The mathematical model of activated sludge has the characteristics of multivariable, multi-time, and multi-space scales. It needs to calculate the input of multiple parameters at the same time, such as sewage inflow and outflow, sewage composition, oxygen content in sewage, input oxygen, concentration of organic microorganisms, concentration of each chemical element, concentration of sludge, clean water outflow, and return flow of young sludge [80, 81]. These variables are nonlinear, which greatly increases the computational complexity and the accuracy of the mathematical model.

In addition, these variables exist on different temporal and spatial scales, including competition among local microbial populations, coupled chemical reactions during growth, and global fluid dynamics. These factors require mathematical models to be

calculated at different levels, which poses a challenge to the dynamic response and regulation capabilities of mathematical models.

The accuracy of the mathematical model requires long-term data accumulation and repeated verification under different environments. Its debugging and optimization require continuous debugging of different parameters, such as microbial decomposition rate, microbial growth rate, organic microbial oxidation rate, nitrification rate, and denitrification rate [82, 83]. The debugging process requires multiple iterations to ensure the accuracy and predictability of the mathematical model.

2.4 Role of Dissolved Oxygen in Wastewater Treatment Processes

2.4.1 Importance of dissolved oxygen in biochemical reactions in ASWWTP

Dissolved oxygen is an essential chemical element in the activated sludge process for sewage purification. It is essential for the chemical reaction process that removes harmful substances from the environment through biodegradation. Dissolved oxygen is a chemical element that promotes the growth and respiration of organic microorganisms, as described in [84, 85]. In addition, dissolved oxygen is an indispensable catalyst in the nitrification process. When the dissolved oxygen concentration is insufficient,

organic microorganisms will undergo anaerobic phenomena, which will lead to a decrease in the sewage purification rate, as described in [86].

The air supply provides oxygen while the microorganisms perform aerobic respiration. Microorganisms use the process of aerobic respiration to break down organic pollutants, converting them into carbon dioxide, water, and new cell material, as described in [87]. High concentrations of dissolved oxygen can increase the efficiency of microorganisms in breaking down organic matter. Conversely, low concentrations of dissolved oxygen can turn organic microorganisms into anaerobic microorganisms, as discussed in [88]. The chemical formulation for nitrification reaction can be expressed as follows:

$$NH_4^+ + 2O_2 \rightarrow NO_3^- + H_2O + 2H^+ \qquad (2.4.1\text{-}1)$$

Where: NH_4^+ represents ammonia nitrogen, O_2 represents oxygen, NO_3^- nitrate, H_2O represent water, and H^+ represents hydron.

Dissolved oxygen is an essential biochemical element in the processes of denitrification and biological phosphorus removal. Its concentration determines the efficiency of denitrification and phosphorus removal, as described in [89]. In the denitrification process, dissolved oxygen is a catalyst for nitrification. Nitrifying bacteria require a

high concentration of dissolved oxygen, usually maintained at 1.5-2.5 mg/l, as described in [90]. The chemical formulation for denitrification reaction is illustrated as follows [91]:

$$NO_3^- + CH_2O + 2H^+ \rightarrow N_2 + CO_2 + H_2O \quad (2.4.1\text{-}2)$$

Where: NO_3^- represents nitrate. CH_2O represents formaldehyde, H^+ represents hydron. N_2 represents nitrogen, and CO_2 H_2O represents water.

During the biochemical reaction of denitrification, the dissolved oxygen concentration must be maintained at a high level. As described in [92], nitrifying bacteria convert nitrogen into nitrogen gas during the denitrification process, thereby achieving the purpose of denitrification.

Finally, in the biological phosphorus removal process, dissolved oxygen interacts with polyphosphate bacteria and absorbs phosphorus into polyphosphate bacteria, thereby achieving phosphorus removal, as described in [93]. Its chemical formula is:

$$PO_4^{3-}\text{(wastewater)} - PO_4^{3-}\text{(intracellular) (stored in PAO cells)} \quad (2.4.1\text{-}3)$$

Where: PO_4^{3-} is phosphorus, PAO is polyphosphate – accumulating organisms.

2.4.2 Dissolved oxygen's role in nutrient removal and organic matter decomposition

The percentage of the nutrient removal is a standard factor for evaluating wastewater discharge. Excessive nutrients remaining in the discharged water can promote the overgrowth of algae and other plants, leading to the phenomenon known as algal bloom. This disruption of the aquatic ecosystem balance can result in hypoxia in water bodies [94].

The term 'nutrient' refers to the organic carbon, nitrogen, and phosphorus, all of which require a series of oxygen-dependent biochemical reactions for removal. The removal of organic carbon is crucial to preventing the overgrowth of microorganisms, as carbon is a nutrient source for their growth and reproduction. Carbon is the basis for nitrogen and phosphorus removal. Therefore, maintaining carbon concentration is necessary in wastewater purification.

First, the removal of organic carbon is divided into two categories: soluble carbon and insoluble carbon, both of which react biologically with dissolved oxygen [95, 96]. Through metabolic processes promoted by microorganisms, soluble carbon is degraded into biomass, carbon dioxide and water; insoluble carbon exists in suspended particles in wastewater. This form of carbon is degraded externally into soluble carbon, which is absorbed and utilized by microorganisms, further undergoing biological reactions and

purifying wastewater. These biochemical processes occur slower than the metabolism of soluble carbon. This is an important factor that needs to be considered when establishing mathematical models and designing control systems. Soluble carbon is oxidized to produce carbon dioxide and biomass, as shown in Figure 2-3.

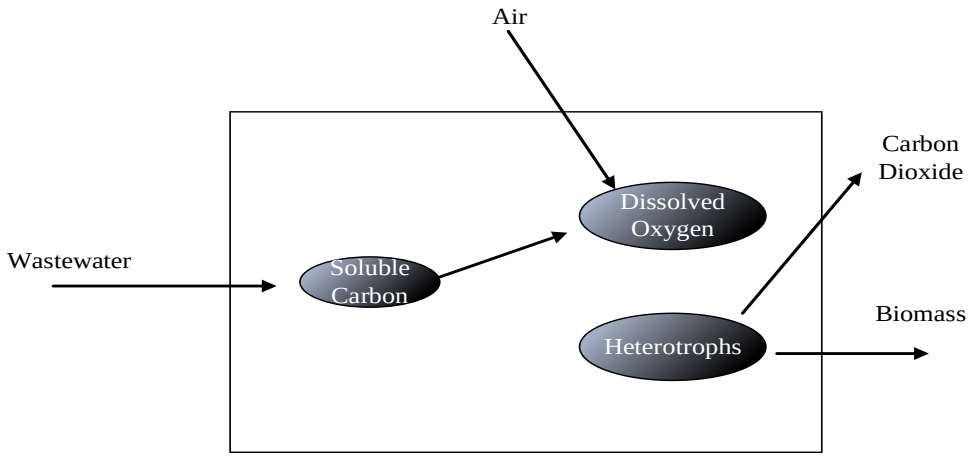

Figure 2- 3 The function of DO in carbon removal

Secondly, denitrification is essential to prevent eutrophication of water bodies, prevent excessive growth of aquatic plants such as algae, reduce odor and corrosion, and improve purification effects. Excessive nitrogen content in wastewater will produce ammonia gas, causing air pollution. Nitrogen content is one of the criteria for wastewater discharge purification.

Denitrification chemical reactions include aerobic digestion reactions and anoxic denitrification reactions. In the aerobic denitrification process, soluble carbon and ammonium compounds react biochemically with dissolved oxygen to produce nitrite and biomass. At the same time, in the anoxic denitrification process, soluble carbon

reacts biochemically with nitrite to produce nitrogen gas and biomass, as shown in Figure 2-4.

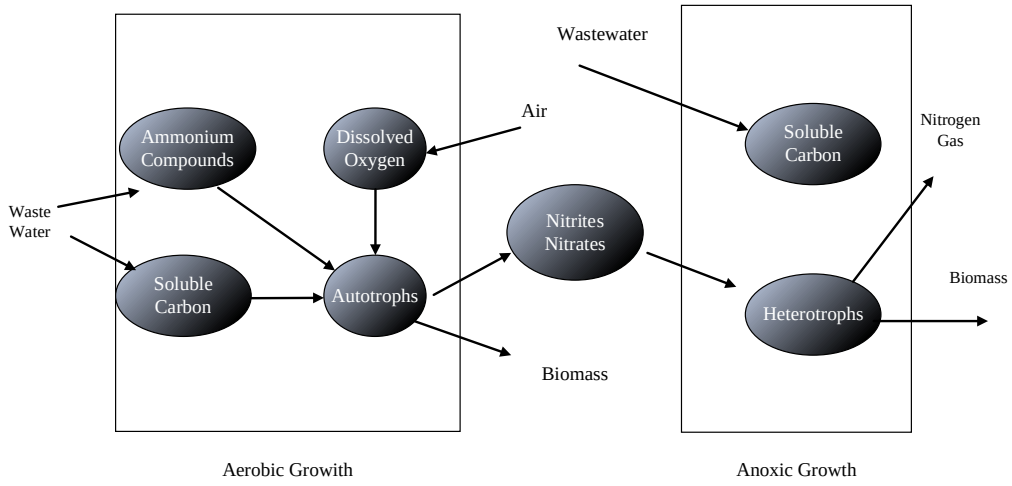

Figure 2- 4 The function of DO in nitrogen removal

Finally, excessive algae growth, algae death, or decomposition can cause water bodies to turn green and emit foul odors because of excessive phosphorus concentrations, which leads to a decrease in oxygen content in the water. Biological phosphorus removal consists of two steps: the first anaerobic reaction and the second aerobic reaction.

Anaerobic reaction process:

Carbon-based biomass in the wastewater reacts to form polyhydroxyalkanoates (PHA). Next, new biomass converts into polyphosphates (PP).

Aerobic reaction process:

During the aerobic process, dissolved oxygen interacts biologically with PHA and soluble phosphates. After these processes, the soluble phosphates are produced, as shown in Figure 2-5. The biological nutrient removal model was designed by the International Association for Water Quality (IAWQ) [94].

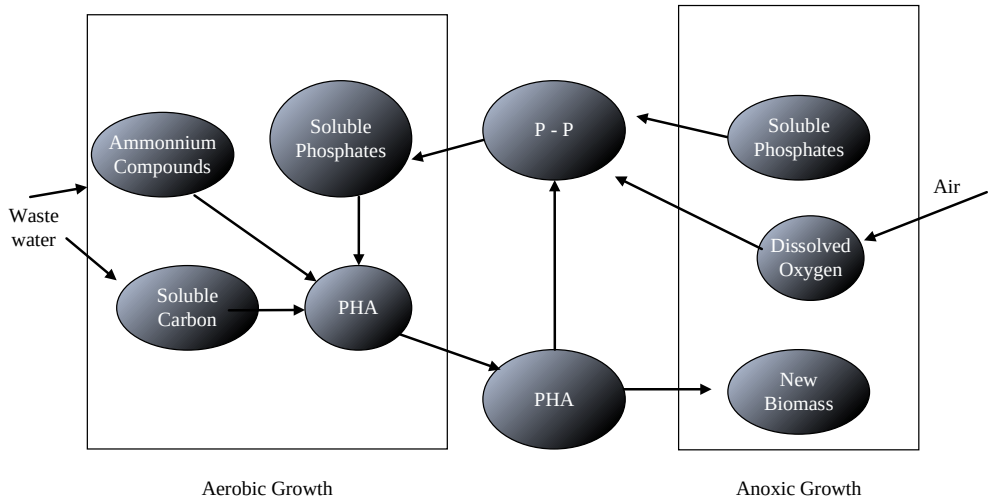

Figure 2- 5 The function of DO in phosphorous removal

As described in [97], the nutrient removal process involves the mass transfer of nutrients. During The biochemical reactions of oxidation and degradation include the transfer of oxygen ions to organic matter and metals. The process produces gas and solid particles; the solid particles settle at the bottom of the primary sedimentation tank, while the gas and sludge are discharged simultaneously. In order to meet specific clean water discharge standards, the treated water from the primary sedimentation tank typically requires further treatment, such as membrane filtration or the addition of

chemical agents, before it can be discharged or reused [98]. The rate of biochemical reactions is related to the increased gas-liquid and liquid-solid contact areas and the oxygen consumption [99].

Oxygen is an essential chemical element in the wastewater purification process and directly affects the balance between wastewater purification efficiency and energy consumption, which usually tend to increase proportionally. Therefore, it is necessary to find the most economical and effective way to adjust the oxygen ratio in the wastewater purification process through a suitable control system. The appropriate ratio of dissolved oxygen concentration to wastewater mixing can enhance the efficiency of biochemical reactions [100]. In the biochemical nutrient removal process, each biochemical reaction occurs at a different rate, depending on the characteristics of each biochemical component [101]. The details of the oxygen transfer function are discussed in Chapters 3, 4, and 5.

2.4.3 Influence of dissolved oxygen concentration on energy efficiency in wastewater treatment

In the process of activated sludge wastewater purification, dissolved oxygen is a key factor that directly affects the biological growth of organic microorganisms and the efficiency of biochemical reactions. Dissolved oxygen is produced by the blower,

which consumes the most energy in the sewage purification process. This is because only in an environment with high concentrations of dissolved oxygen can the removal of organic microorganisms and nutrients be maintained efficiently. Maintaining a high concentration of dissolved oxygen requires blowers to continuously produce and output air to the biochemical reaction tank, so the blower requires a lot of energy to support its continuous operation. This is the most energy-consuming component in the wastewater purification process, as discussed in [102].

Although high concentrations of dissolved oxygen can ensure efficient sewage purification, considering energy consumption, sewage purification plants generally adjust dissolved oxygen concentrations within a reasonable range according to sewage discharge standards. As mentioned in [103], it is difficult to achieve a balance between energy consumption and purification efficiency because their direct relationship is nonlinear. As discussed in [104], in sewage purification plants with different sewage sources, reducing dissolved oxygen concentrations can improve denitrification efficiency and thus reduce energy consumption, which illustrates the feasibility of reducing dissolved oxygen. The mathematical model used to describe the sewage purification process has strict requirements.

2.4.4 Impact of dissolved oxygen control on system performance and stability

As mentioned in [105], the activity of microorganisms depends on the concentration of dissolved oxygen. The dissolved oxygen concentration required by different microbial communities to maintain their high growth and high metabolic rates depends on different dissolved oxygen concentrations. In the wastewater purification process, efficient metabolism and reproduction of single or multiple microbial populations are not feasible. Due to the inhibition and inability of other microbial populations to grow, as discussed in [106, 107], maintaining a balance in the growth of each biological population is one of the key performance factors of the control system.

The accuracy of the dissolved oxygen concentration control system directly affects the sewage purification rate because the decomposition rate of organic microorganisms and the efficiency of nitrogen and phosphorus removal depend on the dissolved oxygen concentration. In addition, the dissolved oxygen concentrations they require are different. As discussed in [108], dissolved oxygen has the effect of increasing the efficiency of microbial decomposition at high concentrations. However, at high concentrations of dissolved oxygen, the efficiency of denitrification decreases. Therefore, the performance and stability of the dissolved oxygen control system affect the quality of purified water.

As mentioned in [109], current sewage purification plants achieve a balance between efficient purification and energy consumption by utilizing adaptive control or artificial intelligence control systems to adjust the concentration of dissolved oxygen in real time.

2.5 Challenges in Dissolved Oxygen Control System for ASWWTP

2.5.1 Complexity of dissolved oxygen in nonlinear and environments

As mentioned in [110], the flow of sewage from a sewage treatment plant will change due to the influence of the external environment, such as climate change and sewage sources. There are sudden and large fluctuations in sewage sources. Since the sewage flow is not constant for 24 hours, urban sewage sources are cyclical. As discussed in [111], when the sewage inflow increases or decreases in a short period of time, the demand for dissolved oxygen changes. If the dissolved oxygen control system cannot meet the urgent oxygenation demand, it will lead to a decrease in the degradation rate of organic microorganisms or the occurrence of anaerobic conditions. In this case, the requirement for predictability and robustness of the dissolved oxygen control system is a challenge. As studied in [112], the decomposition of organic microorganisms is

affected by multiple factors, leading to rapid growth or growth inhibition. Therefore, it poses a challenge to the accuracy of the control system. As described in [113], the decomposition of organic microorganisms is affected by a variety of factors, resulting in their rapid growth or growth inhibition. Therefore, the requirements for the control system are a challenge.

As described in [114], the oxygen supply system is a nonlinear system. Because it needs to consider the amount of sewage flowing in, it also needs to consider the oxygen conversion efficiency. When the oxygen conversion efficiency is low, increasing the power of the blower does not directly increase the dissolved oxygen concentration because the ambient temperature of the chemical reaction must also be considered. The nonlinear nature of the oxygen supply system requires precise control of the dissolved oxygen levels, especially when sewage flow is high, as discussed in [115]. To ensure high dissolved oxygen levels that support microbial growth, blowers often provide extra air. However, this increases energy consumption significantly, as mentioned in [116]. The formula for calculating the oxygen transfer efficiency is:

The oxygen transfer modelling in this context is based on the mass balance principle.

The equation of oxygen mass transfer can be expressed as follows:

$$\begin{aligned}(\text{rate of oxygen transfer}) = (\text{mass transfer coefficient}) \times \\ (\text{air-water surface area}) \times (\text{concentration difference})\end{aligned}$$

Mathematical model for the oxygen mass transfer equation can be formulated as follows:

$$r_a = K_L a(DO_{sat} - DO) \tag{2.3.5-2}$$

Where: DO_{sat} and DO represent the saturation of DO concentration and DO concentration, respectively, while K_L and a are constants representing the air flow rate.

Mathematical model for the nutrient mass transfer equation can be written as:

$$N = K_L(W_N - ACF_N) \tag{2.3.5-3}$$

Where: N , K_L represents nutrient mass transfer flux and liquid film mass transfer coefficient. W_N , ACF_N represent nutrient concentration in the aqueous phase and nutrient concentration in activated sludge flocs.

The dissolved oxygen required for the growth of microorganisms is nonlinear, as mentioned in [117]. According to research in [118], high concentrations of oxygen are beneficial for microbial growth, but they result in significant energy consumption. On the contrary, extremely low a concentration of oxygen is beneficial for energy consumption, but it can lead to incomplete decomposition of microorganisms, resulting in a reduced purification rate or the collapse of the control system.

As described in [119], the dissolved oxygen control system must be able to predict changes in organic microorganism concentrations due to the time delay in supplying the oxygen required by these microorganisms.

2.5.2 Energy consumption and efficiency trade-offs in aeration

As demonstrated in [120], according to the physical principles of sewage purification, to provide efficient sewage purification rates, the air supply system will continuously generate and supply air to microorganisms, even exceeding the amount of air required for microbial growth, so that they can have enough dissolved oxygen to grow. In this case, energy consumption is a heavy burden on sewage treatment plants, especially when wastewater treatment factories are under high load. As demonstrated in [121], excessive dissolved oxygen in the biochemical reaction tank does not accelerate the biochemical reaction rate. They can inhibit some biochemical reactions, like denitrification [122]. According to biological principles, organic microorganisms can only achieve the best growth rate under an appropriate percentage of dissolved oxygen conditions. Therefore, providing excessive dissolved oxygen to microorganisms to increase their growth rate is not possible, as it will inhibit their growth [123].

In activated sludge wastewater purification plants, the air supply system is the component with the highest energy consumption, accounting for 50% to 70% of the

total energy consumption, as mentioned in [124]. To reduce energy consumption while ensuring high purification efficiency, it is necessary to adjust the percentage of dissolved oxygen in the biochemical reaction very accurately and quickly to strike a balance between energy consumption and high purification rate. However, due to the coupling phenomenon between microbial growth and chemical reactions, the balance between energy consumption and a high purification rate is a challenge for the control system [125].

As described in [126], the dissolved oxygen concentration standard in the biochemical reaction tank is determined by the sewage inflow, the clean water effluent standard, and the microbial concentration of the sewage treatment plant, all of which are time-varying and nonlinear. According to the principle of biochemical reaction, the dissolved oxygen concentration ranges from 1.5 to 2.0 mg/l. As shown in [127], reducing the power and energy consumption of the blower can help reduce the ineffective dissolved oxygen in the biochemical reaction tank. Ineffective dissolved oxygen refers to the dissolved oxygen that is unevenly distributed in the biochemical reaction tank. In addition, by real-time monitoring of the sewage inflow, the MPI-Fuzzy control system with strong predictive ability is used to predict and provide dissolved oxygen, which is then stirred in the biochemical reaction tank to make the dissolved oxygen evenly distributed in the biochemical reaction tank so that the dissolved oxygen is fully combined with organic microorganisms to obtain the best microbial growth rate, as described in [128].

The dissolved oxygen concentration can be adjusted in the biochemical reaction tank by zoning, but the requirements for factory hardware are relatively high, as discussed in [129]. In addition, an intermittent blower can be used to generate and transport air to the biochemical reaction tank to provide the dissolved oxygen required by microorganisms and support the efficient growth of organic microorganisms, as mentioned in [130].

When balancing energy consumption and purification efficiency, it is necessary to consider not only the coupled response in the microbial demand for dissolved oxygen, but also the interfering factors that affect the sewage purification efficiency, such as weather, temperature, and rainfall, as discussed in [131].

2.5.3 Robustness and real-time control challenges

As described in [132], during the sewage purification process, the concentration of dissolved oxygen is subject to unpredictable external disturbances. These disturbances have irreversible effects on the sewage composition and flow rate. In addition, it poses a challenge to the robustness of the control system. These disturbances include temperature, rainfall, and seasonal water quality changes. Temperature can affect the activity of organic microorganisms, which depends on the biological characteristics of different microorganisms. The activity criteria for each microbial population are

different, as described in [133]. Sewage inflow depends on industrial emission standards and rainfall, as mentioned in [134]. Seasonal changes are the factors affecting sewage flow. For example, during the rainy season, the concentration of organic microorganisms decreases, while in the dry season, it increases, as described in [135]. Based on the impact of these uncertainties on the sewage purification rate, these influences pose a challenge to the robustness of the dissolved oxygen control system.

According to the principle of adaptive control, it can make real-time predictions and collect data based on external interference. Dissolve oxygen control parameters are adjusted in real time based on external disturbances, ensuring the stable operation of sewage purification.

As described in [136], the need to monitor and adjust the operating parameters of activated sludge wastewater treatment plants in real time poses challenges to sensor performance and control system response speed. Sensor performance refers to the accuracy and reliability of detection, as well as the speed and error magnitude of data acquisition. The control system must handle data transmission delays and respond quickly to maintain effective operation. Therefore, advanced dissolved oxygen control systems are essential. As described in [137], an MPI controller is used to predict future wastewater treatment system parameters and adjust dissolved oxygen concentration to achieve efficient wastewater treatment. However, the results show that the accumulated

error of the MPI dissolved oxygen control system is unacceptable, which impairs the stability of the control system [138].

As described in [139], the dissolved oxygen control system has the ability to resist external environmental disturbances and changes in sewage load while achieving data optimization to improve purification efficiency and system stability. The design of the adaptive controller must consider the problem of regulating dissolved oxygen while also considering resistance to external and internal disturbances in the purification system; however, when the control parameters are adjusted quickly, the accumulated superposition errors will cause the control system to be unstable. Chapters 3, 4, and 5 provide detailed solutions for various sewage purification plants.

2.6 Advanced Control Strategies for Dissolved Oxygen in ASWWTP

2.6.1 Traditional control methods: MPID and NMPC

As discussed in [140], activated sludge wastewater treatment plants use an MPI control system to regulate dissolved oxygen concentration. However, this control system has insufficient regulation accuracy, slow response speed, and high computing ability

requirements. As described in [141], the MPI controller also has difficulty handling system delays and lacks adaptive capabilities.

As described in [142], activated sludge wastewater treatment plants use NMPC control systems to regulate dissolved oxygen concentration. The predictive capability of the NMPC controller is limited, and it requires the mathematical model to be highly accurate. As mentioned in [143], NMPC is not suitable for regulating dissolved oxygen concentration because its calculation is very complicated, and its real-time adjustment capability is limited. It is unable to meet the requirements for real-time dissolved oxygen control. In addition, the robustness of NMPC control systems is limited, which reduces the ability to resist external and internal interference in the sewage treatment process. As described in [144], the high-frequency regulation actions of NMPC controllers in nonlinear sewage systems bring complexity and higher error rates.

As mentioned in [145], activated sludge wastewater purification plants use fuzzy controllers to quickly adjust dissolved oxygen concentrations. However, fuzzy controllers rely heavily on engineers' experience to formulate rules, so they are less efficient in dealing with emergencies. As described in [146], fuzzy controllers require too many rules to adjust dissolved oxygen concentrations, which requires high computing power. Although this type of controller does not require an accurate mathematical model, it is much more difficult to quantitatively analyse and adjust than PI and PID controllers, and optimization is still challenging [147].

2.6.2 Adaptive control system: direct model reference adaptive control for ASWWTP - advantage and challenge

As described in [148], DMRAC can monitor the parameters of the wastewater purification system in real time and dynamically adjust the control parameters to achieve an efficient purification process. It also has the advantage of fast response speed. In addition, compared with other controllers, its performance optimization is relatively simple.

In addition, compared with PI and PIC controllers, it shows stronger robustness and adaptability in solving the problems of fluctuations in sewage inflow, pollutants, and dissolved oxygen concentration in sewage. Since DMRAC can quickly and dynamically adjust the parameters of dissolved oxygen, it can improve the efficiency of the sewage purification system and achieve a balance between sewage purification rate and energy consumption.

The design and application of DMRAC in regulating dissolved oxygen concentration requires several key points: 1) The design of the control system relies on an accurate mathematical model that describes the activated sludge purification process. 2) In the activated sludge purification processes, the growth and biochemical reactions of organic microorganisms occur on multiple time scales. There are multiple coupling phenomena in the biochemical reactions, which increase the complexity of the

mathematical model. Therefore, it is a challenge to establish a reference model. 3) Errors will continue to accumulate in the operation of the long-term control system, which will cause the drift of the adaptive control parameters and cause the instability of the control system. Therefore, the long-term stability and efficient operation of the control system are challenges. 4) The optimization of the DMRAC control system is to continuously debug the initial parameters of the control system and the adaptive algorithm. This process is very complex, especially in sewage purification; there are many unknown system parameters, which are in multiple different time scales and spaces.

Direct model reference adaptive control, which addresses complex, time-varying, and uncertain systems, demonstrates strong adaptability, as described in [169]. The controller is modified based on the guidance of a reference model. This method involves comparing the real output with the reference output and adjusting control parameters accordingly to make the controller output approach the reference output. This reference model represents the expected output under ideal conditions over time.

In a first-order linear system, the DMRAC can be expressed as follows [149]：

$$y_p(k+1) = a_p y_p(k) + b_p u(k) \tag{2.6.1-1}$$

Where: $u(k)$ is the system input, and $y_p(k)$ is the system output. The a_p and b_p are system parameters.

Based on the expected real-time output ability of the system, the reference model provides the anticipated system response; this enables the controller to adjust the system input to make control output close to reference output [140]. Thus, the model reference equation can be expressed as：

$$y_m(k+1) = a_m y_m(k) + b_m r(k) \qquad (2.6.1\text{-}2)$$

Where: $r(k)$ is the reference model input. $y_m(k)$ is the reference model output. Both a_m and b_m are reference model system parameters.

The goal of direct model reference adaptive control is to adjust the system input ($u(k)$), in order to make system output ($y_p(k)$) converge as close as to reference model output ($y_m(k)$).

The structure of adaptive control can be expresses as:

$$u(k) = \theta^T(K)\sigma(K) \qquad (2.6.1\text{-}3)$$

Where $\theta(k)$ is adaptive parameter vector , $\sigma(k)$ is the system state vector .

The update rule for adaptive parameters can be written as:

$$\theta(k+1) = \theta(k) + \psi\sigma(k)e(k) \qquad (2.6.1\text{-}4)$$

$$e(k) = y_p(k) - y_m(k) \qquad (2.6.1\text{-}5)$$

Where: ψ is adaptive rate, e is error dynamic.

The analysis of control stability is indispensable for ensuring the smooth operation of the system. Typically, stability analysis in DMRAC utilizes a Lyapunov function [150] and can be expressed as follows:

$$V(\theta, e) = \frac{1}{2}\theta^T R\theta + \frac{1}{2}e^2 \tag{2.6.1-6}$$

$$\dot{V}(\theta, e) = -\theta^T R\sigma(k)e(k) \tag{2.6.1-7}$$

Where: R is small postive constant volume .

To determine the stability or instability of the system, the stability condition is satisfied only when $\dot{V}(\theta, e)$ is less than or equal to zero, and both $\theta = 0$, and $e = 0$ [12].

The DMRAC was designed and implemented based on the dissolved oxygen concentration requirements of the activated sludge wastewater treatment plant for nutrient removal. Various Multiple variations DMRAC designs were developed to meet different objectives, as detailed in Chapters 3.4 and 5.

2.6.3 Two-level control for large-scale ASWWTP - advantage and challenge

The ASWWTP structure adopts a segmented design to help understand and regulate the dissolved oxygen concentration. Each control unit is responsible for a different wastewater purification unit. The purpose of this control structure is to reduce the

burden on the central control unit, thereby improving the reliability and flexibility of the system. As described in [44], the two-level control strategy is also based on online updating of state variables, so it has powerful fault diagnosis and correction capabilities.

The ASWWTP operation employs a hierarchical control system. The upper layer control system is responsible for overall system monitoring and optimization, while the lower layer control system is divided into four independent control systems for the wastewater purification unit [137], as depicted in Figure 2-6. 1) The inlet control system controls the flow rate of sewage according to the sewage load of ASWWTP. Ensure that the subsequent treatment process does not produce unnecessary overload. 2) The aeration control system is responsible for maintaining the appropriate concentration of dissolved oxygen to promote microorganism activity. It employs a dissolved oxygen sensor control system and a blower control system to adjust the aeration volume. 3) The sediment tank control system is responsible for monitoring the sludge interface and effluent quality and controlling the discharge sludge pump operation, ensuring that clear water and sludge are separated and discharged according to required standards. 4) The sludge concentration and dewatering control are applied if required.

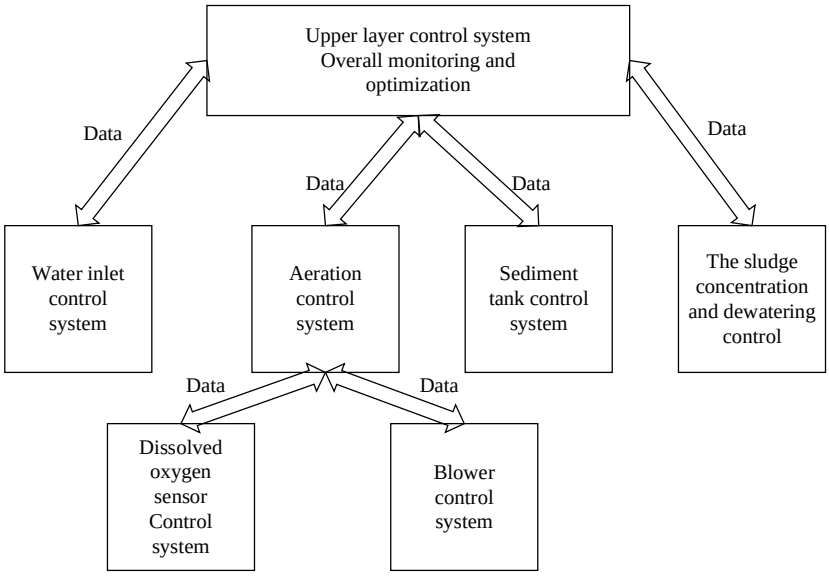

Figure 2- 6 The hierarchical DO concentration control structure of ASWWTP

As discussed in [139], a two-layer control system is used to regulate the dissolved oxygen concentration. In this two-layer control system, local controllers are used to adjust the dissolved oxygen concentration in each biochemical reaction tank separately, especially to solve the sudden demand for dissolved oxygen by microorganisms. The global controller is used to coordinate the aerator and multiple biochemical reaction tanks as a whole and optimize the long-term purification performance. Local and global parameters are on different time scales, so the coordination between them is more difficult. There is a time lag phenomenon when the two-layer control system adjusts the dissolved oxygen concentration. As described in [91], the two-layer control system can resist external interference in the local controller. Therefore, the robustness and anti-interference ability of the two-layer control system are acceptable. The two-layer control system can reasonably coordinate the coupling phenomenon of multiple

variables through the global controller, thereby improving the ability to dynamically adjust the load.

Fast response between global controller and local controller is a difficult problem in two-level control systems. As discussed in [151], if the local control cannot respond quickly to sudden or uncertain disturbances, the global control system will be unstable, resulting in a decrease in the wastewater purification effect. The coordination between the two-level controllers plays a decisive role in the stability of the global control system. The local controller needs to respond quickly to the organic microbial growth and biochemical reactions, which are nonlinear dynamic changes. As discussed in [104], the local controller regulates the urgency and complexity of the parameters of the coupled phenomena, which are system parameters at multiple time scales and different spatial dimensions.

This study considers using a two-layer controller to regulate dissolved oxygen concentration. The upper-level control system uses a fuzzy controller, while the lower-level control system uses an adaptive controller. This two-layer controller can achieve stable and efficient nutrient removal. A detailed study is provided in Chapter 5.

2.7 Addressing Spaces and Capacity Constraints in ASWWTP

2.7.1 Structural optimization of ASWWTP under space constraints

As described in [105], the aeration and sedimentation tanks are arranged vertically and compactly to address space constraints. This design places high demands on the accuracy of the control system. According to [98], the sewage purification components are modularized, with their functions segmented and partitioned to minimize the plant's footprint, although this structure results in higher maintenance costs. As described in [99], integrating multiple functions into a single unit further reduces the plant's footprint, but it inhibits microorganism growth due to numerous coupling effects between microbial growth and biochemical reactions.

In low-flow sewage systems, small biochemical reaction tanks are used to solve the limitations of small areas. However, it has the disadvantage of extending the purification time. A decentralized mass structure is used to solve the limitation of small amounts of sewage and effective area. In addition, an adaptive control system is used to adjust the dissolved oxygen concentration to reduce energy consumption without affecting the purification efficiency, which will be discussed in detail in Chapter 3.

2.7.2 Design of small-space ASWWTP for low-volume wastewater treatment

As mentioned in [152], compact wastewater purification equipment can greatly reduce the use of pipelines, thus solving the problem of unnecessary energy consumption in the dissolved oxygen transfer process. However, this method leads to long purification times and low purification efficiency. As discussed in [153], the use of internal circulation in biochemical reactions can solve the problem of reducing the residence time of the mixed liquid in the sedimentation tank, but this method will lead to extremely complex control system design, increase sewage purification time, and increase maintenance costs. When treating small-flow sewage, the control system requires higher accuracy; otherwise, a lot of energy will be wasted to produce oxygen. Therefore, designing an efficient and stable control system is a challenge.

Multiple biochemical reaction tanks and two-layer control systems are used to meet the limitations of construction space and flow. The concentration of dissolved oxygen is dynamically adjusted to achieve an efficient and stable sewage purification process, which is described in detail in Chapter 4.

2.7.3 Design of small-space ASWWTP for high-volume wastewater treatment

As discussed [97], a vertical multi-layer sewage treatment plant structure was designed to solve the space limitations of the sewage treatment plant. Due to the complex, time-

varying biochemical reactions, the sewage purification efficiency is low. As discussed in [135], the integrated building structure is designed to solve the limitation of small space and large sewage flow in sewage treatment plants. However, its excessive energy consumption is unacceptable. Although the intelligent control system can realize the efficient purification process of large-flow sewage, this type of structure cannot respond quickly to sudden large load fluctuations.

In cases of limited space and high sewage volume, the simple use of advanced purification device structures alone cannot achieve an efficient and stable purification process. It is also necessary to design a highly intelligent control system to adjust the dissolved oxygen concentration. In addition, the dissolved oxygen control system must have a fast response speed, be real-time adjustable, and have strong robustness. which is studied in detail in Chapter 5.

2.8 Summary

This chapter introduces the history, principles, types, limitations and challenges of activated sludge wastewater purification. It also introduces the key components of wastewater treatment plants, such as air supply, biological reaction， and sedimentation units. It focuses on the metabolic process of organic microorganisms and the series of chemical reactions involved in the wastewater purification process.

The challenges in building a mathematical model for the ASWWTP are introduced, such as the process of nutrient removal and the importance of oxygen in the purification process. The importance of the dissolved oxygen control system on the sewage purification rate and energy consumption is also explained. Finally, solutions to the constraints of building an activated sludge sewage purification plant and the dissolved oxygen control system are proposed, which are described in detail in Sections 3, 4，and 5.

CHAPTER 3 Direct Model Reference Adaptive Control of Nutrient Removal at ASWWTP

An architecture of ASWWTP was established to address the need for small-scale sewage purification while reducing construction space and maintenance costs. According to this structure, a direct model reference adaptive control system is designed based on the limited parameters of the ASWWTP to achieve stable and efficient nutrient removal under its global parameters mathematical model. The operating conditions of the air supply system are assumed to be ideal. The mathematical model of ASWWTP is implemented by rewriting ASM 2d based on mass balance principles. The stability of the DMRAC is proven through the Lyapunov function. In addition, MATLAB simulations based on real data records demonstrated that the system was able to operate efficiently and stably while being able to resist disturbances.

3.1 Introduction

According to the previous introduction, the concentration of dissolved oxygen during the operation of ASWWTP can determine its operating efficiency and purification rate. In this chapter, we are developing the DMRAC system based on limited mathematical model parameters and applying it to the mathematical model of global parameters. To

achieve high efficiency of nutrient removal, therefore achieving a stable, effective, and disturbance-resistant wastewater purification process.

The structure design of ASWWTP can efficiently purify small-scale wastewater while minimizing constructed space and maintenance costs. It consists of three treatment units: 1) the wastewater collection unit, which is used for collecting wastewater and performing preliminary filtering; 2) the biological purification unit, which utilizes oxygen to convert the organic matter into harmless substances through degradation; and 3) the primary sedimentation unit, which separates sludge and clear water. This chapter focuses on the growth and degradation processes within the microorganisms in units 2 and 3, as illtreated in Figure 3-1. The wastewater collection treatment unit can be neglected due to its single function and lack of involvement in biochemical reactions for wastewater purification.

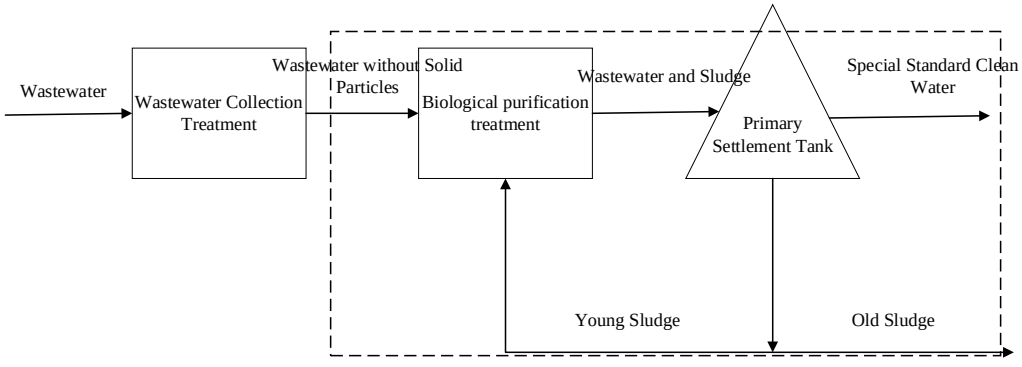

Figure 3- 1 The architecture of the ASWWTP

The ASWWTP operation involves multiple treatment units working together. Therefore, the ASWWTP operation control system involves multiple-layers control systems. The upper layer control system is delivering the wastewater into a bioreaction tank from the first collecting tank. Simultaneously, the lower layer control system provides predictions of the amount of air required for a series of biochemical reactions that vary over time. subsequently, the wastewater delivers into the primary settlement tank,

3.2 Nutrients removal processes

Wastewater flows into the biological reaction tank from the wastewater collection treatment unit, and air is introduced into the biological reaction tank by a blower, which is responsible for generating and delivering air. In addition, young sludge flows back from the settling back to the biological reaction tank. When wastewater, young sludge, and air flow into the bioreaction tank simultaneously, organic microorganisms are fed by oxygen and undergo a series of biochemical reactions to effectively purify the wastewater. These biochemical reactions include microbially adsorbed suspended solids, oxidation of organic matter, and oxygen replacement [154]. The ASWWTP operation involves two-hierarchical DO concentration control structures. The two-hierarchical control system aims to ensure the DO concentration trajectory ($DO(t)$) in the bioreaction tank tacks the reference DO concentration trajectory ($DO^{ref}(t)$), based

on the airflow ($Q_{air}(t)$) provided in the lower layer, as described in [155]. The lower layer control system, through the blower actuator, provides $Q_{air}(t)$ to optimally control the $DO(t)$ to track the $DO^{ref}(t)$. The $DO^{ref}(t)$ of the upper control is derived from the pre-calculating set-points reference airflow ($Q_{air}^{ref}(t)$). The $Q_{air}^{ref}(t)$ is determined by the inflowing wastewater and young sludge.

In our study, we focused on calculating the blower actuator's airflow to ensure that the trajectory of the DO concentration trajectory tracks the reference DO concentration trajectory in the bioreaction tank. The reference airflow is regulated by the upper layer control system in an overall medium-level control structure [113]. The blower actuator is the control input in the lower layer control system. The DO concentration trajectory is discussed in [113], and it is part of the lower layer control system. In this chapter, we utilized DMRAC as the lower layer control system. This controller algorithm is derived from the DMRAC method [156]. Finally, the mixing wastewater flows into the settlement tank, as illustrated in Figure 3-2.

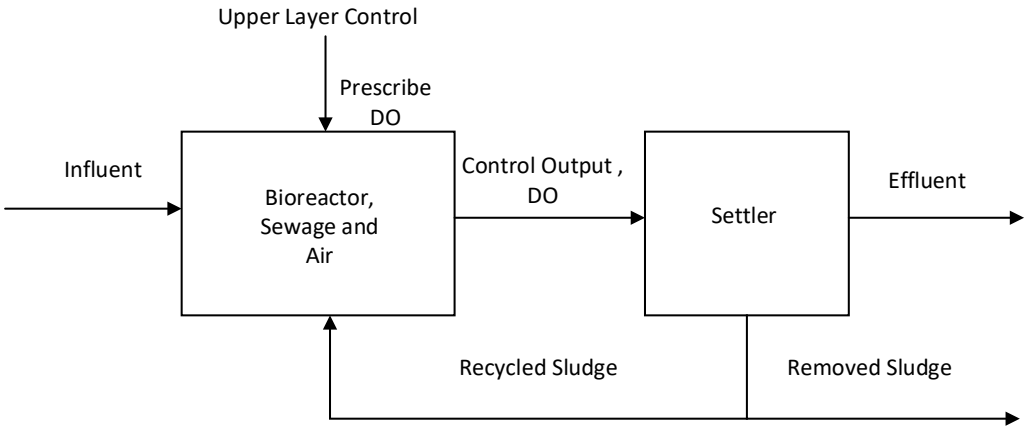

Figure 3- 2 The architecture of ASWWTP for nutrient removal

The settlement tank uses gravity to separate sludge and clean water; this process may take hours or days, as discussed in [34]. The clean water flows out of pipes, waiting for use; if there are special discharge requirements, wastewater must undergo secondary sedimentation in tertiary wastewater treatment [107]. Solid particles and flocs settle to the bottom of the sedimentation tank by gravity, and the sludge at the bottom is divided into aged sludge and new sludge. New sludge flows back to the biochemical reactor to wait for the purification of activated sludge again. Aged sludge is discharged directly or discharged after being concentrated again according to the discharge standards. The organic matter in the young sludge assists microorganisms in ongoing degradation [179]. In this chapter, we assume that the settler is in an ideal state and, therefore, does not require stirring, in contrast to the approach presented in [180], as illustrated in Figure 3-3.

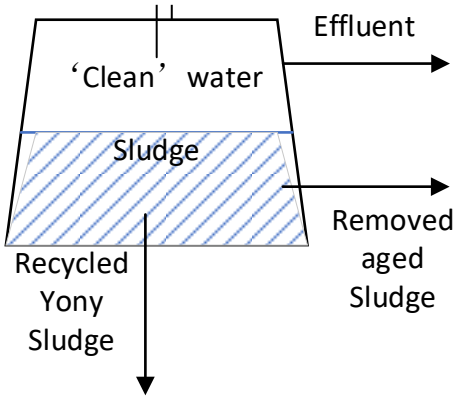

Figure 3- 3 The settlement tank processes

At the biochemical reaction tank, a serial biochemical reaction occurs, involving oxygen consumption [43]. Therefore, following the mass balance principle, we can write an oxygen balance equation to describe the inflow and outflow matter from the bioreaction tank.

In this chapter, we consider the amount of oxygen required to achieve optimal biochemical reactions on the left-hand side of the equation. unlike [11, 160].

3.3 Control problem statement

The state variables in the ASWWTP process cannot be directly detected and measured. A mathematical model that accurately describes the ASWWTP process is established to achieve precise real-time evaluation of purification system parameters in the DO control system and to predict future parameter changes during the estimation process. The mathematical model of ASWWTP describes the biological reaction process,

chemical reaction process, purification system state variable, and the rate of microorganism growth and chemical reaction rates [181].

The architecture of ASWWTP is shown in Figure 3-2. The mathematical model of the ASWWTP can be derived by rewriting ASM 2d based on the mass balance principle. The state-space model, introduced in [182], can be written as follows:

$$\frac{dX}{dt} = \mu(t)X(t) - D(t)(1+r)X + rD(t)X_r(t) \tag{3.3-1}$$

$$\frac{dS}{dt} = -\frac{\mu(t)X(t)}{Y} - D(t)(1+r)S(t) + D(t)S_{in}(t) \tag{3.3-2}$$

$$\begin{aligned}\frac{dDO}{dt} = &-\frac{K_0\mu(t)X(t)}{Y} - D(t)(1+r)DO(t) \\ &+ K_{L\alpha}(Q_{air}(t))(DO_{\max} - DO(t)) + D(t)DO_{in}(t)\end{aligned} \tag{3.3-3}$$

$$\frac{dX_r}{dt} = D(t)(1+r)X(t) - D(t)(\beta+r)X_r(t) \tag{3.3-4}$$

$$\mu(t) = \mu_{\max}\frac{S(t)}{K_s + S(t)}\frac{DO(t)}{K_{DO} + DO(t)} \tag{3.3-5}$$

where

$$D(t) = \frac{Q_{in}}{V_a},\ r = \frac{Q_r}{Q_{in}},\ \beta = \frac{Q_W}{Q_{in}} \tag{3.3-6}$$

$X(t)$, $S(t)$, $DO_{\max}$, $X_r(t)$, $D(t)$, $S_{in}(t)$, $DO_{in}(t)$, Y, $\mu(t)$, $\mu_{\max}$, K_s, K_{DO}, $Q_{air}(t)$, K_0, r, β, $Q_{in}(t)$, $Q_{out}(t)$, $Q_r(t)$, $Q_w(t)$, V_a are biomass concentration, substrate concentration, maximum dissolved oxygen concentration, recycled biomass

concentration, dilution rate, substrate concentration in the influent, dissolved oxygen concentration in the influent, biomass yield factor, biomass growth rate, maximum specific growth rate, affinity constant, saturation constant, aeration rate, model constant, recycled sludge rate, removed sludge rate, influent flow rate, effluent flow rate, recycled flow rate, waste flow rate and aerator volume.

The oxygen transfer function (OTF) $k_{La}(Q_{air}(t))$, presented in equation (3.3-3), is known to be nonlinear. The operation of the blower and the dissolved oxygen consumption by microorganisms over time contribute to this nonlinearity [105]. Under these conditions, the OTF can be written as follows:

$$k_{La}(t) = \alpha Q_{air}(t) + \delta \tag{3.3-7}$$

Where: α and δ are known constants for the oxygen transfer function.

We only considered accurate output DO as control output. Therefore, ASM 3 is not appropriate for describing this ASWWTP process, as it is modelled for specific treatment environments [157]. However, ASM 1 has been found to have limitations in adjusting the ASWWTP‘s parameter, as demonstrated in [158]. Furthermore, ASM 2 has demonstrated low accuracy due to its one-dimensional nature; it is unable to consider both time and space, as described in [159].

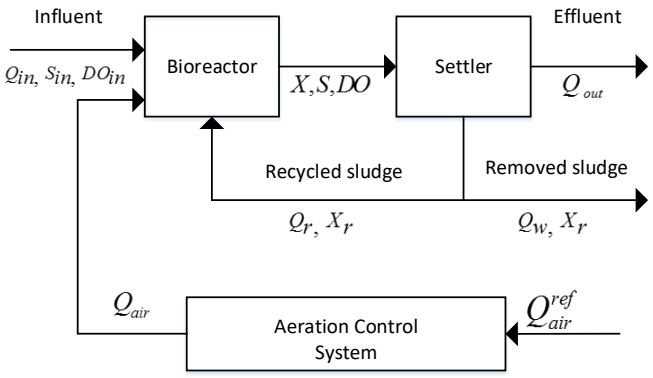

Figure 3- 4 The architecture of ASWWTP with airflow actuator

The architecture of the ASWWTP with a blower is depicted in Figure 3-4, where the blower is used for producing oxygen. The time scale of the blower operation differs from that of the bioreactor operation. The blower actuator state belongs to the lower layer control system and determines the airflow ($Q_{air}(t)$), while the bioreactor belongs to the upper layer control system and reference airflow ($Q_{air}^{ref}(t)$) [20]. Additionally, the state variables of the ASWWTP are on different time scales; it has been discussed in Chapter 2.4 and in [160].

However, the design of the blower control system has been detailed in [36]. In this chapter, we ignore the discussion of the blower controller design. It is assumed that the ideal blower operation exists; hence, the blower control output is equal to the reference airflow, $Q_{air}^{ref}(t) = Q_{air}(t)$, it has demonstrated in [83]. The ASWWTP disturbance inputs include influent flow rate Q_{in}, substrate concentration S_{in}, and dissolved oxygen concentration in the fluent DO_{in}. Moreover, those disturbance inputs are time varying,

and the control output is DO concentration. The structure of the DO control system, assuming the existence of an ideal DO concentration sensor as shown in Figure 3-5, employs the DMRAC system to estimate the ideal DO concentration sensor using adaptive control laws. Therefore, respiration does not need to be estimated. This represents a different control method compared to that described in [83]. Our aim is to design a DMRAC control system where the output trajectory $DO(t)$ can quickly and accurately follow the reference DO ($DO^{ref}(t)$) trajectory, while also maintaining robust performance against interference.

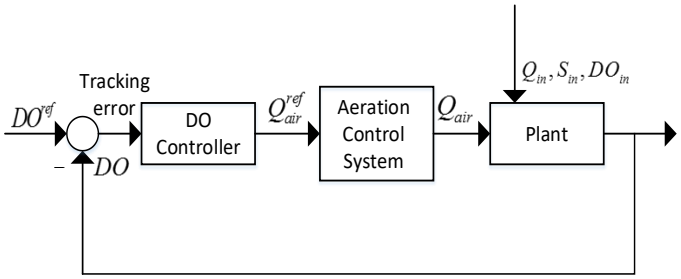

Figure 3- 5 The architecture of ASWWTP with aeration

The equations (3.3-1), (3.3-2), (3.3-3), (3.3-4), and (3.3-5) represent the ASWWTP dynamics. It is characterized as a fourth-order nonlinear complex system with different time-scale dynamics models. The PI control system is unsuitable for implementation on a full range of process conditions, due to its uncertainty and varying. Moreover, it exhibits lower response times and large error dynamics [63]. Furthermore, being a

linear control system, it is unsuitable for this nonlinear ASWWTP system. As discussed in [3], the application of the MPC control system on the ASM 2d is extremely complex. This complexity arises from the ASM 2d being a two-dimensional mathematical model, which necessitates calculations at multiple points across both time and spatial dimensional [124]. Considering the features of the ASM 2d model, although it focuses on a single unit (bioreaction tank), it still involves multiple inputs existing that interact and must be considered together. Therefore, fuzzy logic control is unsuitable for this plant [113].

In this chapter, adaptive control is considered, which is different from the previous [12]. The design of the DMRAC is based on the SISO model of dissolved oxygen dynamics in equation 3.4-1, achieved through a reasonable arrangement of the state space model equations (3.3-1), (3.3-2), (3.3-3), and (3.3-4). The mathematical model of the ASWWTP has unmeasured state variables related to air quantity. We integrated those state variables into one term, which is respiration. The adaptive controller estimates the respiration rate, and it is updated by the adaptive control laws, which are set indirectly and automatically [83].

Subsequently, design and implement a direct model reference adaptive control that applies to DO concentration dynamics at ASWWTP. Following implementation, validate the stability of the controller through simulation results and the application of a Lyapunov function.

3.4 Dissolved oxygen controller design

The state space equation of the ASWWTP system has been described by equations (3.3-1) … (3.3-4) and (3.3-5) in the previous section and contains highly nonlinear and unknown system state variables. While system state variables such as $X_r(t)$, $X(t)$, and $S(t)$ are remain unmeasurable, other parameters such as $Q_{in}(t)$ and $Q_w(t)$ can be detected online. In addition, the dissolved oxygen dynamic model is formulated as a first-order SISO system. The dissolved oxygen dynamic trajectory is influenced by both state variables and disturbances. The stability and effectiveness of the DO dynamic controller depend on the global state parameters and disturbances of the wastewater purification process. The mathematical ASM 2d model of ASWWTP is relatively accurate compared to other models [161]. However, in the wastewater purification system, there are uncertain disturbance inputs and unpredictable system state variables. Therefore, the first order of the SISO DO dynamic equation is the basis for adaptive controller design. According to the online update characteristics of the adaptive control system, it can exploit robustness to handle these unknown system state variables and unknown disturbances.

The DMRAC structure is represented in Figure 3-6.

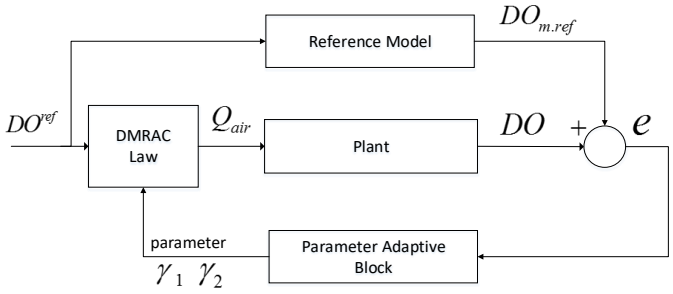

Figure 3- 6 The structure of direct model reference adaptive control

Starting with equation (3.3-3), the SISO model for DO concentration is constructed by substituting $\mu(t)$ (3.3-7) with equation (3.3-5). The DMRAC design is based on the equation (3.4-1). The resulting input-output model is presented below:

$$\begin{aligned}\frac{dDO}{dt} &= -D(t)(1+r)DO(t) - \frac{K_0 X(t)}{Y}\mu(t) \\ &\quad + (\alpha Q_{air}(t) + \delta)(DO_{\max} - DO(t)) + D(t)DO_{in}(t)\end{aligned} \tag{3.4-1}$$

The fourth term in equation (3.4-1) represents the slowly varying component, indicating that the inflow rate of DO in the wastewater entering the biological reactor changes gradually. Consequently, the magnitude of the fourth term $D(t)DO_{in}(t)$ becomes extremely small and can be neglected. As a result, the SISO model for DO concentration is reformulated, and input is Qair (t) and output is DO(t), as follows:

$$\begin{aligned}\frac{dDO}{dt} &= -a_p(t)DO(t) - c_p(t)\,f(DO(t)) \\ &\quad + b_p(t)Q_{air}(t) + d_p\end{aligned} \tag{3.4-2}$$

Where: $a_p(t), c_p(t), b_p(t)$ and d_p are the model parameters and

$$
\begin{aligned}
a_p(t) &= \frac{Q_w(1+r)}{\beta V_a} \\
c_p(t) &= \frac{K_0 X(t)}{Y} \frac{\mu_{\max} S(t)}{(K_s + S(t))} \\
f(DO(t)) &= \frac{DO(t)}{(K_{DO} + DO(t))} \\
b_p(t) &= \alpha(DO_{\max} - DO(t)) \\
d_p &= \beta DO_{\max}
\end{aligned}
\tag{3.4-3}
$$

The parameter d_p consists of β and $DO_{\max}$, both of which are known and exhibit slowly variations over time. Additionally, $X(t)$ and $S(t)$ represent internal dynamic biological state variables. When compared to the components of $DO(t)$ [19, 115], these parameters are varying slowly. Hence, the parameter $c_p(t)$ is both slow-varying and unknown. The time scale associated with variables $Q_r(t)$ and $Q_w(t)$ are dependent on the upper layer control. In comparison to the time scale of $DO(t)$, these time scales are slow. The variables recycled flow rate ($Q_r(t)$) and waste flow rate ($Q_w(t)$) are associated with the operation time of the upper layer control system, and their time scales are the same as the time scales of disturbance inputs $Q_{in}(t)$, $S_{in}(t)$, and $DO_{in}(t)$. Moreover, the internal state variable DO has a faster time scale compared to the variables recycle flow rate and waste flow rate. Therefore, the parameter $a_p(t)$ can be deemed a rapidly fluctuating yet known variable, as discussed in [124] and [160]. Finally, the parameter $b_p(t)$ is dependent on $DO(t)$ and $DO_{\max}$, however, they have the same time scale, as indicated by equation (3.4-3). Because the known oxygen

transfer constant, parameter $b_p(t)$ can be classified as a rapidly fluctuating and known variable.

In the closed-loop to achieve the control output $DO(t)$ trajectory fast and stable tracks the prescribed DO reference dynamics ($DO_{m.ref}(t)$). The reference DO trajectory is derived from the reference air set by upper layer control [113]. The model reference dynamics ($DO_{m.ref}(t)$) (MRD) equation can be written as:

$$\frac{dDO_{m.ref}}{dt} = -a_m DO_{m.ref}(t) + b_m DO^{ref}(t) \tag{3.4-4}$$

Where: $DO_{m.ref}(t)$ defines the model reference dynamic output $DO(t)$, and model reference parameters a_m and b_m are defined as constants determined by designer. Hence, $a_m = b_m$.

As mentioned in [44], the expanded model reference adaptive control laws can be written as follows.

$$\begin{aligned} Q_{air}(t) = {} & a_{DO}(t)DO(t) + a_f(t)\, f(DO(t)) \\ & + a_{DO^{ref}}(t)DO^{ref}(t) - \frac{\beta DO_{\max}}{b_p(t)} \end{aligned} \tag{3.4-5}$$

The equation (3.4-4), which represents the model reference dynamic (MRD), is linear. Additionally, in equation (3.4-5), the second and fourth terms can asymptotically cancel the effects of the nonlinear term and the additional term in (3.4-2) in a closed loop, respectively.

The parameters of the direct model reference adaptive control law (DMRACL) are denoted as $a_{DO}(t)$, $a_f(t)$, and $a_{DO^{ref}}(t)$. When the MRD is in a closed loop, We assume that ideal parameters exist. The close-loop DMRAC control equation (3.4-1) is achieved by using equation (3.4-5), which leads to the derivation of equation (3.4-6):

$$\begin{aligned}\frac{dDO}{dt} &= -(a_p(t) - b_p(t)a_{DO}(t))DO(t) \\ &\quad -(c_p(t) - b_p(t)a_f(t))f(DO(t)) \\ &\quad + b_p(t)a_{DO^{ref}}(t)DO^{ref}(t)\end{aligned} \tag{3.4-6}$$

and

$$\begin{aligned}-(a_p(t) - b_p(t))\hat{a}_{DO}(t)) &= -a_m \\ -(c_p(t) - b_p(t)\hat{a}_f(t)) &= 0 \\ b_p(t)\hat{a}_{DO^{ref}}(t) &= b_m\end{aligned} \tag{3.4-7}$$

The ideal parameter can be derived by rewriting equation (3.4-7), resulting in:

$$\hat{a}_{DO}(t) = \frac{-a_m + a_p(t)}{b_p(t)}$$

$$\hat{a}_f(t) = \frac{c_p(t)}{b_p(t)} \tag{3.4-8}$$

$$\hat{a}_{DO^{ref}}(t) = \frac{b_m}{b_p(t)}$$

Since the values of b_m and $b_p(t)$ are known, $\hat{a}_{DO^{ref}}(t)$ can be determined online using available data. The model reference adaptive control law can thus be reformulated as follows:

$$\begin{aligned} Q_{air}(t) = {} & a_{DO}(t)DO(t) + a_f(t)\,f(DO(t)) \\ & + \frac{b_m}{b_p(t)} DO^{ref}(t) - \frac{\delta DO_{\max}}{b_p(t)} \end{aligned} \tag{3.4-9}$$

Unlike the [156], the MRAC control law does not include the adaptive control parameter $a_{DO^{ref}}(t)$. The corresponding closed-loop SISO dynamic $DO(t)$ by equation (3.4-9) can be rewritten as:

$$\begin{aligned} \frac{dDO}{dt} = {} & -(a_p(t) - b_p(t)a_{DO}(t))DO(t) \\ & -(c_p(t) - b_p(t)a_f(t))\,f(DO(t)) \\ & + b_p(t)\frac{b_m}{b_p(t)} DO^{ref}(t) \end{aligned} \tag{3.4-10}$$

The parameters $a_{DO}(t)$ and $a_f(t)$ in equation (3.4-8) can be determined on-line using parameter adaptive laws. However, system parameters $a_p(t)$ and $c_p(t)$ remain

unknown. Using parameter adaptive laws to calculate $a_{DO}(t)$ and $a_f(t)$ necessitates knowing the error dynamics between the $DO(t)$ dynamic and the $DO_{m.ref}(t)$. The dynamic of the error equation is presented below.

$$e(t) = DO(t) - DO_{m.ref}(t) \tag{3.4-11}$$

As discussed in [162], the parameter adaptive law that ensues the stability of the adaptive control system is derived. The adaptive control system is applied to the SISO dynamic system. This first-order dynamic system includes uncertain time-varying constants, nonlinear additive structure, and known parameters. By applying these parameter adaptive laws to equation (3.4-1), the parameter adaptive of DMRAC applied to the ASWWTP system can be obtained as follows:

$$\frac{da_{DO}}{dt} = -\gamma_1 e(t) DO(t) \tag{3.4-12}$$

$$\frac{da_f}{dt} = -\gamma_2 e(t) f(DO(t)) \tag{3.4-13}$$

In equations (3.4-12) and (3.4-13), γ_1 and γ_2 represent adaptive gains parameters, both of which are small positive constants. These parameters can be used to adjust the rate of adaptive control. By adjusting these gains, the adaptive rate can be changed to rapidly respond to parameter changes during the operation of the ASWWTP. Therefore, the

adaptive rate must be coordinated with the rate of change of the ASWWTP parameters to ensure the stability of the closed-loop system.

3.5 Stability analysis

The on-line updates for estimated parameters $a_{DO}(t)$ and $a_f(t)$ are provided by the parameter adaptive laws. as shown in equations (3.4-12) and (3.4-13). Hence, the difference between the ideal adaptive law parameters and the estimated adaptive law parameters is represented by $\Delta a_{DO}(t)$ and $\Delta a_f(t)$, respectively.

$$\Delta a_{DO}(t) = a_{DO}(t) - \hat{a}_{DO}(t) \tag{3.5-1}$$

$$\Delta a_f(t) = a_f(t) - \hat{a}_f(t) \tag{3.5-2}$$

The Lyapunov function is employed in the stability analysis of DMRAC. The Lyapunov function utilized in this analysis is presented below；

$$V(t) = \frac{1}{2}e^2(t) + \frac{1}{2}\Delta a_{DO}{}^2(t) + \frac{1}{2}\Delta a_f{}^2(t) \tag{3.5-3}$$

The equation (3.5-3) can be expanded as follows:

$$\begin{aligned}\frac{dV(t)}{dt} = {} & e(t)\dot{e}(t) + (a_{DO}(t) - \hat{a}_{DO}(t))(\dot{a}_{DO}(t) - \dot{\hat{a}}_{DO}(t))\frac{1}{\gamma_1} \\ & + (a_f(t) - \hat{a}_f(t))(\dot{a}_f(t) - \dot{\hat{a}}_f(t))\end{aligned} \tag{3.5-4}$$

The real dynamic $DO(t)$ in equation (3.4-1) and the model reference $DO^{ref}(t)$ in equation (3.4-10) are both substituted into equation (3.4-11) to derive the error dynamics.

$$\begin{aligned}\dot{e}(t) = &-(a_p(t) - b_p(t)a_{DO}(t))DO(t) \\ &-(c_p(t) - b_p(t)a_f(t)f(DO(t)) \\ &+a_m DO_{m.ref}(t)\end{aligned} \tag{3.5-5}$$

Additionally, the term $a_m DO(t)$ is added and subtracted on the right-hand side of equation (3.5-5) of the Lyapunov function as follows:

$$\begin{aligned}\dot{e}(t) = &-a_m e(t) - ((a_p(t) - b_p(t)a_{DO}(t)) - a_m)DO(t) \\ &-(c_p(t) - b_p(t)a_f(t))f(DO(t))\end{aligned} \tag{3.5-6}$$

By substituting equations (3.4-10) and (3.4-11) into equation (3.5-4) can be expressed as:

$$\begin{aligned}\dot{e}(t) = &-a_m e(t) + (a_{DO}(t) - \hat{a}_{DO}(t))b_p(t)DO(t) \\ &+(a_f(t) - \hat{a}_f(t))b_p(t)f(DO(t))\end{aligned} \tag{3.5-7}$$

By substituting equations (3.5-7), (3.4-12), and (3.4-13) into equation (3.5-4), it can be expressed as:

$$\begin{aligned}\frac{dV(t)}{dt} = &-a_m e^2(t) \\ &+(a_{DO}(t) - \hat{a}_{DO}(t))[e(t)b_p(t)DO(t) - e(t)DO(t) - \dot{\hat{a}}_{DO}(t)\frac{1}{\gamma_1}] \\ &+(a_f(t) - \hat{a}_f(t))[e(t)b_p(t)f(DO(t)) - e(t)f(DO(t)) - \dot{\hat{a}}_f(t)\frac{1}{\gamma_2}]\end{aligned} \tag{3.5-8}$$

A quadratic function of the squared error constitutes the right-hand side of equation (3.5-8). From the equation (3.5-8), it can be easily determined that the $e(t)^2$ is positive and the $-a_m < 0$. Therefore, the first term of the equation (3.5-8) is negative. Hence, the left-hand side of the equation (3.5-8) is negative for $\frac{dV(t)}{dt} < 0$ to hold. The derivation is in Appendix A. By squaring equation (3.5-8), it is easily illustrated that $\frac{d^2V(t)}{dt}$ is bounded.

Perform a stability analysis of the Lyapunov function result using Barbalat's lemma.

If the dynamics of the plant's initial conditions and equations (3.4-12), (3.4-13) approach the equilibrium point, and the parameter adaptive rates γ_1 and γ_2 are chosen to be sufficiently small, then.

1) The parameter adaptive rates are bounded by the model reference adaptive control law.

2) Hence, the output $DO(t)$ of the direct model reference adaptive control can achieve asymptotic tracking of the model reference $DO^{ref}(t)$, and the ideal parameters $\hat{a}_{DO}(t)$ and $\hat{a}_f(t)$ remain bounded.

3)The parameters $a_{DO}(t)$ and $a_f(t)$ of the parameter adaptive laws are bound by the squared error dynamics.

The stability analysis, employing the Lyapunov function and Barbalat's lemma, easily proves that DMRAC is stable. MATLAB simulation results demonstrate that the stability of DMRAC is bounded by estimates of the model reference and adaptive gain.

3.6 Simulation results and discussion

This section presents the simulation results of DMRAC applied to the ASWWTP to control the dissolved oxygen dynamic. These results verify the stability and robustness of the DMRAC system using real data records [161].

The initial plant state parameters are: $X(0)=15mg/l$, $S(0)=200mg/l$, $DO(0)=3mg/l$, $X_r(0)=18mg/l$, $DO_{\max}=10mg/l$, $S_{in}(0)=600mg/l$, $D(0)=3$, $DO_{in}(0)=0.5mg/l$. The plant process constant parameters are $\alpha=3.34m^{-3}$, $\delta=3.54h^{-1}$, K_0=0.5. The kinetic parameters are: $\mu_{\max}=0.15mg/l$, $K_s=100mg/l$, K_{DO}=$2mg/l$. The plant disturbance inputs are piecewise variable, as illustrated in Figure 3-7, 3-8 and 3-9.

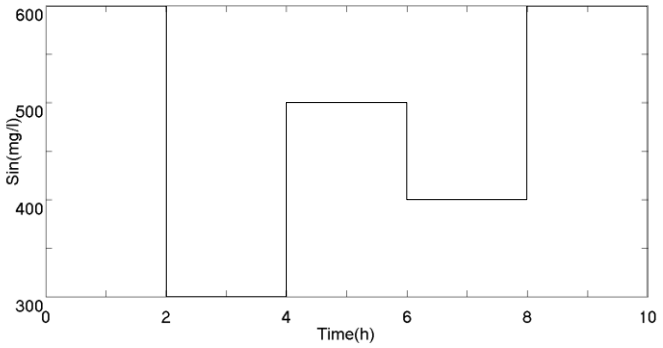

Figure 3- 7 Influence substrate $S_{in}(t)$

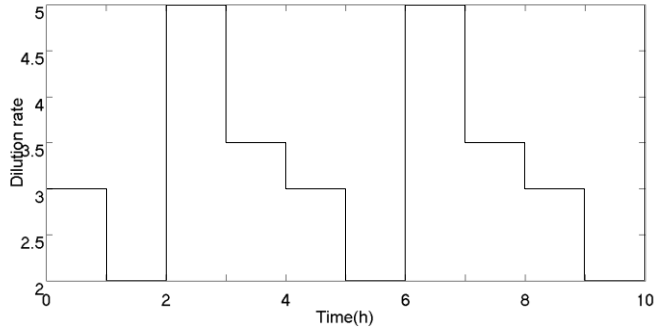

Figure 3- 8 Dilution rate $D(t)$

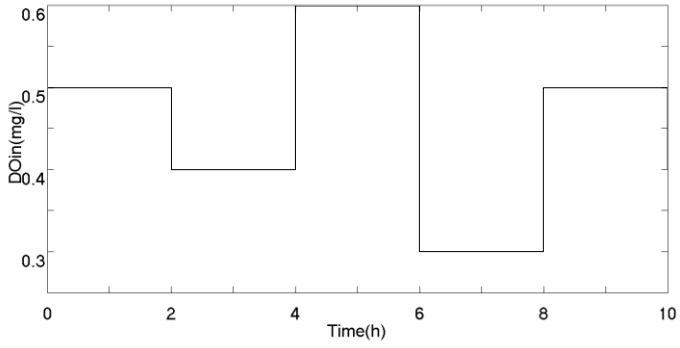

Figure 3- 9 Influent dissolved oxygen $DO_{in}(t)$

The model reference parameters were $a_m = 30$ and $b_m = 30$. The ASWWTP mathematical model of global variables uses the ASM 2d. The model reference for

dissolved oxygen $DO^{ref}(t)$ was taken piecewise constant. The results show that controlling the output DO concentration trajectory under the slow adaptive rates yields good tracking performance and stability, as demonstrated in Figure 3-10. Figure 3-11 shows that under the slow adaptive rate, the control output DO concentration trajectory effectively suppresses the disturbance input and has good stability and tracking performance.

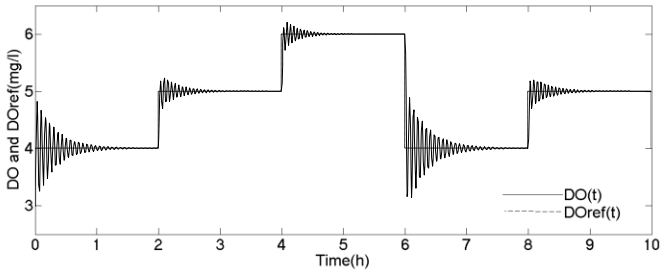

Figure 3- 10 The dynamics trajectories of $DO(t)$ and $DO^{ref}(t)$ under conditions of no disturbance inputs and slow adaptive rates $\gamma_1 = 0.5$, $\gamma_2 = 0.5$.

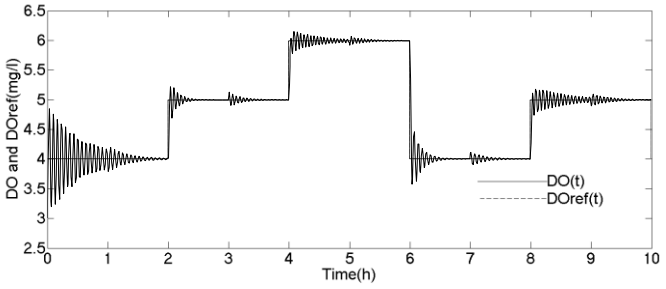

Figure 3- 11 The dynamics trajectories of $DO(t)$ and $DO^{ref}(t)$ under conditions of disturbance inputs and slow adaptive rates $\gamma_1 = 0.5$, $\gamma_2 = 0.5$.

The same initial conditions as in Figure 3-11 are used in Figure 3-12. and it uses some piecewise constant model reference, but the adaptive rates are faster than before, as indicated by $\gamma_1 = 5$, $\gamma_2 = 5$. The dissolved oxygen response tracking trajectory depicted in Figure 3-12 is unstable. The utilization of high adaptive rates reduces robustness and causes the adaptive parameters $a_{DO}(t)$, $a_f(t)$ to become unconstrained by the error dynamics. Consequently, the DMRAC output ($DO(t)$) trajectory is unable to rapidly and stably track the reference ($DO^{ref}(t)$)trajectory.

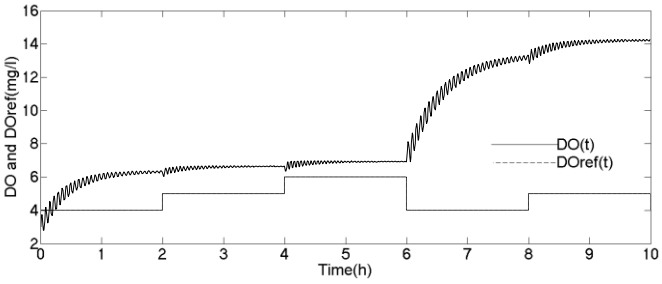

Figure 3- 12 Unstable $DO(t)$ response with fast adaption rates $\gamma_1 = 5$, $\gamma_2 = 5$, and without disturbance inputs

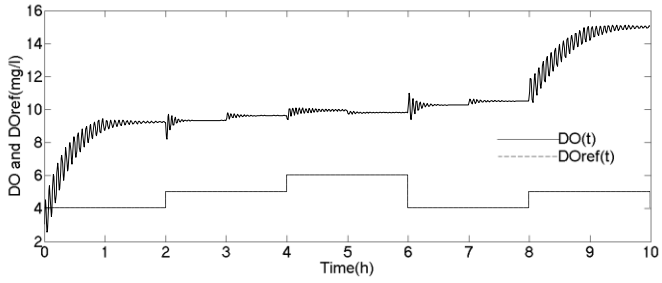

Figure 3- 13 Unstable $DO(t)$ response with fast adaption rates $\gamma_1 = 5$, $\gamma_2 = 5$, and with large disturbance inputs

Figure 3-13 uses the same initial condition and model reference as Figure 3-11, but with large disturbance inputs. The results clearly indicate that the closed-loop adaptive control system becomes unstable under such conditions. This instability is caused by the large unknown disturbance input and the excessive gain scheduling, leading to an unstable response of the adaptive control system.

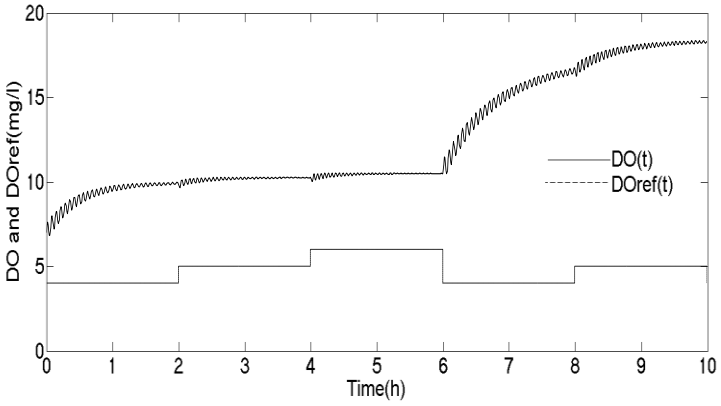

Figure 3- 14 The initial conditions of the ASWWTP are significantly distant from the equilibrium point, and the dynamics of $DO(t)$ fail to track the trajectory of $DO^{ref}(t)$, thus rendering the system unstable under conditions characterized by the absence of perturbation input and slow adaptive rates $\gamma_1 = 0.5$, $\gamma_2 = 0.5$

The initial conditions of the ASWWTP are deliberately selected to be distant from the anticipated equilibrium point. The initial plant conditions are $X(0) = 30mg/l$, $S(0) = 960mg/l$, $X_r(0) = 7mg/l$, $DO(0) = 7mg/l$. Results indicate that, despite employing slow adaptive rates, the $DO(t)$ dynamic tracking trajectory performance of the control system output is unstable. This instability arises due to the excessively long convergence time of the adaptive control system and the time delay in the dynamics

response of the purification system. Therefore, the parameters of the adaptive control system are deemed invalid, as depicted in Figure 3-14. The simulation results validate the stability analysis presented in Chapter 3.5.

3.7 Conclusions

According to the requirements of small wastewater treatment volume and small available space, a new architecture of ASWWTP is designed, which consists of a bioreactor unit, a blower, and a sedimentation unit. The mathematical model is established by mass balance and rewriting ASM 2d. The mathematical model of the ASWWTP is based on the principle of mass balance and ion kinetic energy conservation and is formed by rewriting the ASM 2d model.

A direct model reference adaptive control system is designed to adjust dissolved oxygen concentration in the ASWWTP system, utilizing limited ASWWTP parameters and applying it to the mathematical model of global ASWWTP parameters. The adaptive control parameters are adjusted through MATLAB simulation to meet design requirements. The MATLAB simulation results demonstrate the stability and effectiveness of the ASWWTP system, also demonstrating its resilience against disturbances. Stability of the control system is further verified using a Lyapunov function.

CHAPTER 4 Direct Model Reference Adaptive Control of Nutrient Removal at ASWWTP with Blower Constraint

The architecture of the ASWWTP used in this chapter remains the same as in Chapter 3. However, we assume that the ASWWTP operates under unknown disturbances. A blower supplies excessive air into the bioreactor to facilitate the growth and degradation of microorganisms. The DMRAC with filter design is based on the limited ASWWTP mathematical model parameters and is applied to the global parameter model of the ASWWTP. This control system ensures stable and efficient operation of the ASWWTP under disturbances while filtering out excess airflow. The mathematical model of the ASWWTP is developed based on mass balance and kinetic energy conservation principles, with modifications to the ASM2d model. MATLAB simulations, using real data, were performed to verify the performance of the DMRAC system [53].

4.1 Introduction to ASWWTP operation with blower constraint

In actual wastewater purification plant operations, it is often challenging to maintain the ideal ASWWTP operating state due to unpredictable disturbances. During the ASWWTP process, the system may encounter airflow overload conditions, leading to instability, which can be caused by a sudden influx of large amounts of air or failures in dissolved oxygen sensors. In this chapter, we focus on the issue of blowers generating and transferring excess air.

As previously discussed in [193], a high concentration of DO in the bioreaction tank leads to a decrease in the degradation rate of microorganisms, a reduction in oxidative displacement rate, and the generation of oxidative by-products. Leading to the amounts of aerobic microorganisms decreasing and an increase in anaerobic microorganisms. Thus, an imbalance in microbial populations will affect the overall denitrification process. Moreover, the high DO concentration results in reduced nitrogen removal efficiency.

The design and application of DMRAC with a filter aim to address the challenge of maintaining a suitable DO concentration to achieve stable and highly efficient ASWWTP operation when the ASWWTP system operates in an air overload state. The mathematical model of the ASWWTP rewrites ASM 2d based on the mass balance

principle. Demonstrating the stability and anti-disturbance performance of DMRAC with filter through Lyapunov function analysis and MATLAB simulation.

4.2 The architecture of ASWWTP

The architecture of the ASWWTP consists of both primary and secondary wastewater treatment components. In the primary wastewater treatment unit, large pollutant particles are collected and filtered. Next, the wastewater flows into the secondary wastewater treatment unit, which includes a bioreaction tank, sedimentation tank, and blower. The blower's operating condition is crucial for the growth and degradation of microorganisms because it produces and delivers airflow into the bioreaction tank. The sedimentation tank separates the clear water from the sludge by gravity. The architecture of the ASWWTP is depicted in Figure 4-1. We consider the DO concentration trajectory, tracking the reference DO concentration trajectory in the bioreaction tank, which involves highly nonlinear dynamics.

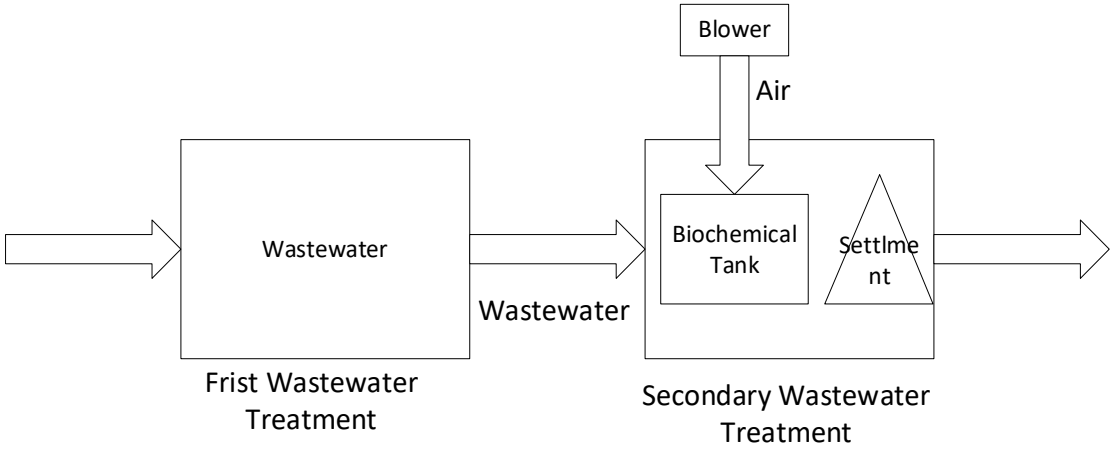

Figure 4- 1 The architecture of ASWWTP

4.3 Aeration station processes

After filtering out large particles, the wastewater flows into the bioreaction tank. In the biological reaction, wastewater, dissolved oxygen, and young sludge are mixed to initiate a biochemical process. Dissolved oxygen acts as a catalyst for microbial growth and degradation, while young sludge is maintained in the bioreaction tank to sustain the microbial population. After a series of biological reactions, the wastewater flows into the sedimentation tank, where clean water and sludge are separated by gravity. Dissolved oxygen is supplied by a blower, which serves as a control input, as shown in Figure 4-2. By adjusting the dissolved oxygen concentration, the level required for microbial growth and degradation in the bioreaction tank is achieved. Microorganisms carry out the removal process during the biochemical reaction.

As discussed in [19, 156], the purpose of the two-layer control system is adjust to DO concentration trajectory ($DO(t)$) to track the reference DO concentration trajectory ($DO^{ref}(t)$) in the bioreaction tank. The upper control system determines $DO^{ref}(t)$ based on the pre-established set-points reference airflow ($Q_{air}^{ref}(t)$). The lower layer control system output $DO(t)$ is derived from the optimized airflow ($Q_{air}(t)$) to ensure that $DO(t)$ trajectory to track $DO^{ref}(t)$ trajectory. The $Q_{air}^{ref}(t)$ is derived from the inflow of wastewater and young sludge in the biochemical reaction tank. In the blower operation with ideal conditions, the airflow equivalent to the reference airflow has been discussed in [126]. Additionally, in Chapter 3, when the output of the blower actuator matches the blower output, the DMRAC output allows the DO concentration trajectory to rapidly and stably track the reference DO concentration trajectory. Thus, the microorganisms in the biochemical reaction tank can obtain the required dissolved oxygen. The lower layer control system employing an MPC controller was demonstrated in [163]. Our study utilizes the DMRAC with a filter as the lower layer control system. This controller algorithm is based on the DMRAC method [156].

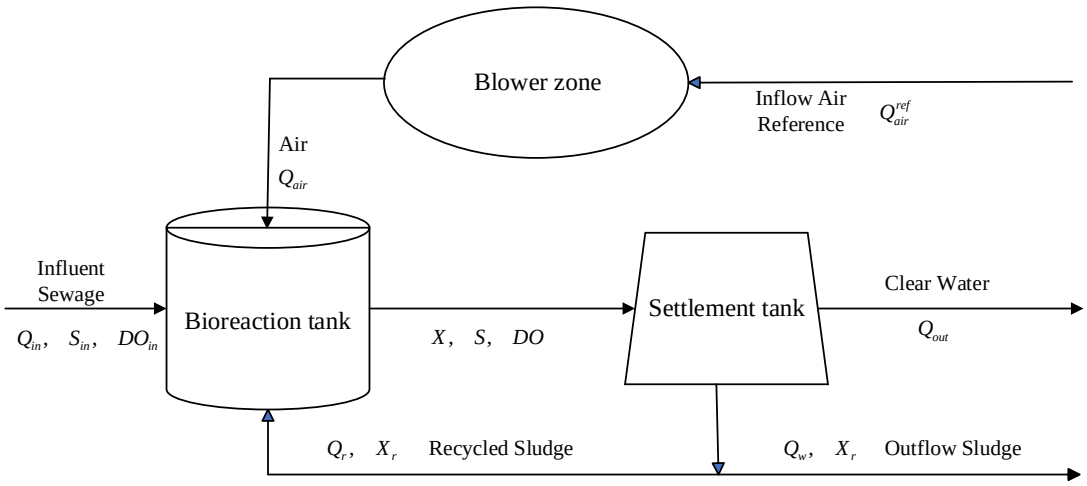

Figure 4- 2 The architecture of nutrient removal with blower

In our study, assume that the lower layer control system blower is unable to produce airflow that matches the reference airflow provided by the upper layer control system. In addition, we assume that the actual air volume exceeds the reference air volume, resulting in an excessively high DO concentration in the bioreactor. As described in the [51], high DO concentrations will reduce the degradation capacity of anaerobic microorganisms and have a negative impact on the denitrification reaction, thereby reducing the overall denitrification efficiency. On the contrary, aerobic microorganisms will settle, resulting in reduced water quality. Therefore, ensuring an appropriate DO concentration during the biochemical reaction is the focus of the control system.

4.4 Dissolved oxygen concentration problem statement

The ASWWTP mathematical model is used to study the design and operation of the ASWWTP. It was established by IWA, and those models include: ASM 1, ASM 2, ASM 2d and ASM 3 [33]. The ASM 1 employs one dimension to describe organic matter degradation, nitrification, and denitrification processes, with specific details of organic matter removal processes. Additionally, the ASM 2 is one dimension to describe the microorganism growth and degradation, specific to the phosphorous absorption and release process. Moreover, the ASM 2d is two-dimensional to describe microorganism growth and degradation, specific to the more detailed denitrification and phosphorus. Finally, the ASM 3 is two-dimension to describe all biochemical reaction processes [164].

The state variables of the ASWWTP cannot be accurately monitored by a hard sensor. These state variables involve a range of biochemical reactions occurring over time. each interdependent and simultaneous in nature. Since we focus on the DO concentration as the control output. The mathematical model of ASWWTP rewrites ASM2d and utilizes mass balance to demonstrate the ASWWTP process, as depicted in the following equation (3.3-1) … (3.3-6). Figure 4-3 illustrates the architecture of the ASWWTP for nutrient removal, incorporating a blower.

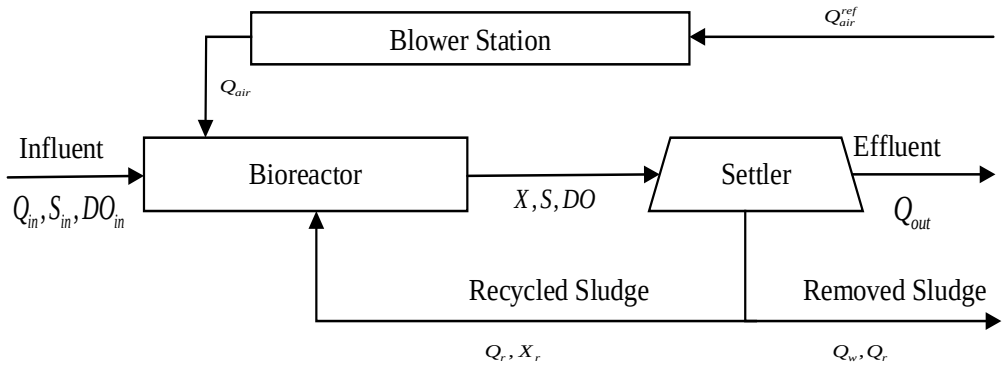

Figure 4- 3 The architecture of ASWWTP for nutrient removal with a blower

The function $k_{La}(Q_{air}(t))$ represents the oxygen transfer function derived from the mathematical mode of the ASWWTP in equation (3.3-3). This oxygen transfer function is dependent on the blower's operating state, as demonstrated in [105]. Therefore, the oxygen transfer function can be expressed as follows:

$$k_{La}(t) = \alpha Q_{air}(t) + \delta \tag{4-1}$$

Where: α and δ are constants known to represent oxygen transfer factors.

As discussed in [112, 155], a two-layer control system is employed with the objective of ensuring that the DO concentration trajectory ($DO(t)$) tracks the reference DO concentration trajectory ($DO^{ref}(t)$). The upper layer controller computes the reference airflow ($Q_{air}^{ref}(t)$) necessary to achieve the desired reference DO concentration trajectory ($DO^{ref}(t)$). The lower controller utilizes the blower actuator to generate airflow ($Q_{air}(t)$), which directly affects the actual DO concentration trajectory ($DO(t)$) in the biochemical reaction tank. As demonstrated in [19], a blower operation under ideal conditions, the blower actuator can produce the airflow ($Q_{air}(t)$) same to the reference

airflow ($Q_{air}^{ref}(t)$), thereby ensuring that the DO concentration trajectory ($DO(t)$) tracks the reference DO concentration trajectory ($DO^{ref}(t)$). This guarantees that microorganisms receive sufficient DO for growth and degradation. In our study, we consider that the blower is unable to generate airflow ($Q_{air}(t)$) equal to the reference airflow ($Q_{air}^{ref}(t)$)， but can only produce airflow that exceeds the reference airflow ($Q_{air}(t) > Q_{air}^{ref}(t)$).

The operation of ASWWTP is affected by input disturbances, such as influent flow rate ($Q_{in}(t)$), the substrate concentration in the influent ($S_{in}(t)$) and dissolved oxygen concentration in the fluent ($DO_{in}(t)$). These disturbances are unknown, uncertain, and unpredictable. Moreover, they are nonlinear dynamics. Therefore, to address these issues, the control system must be capable of updating ASWWTP's parameter online.

In our study, we assumed that the blower produces excessive airflow ($Q_{air}(t)$) compared to reference airflow ($Q_{air}^{ref}(t)$). The control system is designed to filter out this excess airflow while incorporating anti-disturbance capabilities and, moreover, ensuring the system's operation is stable.

The equations (3.3-1) to (3.3-6) show that the dynamics of ASWWTP form a complex nonlinear system. As demonstrated in various [21, 165, 166] simple feedback control methodologies like PI control, nonlinear MPI control, and Intelligent-PID were used to solve nutrient removal issues at the ASWWTP. However, these approaches generally

produce unacceptable results. The MIMO quantitative robust controller-design methodology implemented for nutrient removal at the ASWWTP with the additional airflow control modules was described in the [167], but it proved to be extremely complex.

The structure of the DO control system, assuming the existence of an ideal DO concentration sensor, is illustrated in Figure 4-4. This ideal DO concentration is estimated using adaptive control law, eliminating the need for respiration estimation. This approach differs from that described in [168].

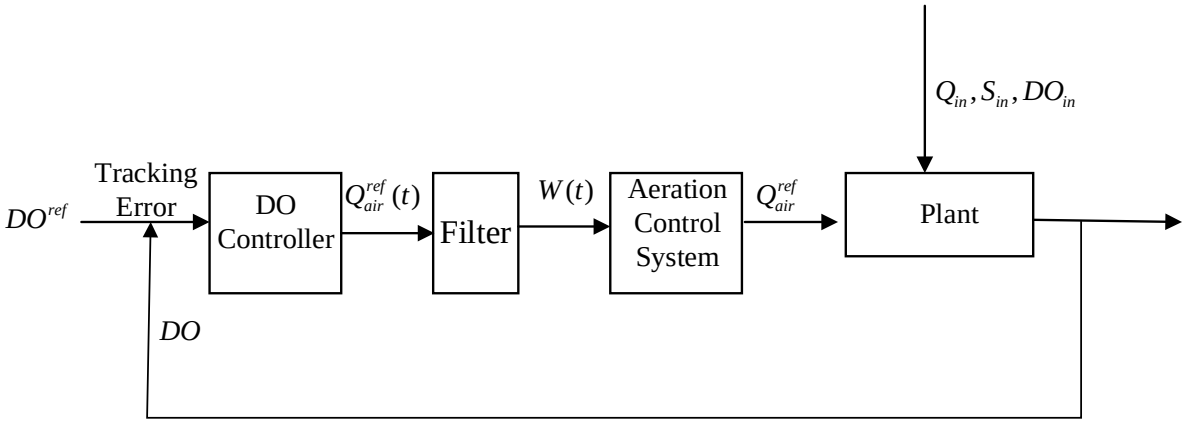

Figure 4- 4 Structure of dissolved oxygen control system

Due to the characteristic of ASWWTP operation, there are some ASWWTP state variables that cannot be measured by a hard sensor. Therefore, we utilize a DO controller to update online these time-varying variables and use these plant parameters to adjust the DO concentration trajectory of the output. The goal of the DMRAC with

filter is to maintain a stable output DO concentration trajectory and tracking reference DO trajectory (DO^{ref})while rejecting excess airflow and unknown disturbances.

4.5 Dissolved oxygen controller design with input constraints

The state-space model of an ASWWTP is described in equations (3.3-1) - (3.3-6), based on a modified ASM 2d and mass balance. The mathematical model of the ASWWTP was developed by IAWQ and tested. As previously mentioned, only the DO concentration is considered the control output, which is a nonlinear and uncertain plant parameter. The state variables $X_r(t)$, $X(t)$, and $S(t)$ are unmeasurable, while other plant parameters such as $Q_{air}(t)$, $Q_{in}(t)$, and $Q_W(t)$ are detectable by a soft sensor. The parameter DO can be estimated by an adaptive controller and updated online.

The first-order single input-output format is rewritten to derive a dynamic model for DO, which includes three main elements: 1) the state variables; 2) the control input with saturation constrain; and 3) the disturbance inputs. Furthermore, the design of the DMRAC with input constraints will entail estimating an uncertain state variable, extra air inflow, and unknown disturbances. This estimation mechanism will be continuously updated online to accommodate unknown parameters.

By substituting equations (3.3-5) and (3.3-7) into equation (3.3-3), the dynamic model $DO(t)$ is derived. The DMRAC with filter design is based on this equation (4-5-1). The resulting SISO model for dissolved oxygen concentration is as follows:

$$\begin{aligned}\frac{dDO}{dt} &= -D(t)(1+r)DO(t) - \frac{K_0 X(t)}{Y}\mu(t) \\ &\quad + (\alpha Q_{air}(t) + \delta)(DO_{\max} - DO(t)) \\ &\quad + D(t)DO_{in}(t)\end{aligned} \tag{4.5-1}$$

The term $D(t)DO_{in}(t)$ in the state-space model is significantly smaller compared to other state variables because of the dependency of the term $D(t)$ on both $Q_{in}(t)$ and V_a, as illustrated in equations (3.3-6). Hence, the impact of $D(t)DO_{in}(t)$ can be neglected. Rewriting equation (4.5-1) yields:

$$\begin{aligned}\frac{dDO}{dt} &= -a_p DO(t) - c_p f(DO(t)) + b_p Q_{air}(t) \\ &\quad + d_p + D(t)DO_{in}(t)\end{aligned} \tag{4.5-2}$$

Where: $a_p(t), c_p(t), b_p(t)$, and d_p are the SISO DO parameters.

$$\begin{aligned}a_p(t) &= \frac{Q_w(1+r)}{\beta V_a} \\ c_p(t) &= \frac{K_0 X(t)}{Y}\frac{\mu_{\max} S(t)}{(K_s + S(t))} \\ f(DO(t)) &= \frac{DO(t)}{(K_s + S(t))} \\ b_p(t) &= \alpha(DO_{\max} - DO(t)) \\ d_p &= \beta DO_{\max}\end{aligned} \tag{4.5-3}$$

The parameter $a_p(t)$, dependent on the variable $Q_{in}(t)$ in equation (3.4-6), pertains to the operating time scale of the upper layer's control system. Compared to the time scale of $DO(t)$, $a_p(t)$ are varies slowly.

The parameter $c_p(t)$ also varies slowly and is unknown due to its dependence on the plant's biological state variables $X(t)$ and $S(t)$, which exhibit slower variations in the time scales compared to $DO(t)$ [12, 19].

The time-varying of $f(DO(t))$ is determined by the time scale of $DO(t)$. K_{DO} is also a small constant relative to the time scale.

The parameter $b_p(t)$ varies depending on the time scale of $DO(t)$ in equation (3.4-3) and the parameter α, which represents the oxygen transfer constant and is known in equation (3.4-7). The plant parameter $DO(t)$ has a faster varying time scale compared to other plant state variables. Hence, the parameter $b_p(t)$ is also the time scale of rapidly changing, as discussed in [169].

The adaptive model references dynamics, when the adaptive controller' output $DO(t)$ tracks the $DO_{m.ref}(t)$ in a closed loop, as described in the following equation.

$$\frac{dDO_{m.ref}}{dt} = -a_m DO_{m.ref}(t) + b_m DO^{ref}(t) \qquad (4.5\text{-}4)$$

Where: $DO_{m.ref}$ represents the adaptive mode reference dynamic output, with parameters a_m and b_m being model reference constants. During the simulation experiment, we assumed a_m to be equal a small constant, denoted as b_m.

By rearranging equation (4.5-2), the saturation input limitation of the $DO(t)$ dynamic of a single input-output model is as follows:

$$\frac{dDO}{dt} = -a_p(t)DO(t) - c_p(t)\,f\,(DO(t)) + b_p(t)W(t) + d_p \tag{4.5-5}$$

Where: $W(t)$ represents assumed to be the saturation control input under constraints (SCIC).

$$W(t) = saturation(Q_{air}(t)) \tag{4.5-6}$$

and $W(t)$ constraints are expressed as:

$$W(t) = \begin{cases} Q_{air}^{L}(t), & if \quad Q_{air}(t) > Q_{air}^{L}(t) \\ Q_{air}(t), & if \quad Q_{air}^{L}(t) \le Q_{air}(t) \le Q_{air}^{U}(t) \\ Q_{air}^{U}(t), & if \quad Q_{air}(t) < Q_{air}^{U}(t) \end{cases} \tag{4.5-7}$$

Where: Q_{air}^{L} and Q_{air}^{U} represent the lower and upper bounds of the actuator's constant limitation, respectively. If the input saturation condition is met, the tracking error of filter $n(t)$ is increases. The model reference adaptive control law with saturation input is shown in equation (4.5-4). This motivates us to develop an adaptive control law

explicitly considering the influence of the actuator's saturation input nonlinearity, in comparison with Chapter 3.

The dynamics of the filter tracking error are applied as follows:

$$n(t) = e(t) - \lambda(t) \tag{4.5-8}$$

Where: $e(t)$ represents the differences between the control output $DO(t)$ and the adaptive model reference output $DO_{m.ref}(t)$ with on-line updates.

$$e(t) = DO(t) - DO_{m.ref}(t) \tag{4.5-9}$$

The adaptive controller should be capable of rejecting constrained input and disturbance input by defining the auxiliary signal as expressed.

$$\frac{d\lambda}{dt} = b_p \Delta Q_{air}(t) - \Phi\lambda(t) \tag{4.5-10}$$

Where: Φ is a small positive constant auxiliary parameter. The parameter $\Delta Q_{air}(t)$ represents the difference between the control input $Q_{air}(t)$ under SCIC and $W(t)$.

The affine model reference adaptive control law with input constraint is applied as follows:

$$W(t)=\frac{1}{b_p(t)}a_{DO}(t)DO(t)+\frac{1}{b_p(t)}a_f(t)f(DO(t))$$
$$+\frac{1}{b_p(t)}a_{DO^{ref}}(t)DO^{ref}(t)-\frac{1}{b_p(t)}d_p \qquad (4.5\text{-}11)$$
$$-\frac{1}{b_p(t)}\Phi(t)(DO(t)-DO_{m.ref}(t))$$

The model reference dynamic in equation (4.5-4) represents a linear time-varying dynamic. The terms $\frac{1}{b_p}a_f(t)f(DO(t))$ and $\frac{1}{b_p}d_p$ in (4.5-11) can achieve asymptotically cancellation of saturation input within the control system through the closed-loop nonlinear dynamics and additive terms in (4.6-5). The control saturation input is described by the last term in equation (4.6-11). The fourth term of equation (4.5-11) is updated online with time-varying, and the parameters $a_{DO}(t)$, $a_f(t)$, and $a_{DO^{ref}}(t)$ are updated online by the adaptive control law. The model reference dynamics are obtained in the closed-loop for ideal parameters. The closed-loop equation (4.5-5) using equation (4.5-11) can be written as:

$$\frac{dDO}{dt}=-(a_p(t)-a_{DO}(t))DO(t)$$
$$-(c_p(t)-a_f(t))f(DO(t)) \qquad (4.5\text{-}12)$$
$$+a_{DO^{ref}}(t)DO^{ref}(t)$$
$$-\Phi(DO(t)-DO_m(t))$$

and

$$-(a_p(t)-\hat{a}_{DO}(t))=-a_m$$

$$-(c_p(t)-\hat{a}_f(t))=0$$

$$\hat{a}_{DO^{ref}}(t)=b_m \tag{4.5-13}$$

$$-\Phi(DO(t)-DO_m(t))=-\Phi e(t)$$

Where: $\hat{a}_{DO}(t)$, $\hat{a}_f(t)$ and $\hat{a}_{DO^{ref}}(t)$ represent the ideal parameters of the adaptive model reference.

The ideal parameters are obtained as follows:

$$\hat{a}_{DO}(t)=-a_m+a_p(t)$$

$$\hat{a}_f(t)=c_p(t) \tag{4.5 -14}$$

$$\hat{a}_{DO^{ref}}(t)=b_m$$

The parameter adaptive laws that ensure the stability of a DMRAC system with a SISO first-order dynamic system are derived in [166]. This SISO first order dynamic system includes a linear unknown constant, known parameters, and a nonlinear additive structure. The linear unknown constant remains constant over time. Using these parameters adaptive laws implemented on equation (4.5-1), the parameters adaptive laws of DMRAC control system in ASWWTP are represented by equations (4.5-15), (4.5-16), and (4.5-17), as follows:

$$\frac{da_{DO}}{dt}=-\gamma_1 e(t)DO(t) \tag{4.5-15}$$

$$\frac{da_f}{dt} = -\gamma_2 e(t) f(DO(t)) \tag{4.5-16}$$

$$\frac{da_{DO^{ref}}}{dt} = -\gamma_3 e(t) DO^{ref}(t) \tag{4.5-17}$$

The constants γ_1, γ_2, and γ_3 are small enough positive values that represent adaptive gains. These adaptive gains are capable of adjusting the adaptive rate. In the closed-loop adaptive control system, adjusting adaptive gain to change the adaptive rate to match the time-vary variables during the ASWWTP process can prove the stability of the adaptive control system. Figure 4-5 depicts the direct model reference adaptive control with constraints on the control input ASWWTP.

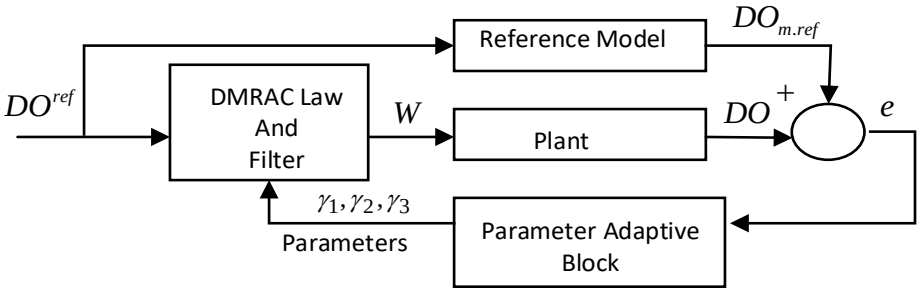

Figure 4- 5 The structure of DMRAC with a filter

4.6 Stability analysis

The parameter adaptive laws (4.5-15), (4.5-16), and (4.5-17) are the online update estimation parameter $a_{DO}(t)$, $a_f(t)$, and $a_{DO^{ref}}(t)$. The difference between estimation

parameters and ideal parameters $\hat{a}_{DO}(t)$, $\hat{a}_f(t)$, $\hat{a}_{DO^{ref}}(t)$ are defined as $\Delta a_{DO}(t)$, $\Delta a_f(t)$, and $\Delta a_{DO^{ref}}(t)$.

$$\Delta a_{DO}(t) = a_{DO}(t) - \hat{a}_{DO}(t) \tag{4.6-1}$$

$$\Delta a_f(t) = a_f(t) - \hat{a}_f(t) \tag{4.6-2}$$

$$\Delta a_{DO^{ref}}(t) = a_{DO^{ref}}(t) - \hat{a}_{DO^{ref}}(t) \tag{4.6-3}$$

Consider the following Lyapunov function:

$$V(t) = \frac{1}{2}n^2(t) + \frac{1}{2}\Delta a_{DO}{}^2(t) + \frac{1}{2}\Delta a_f{}^2(t) + \frac{1}{2}\Delta a_{DO^{ref}}{}^2(t) \tag{4.6-4}$$

Hence,

$$\begin{aligned}\frac{dV(t)}{dt} = {} & n(t)\dot{n}(t) + (a_{DO}(t) - \hat{a}_{DO}(t))(\dot{a}_{DO}(t) - \dot{\hat{a}}_{DO}(t))\frac{1}{\gamma_1} \\ & + (a_f(t) - \hat{a}_f(t))(\dot{a}_f(t) - \dot{\hat{a}}_f(t))\frac{1}{\gamma_2} \\ & + (a_{DO^{ref}}(t) - \hat{a}_{DO^{ref}}(t))(\dot{a}_{DO^{ref}}(t) - \dot{\hat{a}}_{DO^{ref}}(t))\end{aligned} \tag{4.6-5}$$

It follows from equations (4.5-8), (4.5-9), (4.5-4), and (4.5-12) that

$$\begin{aligned}\frac{dn(t)}{dt} = {} & (a_{DO}(t) - \hat{a}_{DO}(t))DO(t) \\ & + (a_f(t) - \hat{a}_f(t))f(DO(t)) \\ & + (a_{DO^{ref}}(t) - \hat{a}_{DO^{ref}}(t))DO_{m.ref}(t) \\ & - \Phi n(t)\end{aligned} \tag{4.6-6}$$

By substituting equations (4.6-6), (4.5-15), (4.5-16), and (4.5-17) into equation (4.5-5) yields:

$$\frac{dV(t)}{dt} = -\Phi n^2(t) \tag{4.6-7}$$

As time approaches infinity, the result of the Lyapunov function tends to zero. In summary, when the Lyapunov function approaches zero, the filter tracking error tends to zero as time approaches infinity. The parameter Φ is a small positive constant, and $n^2(t)$ is a positive variable.

The controller limit boundaries are defined by an auxiliary signal, denoted as $\lambda(t)$, which represents the bounding error between the real DO output and DO model reference output.

$$\lim it\left\{e(t) - \lambda(t)\right\} \le 0 \tag{4.6-8}$$

As time approaches infinity, the $e(t)$ tends to zero. Auxiliary signals can either become positive or negative as time goes to infinity. Now, let us consider the auxiliary signal $\lambda(t)$ by following the Lyapunov function:

$$V_\lambda(t) = \frac{1}{2}\lambda^2(t) \tag{4.6-9}$$

Hence, the derivative of the Lyapunov function is given by the following equation:

$$\frac{dV_\lambda(t)}{dt} = \lambda(t)\dot{\lambda}(t) \tag{4.6-10}$$

By substituting equation (4.5-10) into equation (4.6-10)

$$\frac{dV(t)}{dt} = \lambda(t) b_p(t) \Delta Q_{air}(t) - \lambda(t)\lambda(t)\Phi \qquad (4.6\text{-}11)$$

Assuming the term $b_p(t)\Delta Q_{air}(t) = \Delta Q_{air}^{plant}(t)$ (4.6-12), it follows from equations (4.6-11) and (4.6-12) that

$$\frac{dV_\lambda(t)}{dt} = -\lambda^2(t)\Phi + \frac{1}{2}\lambda^2(t) + \frac{1}{2}\Delta Q_{air}^{plant^2}(t) \qquad (4.6\text{-}13)$$

The small positive constant auxiliary parameter Φ has been mentioned previously. Now, let us assume that $\Phi = \frac{1}{2}a_0$ (4.6-14), where a_0 is a small positive constant parameter, and $a_0 < 0$ (4.6-15). Substitute equation (4.6-14) into equation (4.6-13).

$$\frac{dV_\lambda(t)}{dt} = -2V_\lambda(t)a_0 + \frac{1}{2}\Delta Q_{air}^{plant^2}(t) \qquad (4.6\text{-}16)$$

The second term of equation (4.6-16), denoted by $(\frac{1}{2}\Delta Q_{air}^{plant^2}(t))$, is bounded by the square of $\Delta Q_{air}^{plant^2}(t)$. To determine the bound of the first term, we utilize the integral (4.6-16).

$$V_\lambda(t) = \frac{\Delta Q_{air}^{plant^2}(t)}{4a_0} + (V_{\lambda.0}(t) + \frac{\Delta Q_{air}^{plant^2}(t)}{4a_0})e(t)^{-2a_0} \qquad (4.6\text{-}17)$$

Where: $V_{\lambda.0}(t)$ is the initial value of the $V_\lambda(t)$. As time approaches infinity and a_0 becomes a sufficiently large positive value, the second term of (4.6-17) becomes equal to zero, as shown below.

$$V_{\lambda}(t) = \frac{\Delta Q_{air}^{plant^2}(t)}{4a_0} \tag{4.6-18}$$

It can be deduced from equation (4.6-9) and the constraint on $V_{\lambda}(t)$ being negative or zero, as follows:

$$V_{\lambda}^{2}(t) = \frac{\Delta Q_{air}^{plant^2}(t)}{4a_0}$$

$$\frac{1}{2}\lambda^{2}(t) = \frac{\Delta Q_{air}^{plant^2}(t)}{4a_0} \tag{4.6-19}$$

$$\lambda(t) = \sqrt{\frac{\Delta Q_{air}^{plant^2}(t)}{4a_0}}$$

By rearrange equations (4.6-8) and (4.6-19) as follows:

$$e(t) \le \sqrt{\frac{\Delta Q_{air}^{plant^2}(t)}{4a_0}} \tag{4.6-20}$$

If a_0 is large enough, the tracking error $e(t)$ will tend to zero. Hence, the control system will be asymptotically stable. Further detailed derivations are provided in Appendix B.

Barbalat's Lemma:

We apply Barbalat's lemma to analysis the results of the Lyapunov function. The conclusion states that under the following circumstances, a direct model reference adaptive controller is capable of asymptotic trajectory tracking $DO^{ref}(t)$. It is bounded

by the ideal adaptive parameters and on-line updated parameters ($a_{DO}(t), \hat{a}_{DO}(t), a_f(t), \hat{a}_f(t), a_{DO^{ref}}(t), \hat{a}_{DO^{ref}}(t)$), as follows: if 1) the parameters in the adaptive control law are close enough to the set point in the initial condition, 2) the adaptive rate parameters have small positive values, and 3) the saturation input is small, then the parameters of the direct model reference adaptive controller are bounded, and the control system is stable.

In the subsequent chapter, we will utilize MATLAB simulation results to illustrate the characteristics of the direct model reference controller with input saturation, as implemented in the ASWWTP operation.

4.7 Simulation results and discussion

In this section, we will utilize MATLAB simulation results to demonstrate the stability, robustness, and constraint resistance of the direct model reference adaptive control with filter when applied to the global variables of the blower-limited ASWWTP system. The MATLAB simulation utilized real data as a reference in the [161].

The simulation of ASWWTP operation utilized the following initial conditions: $X(0) = 15mg/l$, $S(0) = 200mg/l$, $DO(0) = 3mg/l$, $X_r(0) = 18mg/l$, $DO_{\max} = 10mg/l$, $DO_{\max} = 10mg/l$, $S_{in}(0) = 600mg/l$, $S_{in}(0) = 600mg/l$ $D(0) = 3$, $DO_{in}(0) = 0.5mg/l$. The process

parameters are listed below: $Y = 0.65$, $r = 0.6$, $\beta = 0.2$, $\alpha = 0.18$, $K_0 = 0.5$. The kinetic parameters are as follows: $\mu_{\max} = 0.15mg/l$, $K_s = 0.15mg/l$, $K_{DO} = 2mg/l$. The auxiliary signal parameter is $\Phi = 0.6$. The reference model parameters are: $a_m = 5$ and $b_m = 5$. The $DO^{ref}(t)$ are assumed to be piecewise constant. The $S_{in}(t)$, $D(t)$, and $DO_{in}(t)$ time-varying disturbance inputs are represented in Figure 4-6, 4.7, and 4-8.

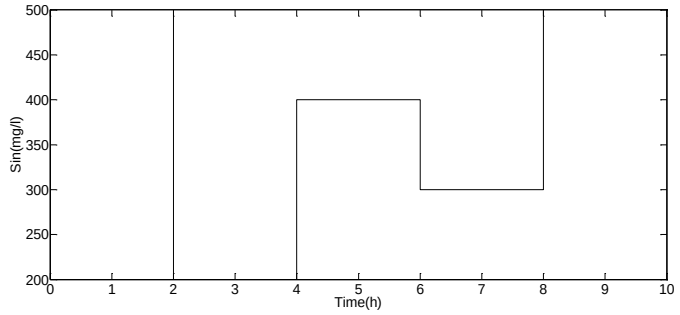

Figure 4- 6 Influent substrate $S_{in}(t)$

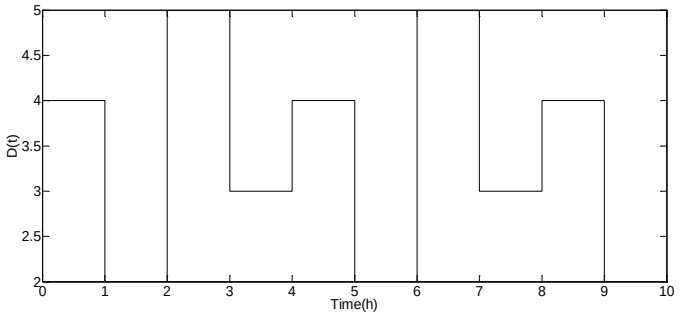

Figure 4- 7 Dilution rate $D(t)$

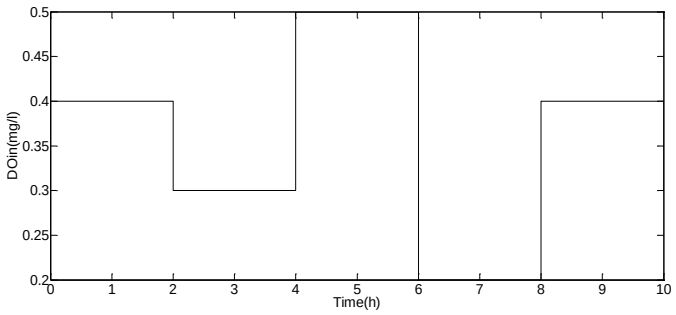

Figure 4- 8 Influent dissolved oxygen $DO_{in}(t)$

During the ASWWTP operation with saturation input and without disturbance input, the output $DO(t)$ of DMRAC exhibits good performance in tracking the trajectory of $DO^{ref}(t)$, as illustrated in Figure 4-9. Moreover, the output of DMRAC demonstrates that the adaptive control output $DO(t)$ can effectively, rapidly, and stably track the trajectory of $DO^{ref}(t)$, indicating that the adaptive controller has good robustness to disturbance inputs and capability to reject saturation inputs in the ASWWTP operation, as illustrated in Figure 4-10.

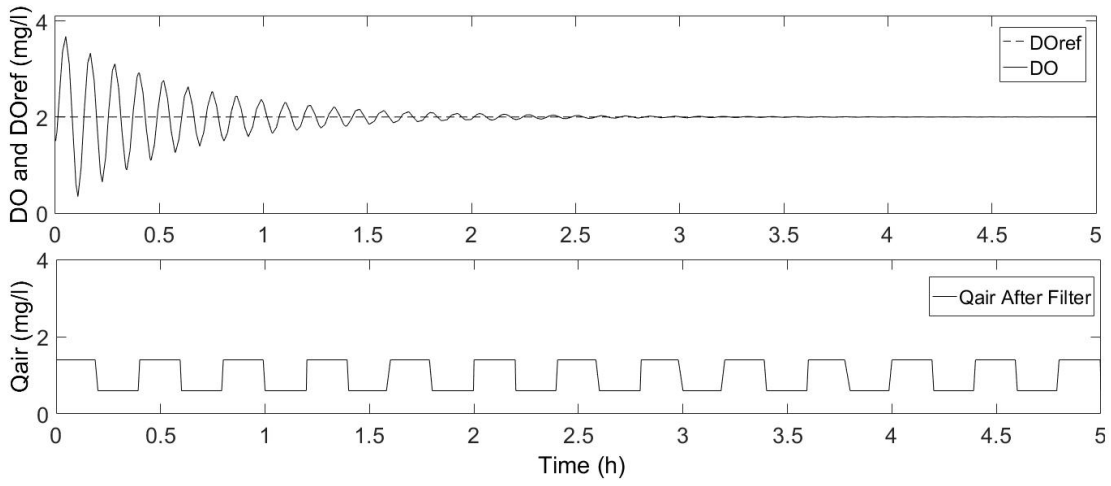

Figure 4- 9 $DO(t)$ and $DO^{ref}(t)$ with saturation input and slow adaptive rates

$\gamma_1 = 0.2, \gamma_2 = 0.2, \gamma_3 = 0.2$ and auxiliary parameter $a_0 = -0.2$

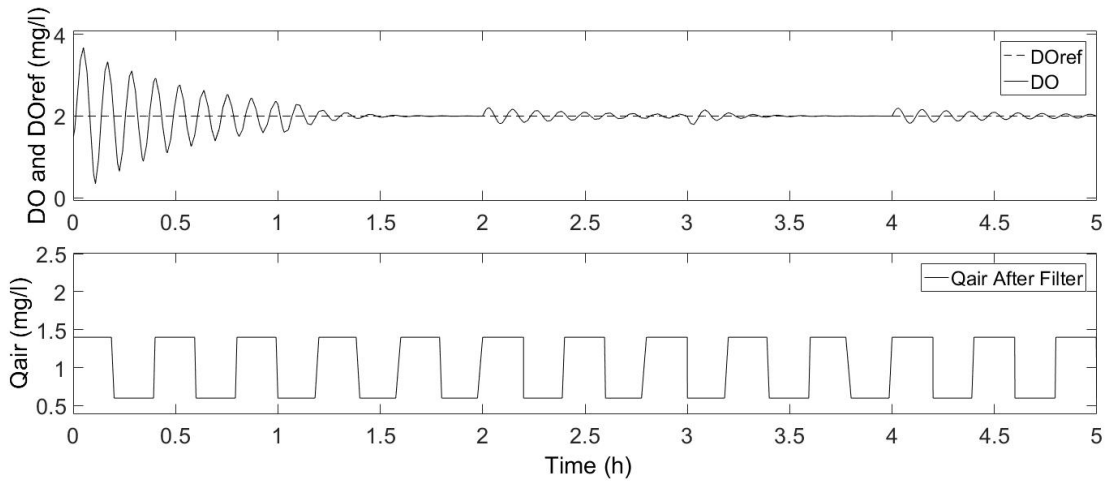

Figure 4- 10 $DO(t)$ and $DO^{ref}(t)$ with saturation input and disturbances input

and slow adaptive rates $\gamma_1 = 0.2, \gamma_2 = 0.2, \gamma_3 = 0.2$ and auxiliary parameter $a_0 = -0.2$

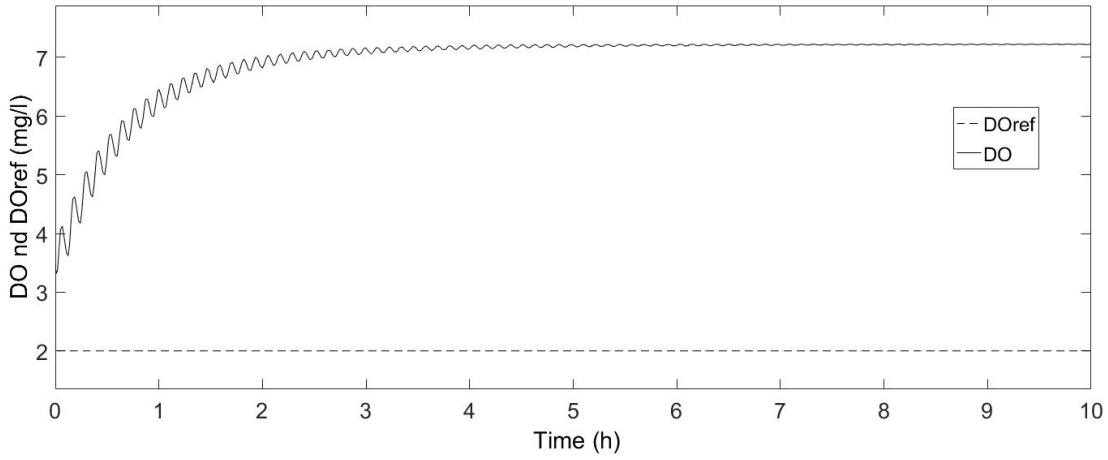

Figure 4- 11 $DO(t)$ and $DO^{ref}(t)$ without disturbances input and with saturation input, fast adaptive rates $\gamma_1 = 6, \gamma_2 = 6, \gamma_3 = 6$ and auxiliary parameter $a_0 = -0.2$.

The initial conditions of the ASWWTP remained consistent with those used previously. The parameter $DO^{ref}(t)$ is consistent with the conditions in Figures 4-9 and 4-1-. The gain of adaptive laws was considered as fast-varying variables ($\gamma_1 = 6, \gamma_2 = 6, \gamma_3 = 6$). Figure 4-11 indicates that the adaptive control output $DO(t)$ is not tracking the $DO^{ref}(t)$ trajectory. Hence, the DMRAC system of the closed-loop system is unstable. Due to increasing the adaptive gain, there is an increase in the parameter adaptive laws, and adaptive rate. Consequently, the adaptive rate becomes extremely fast to match the time-varying parameter of the ASWWTP. Resulting in the auxiliary signal being unable to filter the input saturation. Therefore, rendering the adaptive control parameters unbounded by error.

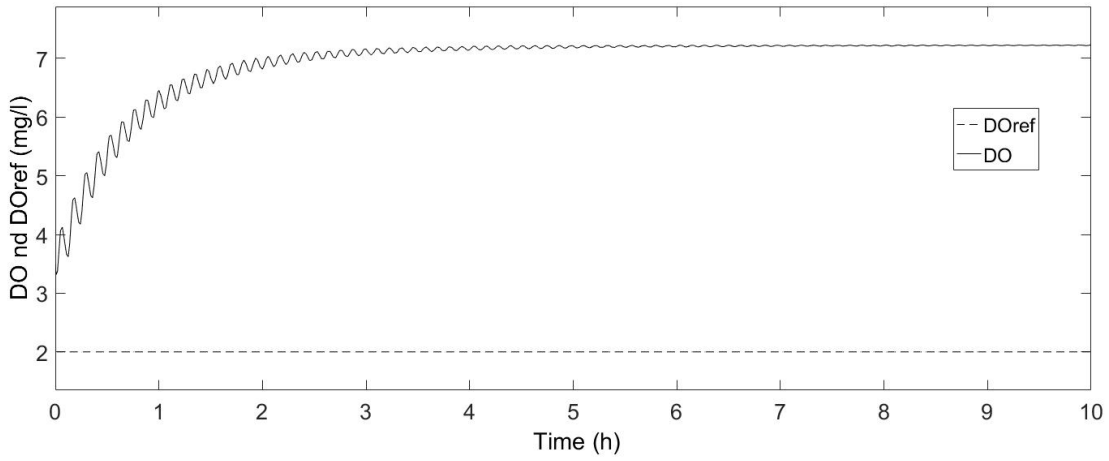

Figure 4- 12 $DO(t)$ and $DO^{ref}(t)$ with saturation input, disturbance input, and with fast adaptive rates $\gamma_1 = 6, \gamma_2 = 6, \gamma_3 = 6$ and auxiliary parameter $a_0 = -0.2$.

In Figure 4-12, the response of the control output $DO(t)$ tends towards infinity, signifying that the adaptive control system becomes unstable in the presence of saturation input, disturbance input, and a rapid adaptive control rate. It indicates that the parameters of the adaptive control law are unable to update online under the matched plant speed scale, leading to a decline in robustness. Hence, the adaptive control parameters $a_{DO}(t)$ and $a_f(t)$ are not bound by the squared error, where the error denotes the deviation between the real control output $DO(t)$ and the trajectory of the model reference output $DO(t)$.

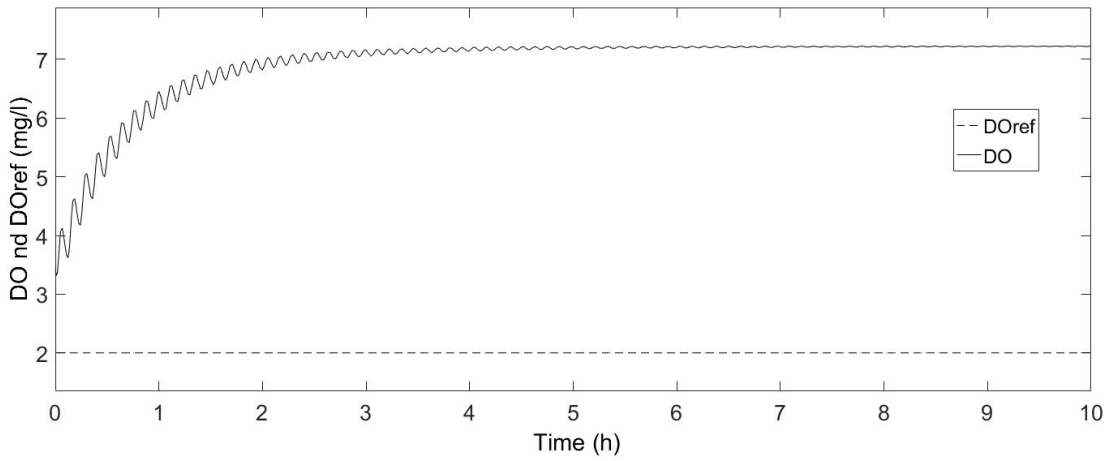

Figure 4- 13 $DO(t)$ and $DO^{ref}(t)$ without disturbance input and with input saturation, adaptive rates $\gamma_1 = 0.6, \gamma_2 = 0.6, \gamma_3 = 0.6$ and large auxiliary parameter $a_0 = -2$

In figure 4-13, the response of the adaptive control output $DO(t)$ is observed not to track the trajectory of the model reference $DO^{ref}(t)$, indicating instability in the

adaptive control system equipped with a filter, where it's under a large auxiliary parameter a_0 . This demonstrates that the saturation input exceeds the auxiliary limitations, hence leading to instability in the control system, as previously analysed for stability. Furthermore, this also indicates the insufficiency of the adaptive control system's robustness to accommodate large input saturation.

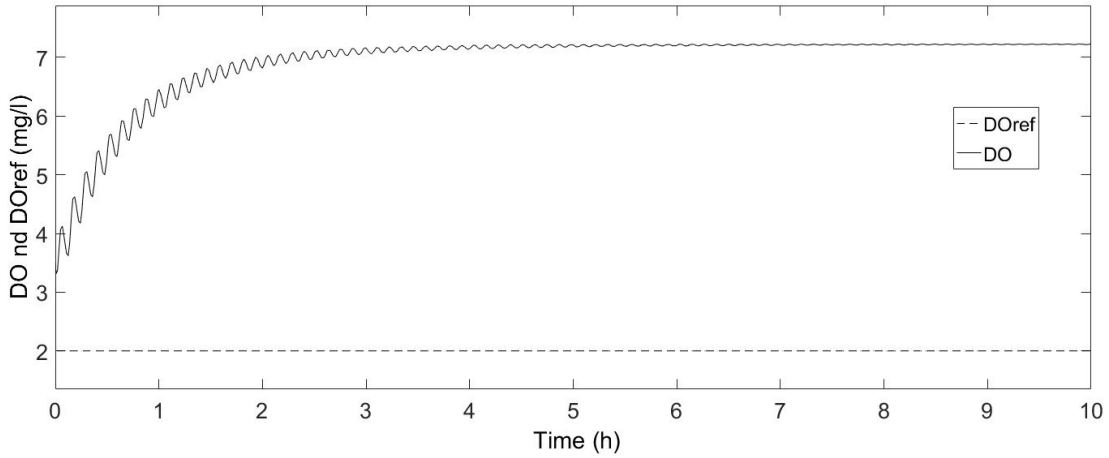

Figure 4- 14 The initial conditions are very fast from the equilibrium point. $DO(t)$ without disturbance and with saturation input, slow adaptive rates $\gamma_1 = 0.2, \gamma_2 = 0.2, \gamma_3 = 0.2$ and auxiliary parameter $a_0 = 0.2$

The initial conditions $X(0) = 30mg/l$, $S(0) = 960mg/l$, and $X_r(0) = 35mg/l$, $DO(0) = 7mg/l$ are very far from the equilibrium point. The response of the adaptive control output $DO(t)$, as shown in Figure 4-14, indicates that the closed-loop control system becomes unstable, which confirms the stability analysis in Chapter 4.6.

4.8 Conclusion

This chapter addresses the dissolved oxygen concentration trajectory tracking issue to achieve nutrient removal at the ASWWTP. Considering the existing architecture of ASWWTP, the blower is operating under conditions of overproduction and excessive air delivery. A dissolved oxygen concentration direct model reference adaptive control system with a filtering function is designed based on limited ASWWTP parameters and applied to the mathematical model of global ASWWTP parameters. The parameters of the adaptive control system are adjusted according to the MATLAB simulation results. The MATLAB simulation results prove that the control system can resist interference while rejecting excess air inflow. At the same time, the stable and efficient operation of the system is guaranteed. The MATLAB simulation results verify the stability of the control system using the Lyapunov function.

CHAPTER 5 Supervised Fuzzy Logic and DDMRAC Two – Level for Nutrient Removal at ASWWTP

5.1 Introduction

In practice, ASWWTP factories often prioritize saving construction space, minimizing maintenance costs, and reducing energy consumption while maintaining stable and efficient operations. As mentioned earlier, the settlement tank occupies a significant amount of space and takes a long time to operate. Additionally, air supply represents the highest cost in ASWWTP operations. To address these challenges, we use a single air supplier and a single settlement tank in coordination with three biochemical tanks arranged in series for ASWWTP operations. This setup effectively manages the large volume of wastewater purification

Due to the varying inflow and outflow of biomass, substrate, dissolved oxygen, and recycled biomass in each biochemical reaction tank, a Fuzzy Logic Decentralized Direct Model Reference Adaptive Controller is designed and implemented in the ASWWTP to rapidly adjust airflow into each bioreaction tank. This allows the real DO concentration to closely follow the reference DO concentration trajectory. The

controller's stability is proven using the Lyapunov function. MATLAB simulation results, based on real data, demonstrate that the ASWWTP operates efficiently and stably, with the capability to reject unknown disturbances.

This study leverages the characteristics of fuzzy logic control and applies it to the regulation of dissolved oxygen concentration in multiple bioreactors, ensuring that the dissolved oxygen concentration in each bioreactor changes appropriately over time, thereby achieving an efficient biochemical reaction rate. To enhance the efficacy of fuzzy logic control in meeting the specific needs of wastewater purification plants, we optimize its adaptability, accuracy, and robustness using Genetic Algorithms.

5.2 The architecture of ASWWTP with a blower and three bioreactors in series

The ASWWTP consists of three biochemical reaction tanks in series, a settlement tank, and a single blower, as illustrated in Figure 5-1. Wastewater from the collection and filtration tanks flows into bioreaction tank 1, where it undergoes a series of biochemical reactions with dissolved oxygen. The wastewater then flows into bioreaction tanks 2 and 3. The blower actuator supplies airflow to each bioreaction tank, acting as the

control input. This ensures that microorganisms receive the necessary dissolved oxygen for growth and degradation.

The reference DO concentration trajectory is provided by a pre-set reference airflow in the upper layer of the overall control system [178]. The quantity and type of substances in the inflow and outflow of each bioreaction tank vary. Finally, after the wastewater completes its bioreaction with dissolved oxygen in bioreaction tank 3, it flows into the sedimentation tank, where sludge is separated from clear water by gravity. The sludge is divided into new sludge and old sludge. The new sludge is returned to bioreaction tank 1, which helps maintain the balance and adaptability of the microbial community.

As discussed in [203], a certain amount of DO must be present in the discharged clean water to maintain the balance of the natural ecosystem. Substrate and biomass concentrations cannot be measured online with hard sensors [35]. The control of DO concentration in the bioreaction tanks during ASWWTP operation has received significant attention in the control community [1, 14, 176].

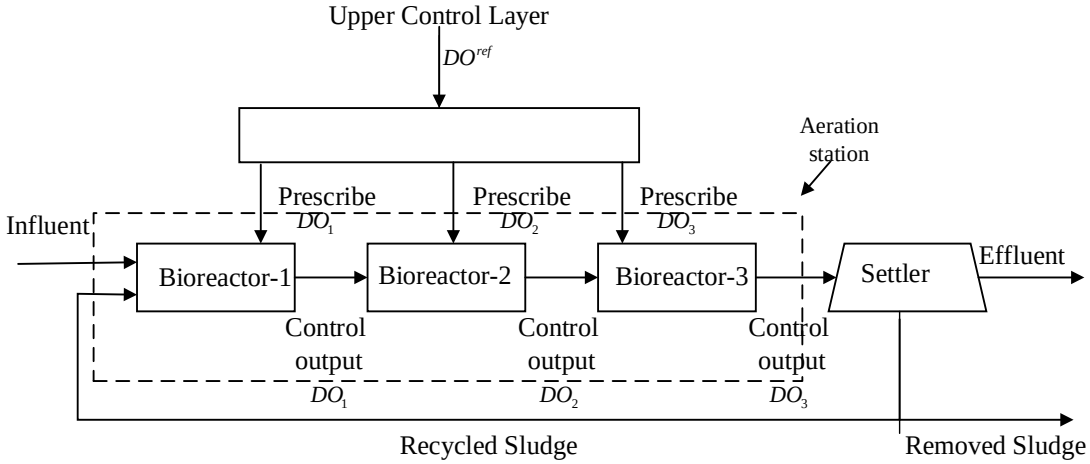

Figure 5- 1 Architecture of ASWWTP with three bioreactors for nutrient removal

As [112, 113] discussed, the two-layer control system implements the DO concentration trajectory ($DO(t)$) output by the lower-layer MPC controller to track the reference DO concentration trajectory ($DO_{ref}(t)$) provided by the upper layer control system. The pre-given $Q_{air}^{ref}(t)$ set-point is obtained by calculating the inflow of wastewater and sludge, and it is the input for the upper layer control system. The lower layer control system optimizes the input - $Q_{air}(t)$, enable $DO(t)$ to track the output $DO^{ref}(t)$ of the upper layer control system. The MPI control system implemented in the lower layer control system for optimizing $Q_{air}(t)$ to ensure that $DO(t)$ tracking the $DO^{ref}(t)$, as demonstrated in [61]. In this chapter, we design and implement a Fuzzy logic – DDMRAC system as the overall lower control system in the ASWWTP, which consists of a single blower and sediment tank, and three bioreaction tanks in a series. The Fuzzy logic -DDMRAC algorithm based on the DMRAC method [156], and fuzzy logic rules.

5.3 Nutrient removal process using single blower and three bioreactors in ASWWTP

Sewage flows from the collection tank into bioreactor 1, and undergoes biochemical reactions with the oxygen delivered by the blower actuator. The biochemical reaction process includes: the growth of microorganisms and the decomposition of organic matter. Next, it flows into bioreactor 2 and 3 in sequence to undergo biochemical reactions. However, the sewage and air flowing into each bioreactor are different, and the amount of air flowing into each biochemical reactor is based on the biomass concentration in each biochemical reactor. The young sludge flows back only to bioreaction tank 1. The microorganisms in all three bioreaction tanks require dissolved oxygen, which is provided by a single blower, as illustrated in Figure 5-2. The detailed process of wastewater flow and airflow injection is as follows:

1) The inflow of bioreaction tank. 1 includes wastewater influent flow rate ($Q_{in}(t)$), airflow ($Q_{air.1}(t)$), DO concentration influent $DO_{in}(t)$, and substrate concentration ($S_{in}(t)$) . The outflows of the bioreaction tank. 1 are $X_1(t)$, $S_1(t)$, and $DO_1(t)$, respectively. This process is the same as that of ASWWTP with a single blower, bioreaction tank, and sediment tank.
2) The inflow of bioreaction tank. 2 is based on the outflow of bioreaction. 1 adding $Q_{aie.2}(t)$. The outflows of the bioreaction tank. 2 are $X_2(t)$, $S_2(t)$, and $DO_2(t)$, respectively. Additionally, the biomass concentration in bioreaction tank

1 is higher than in bioreaction. 2 ($X_1(t) > X_2(t)$), and substrate concentration in bioreaction tank. 1 is lower than in bioreaction. 2 ($S_1(t) < S_2(t)$), as some microorganisms have been degraded.

3) The inflow of bioreaction tank. 3 is based on the outflow of bioreaction. 2 adding $Q_{aie.3}(t)$. The outflows of bioreaction. 3 are effluent flow rate ($Q_{out}(t)$), recycled flow rate ($Q_r(t)$), waste flow rate ($X_r(t)$). As a large portion of microorganisms has been degraded in bioreaction. 3, the substrate concentration is highest, and the biomass concentration is lowest in this tank.

4) Finally, the inflow of sedimentation tank is the same as the outflow from bioreaction tank 3. Clear water and sludge flow out from the bioreaction. 3, respectively. The young sludge flows back to bioreaction 1, while the aged sludge is discharged.

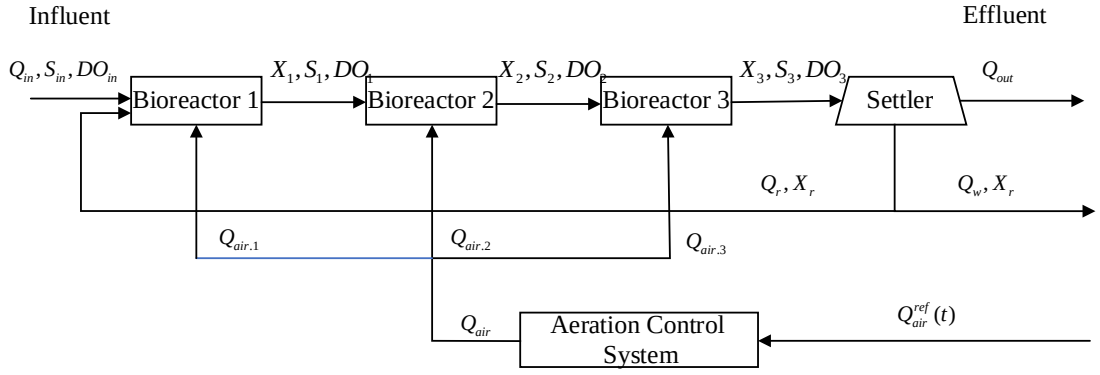

Figure 5- 2 Architecture of ASWWTP with Three Bioreactors in Series

As discussed in [77], the two-layer control system comprises an upper layer that determines the reference DO concentration trajectory based on the pre-setpoint

reference airflow. The lower layer control system optimizes the airflow to ensure that the DO concentration tacks the reference DO concentration. The blower actuator is a complex nonlinear system and ensuring that the airflow output by the blower actuator is equal to the reference airflow is solved using an MPC control system as described in [191]. In our study, we considered the design of a lower-level control system that utilizes a two-layer fuzzy logic-DDMRAC system to determine the DO concentration trajectory, ensuring that it tracks the reference DO concentration trajectory in each bioreactor. This plant employs a single blower actuator to provide the required airflow for three bioreactors. The decentralized DMRAC algorithm is based on the DMRAC method [15].

As discussed in [63], the DO concentration is an important parameter for evaluating the efficiency of wastewater purification in activated sludge treatment. The growth and degradation of microorganisms in the bioreactor depends on the dissolved oxygen concentration in the wastewater. At higher DO concentrations, the growth and activity of microorganisms will be inhibited. At lower DO concentrations, the activity of aerobic microorganisms will be inhibited, thereby systematically reducing the growth and degradation of microorganisms. Therefore, the change trajectory of DO concentration in the bioreactor is crucial to the wastewater purification rate during the operation of ASWWTP.

5.4 Control problem statement

The ASWWTP mathematical model can enhance understanding of any biochemical process involving nutrient removal and biomass transfer. The mathematical model family of ASWWTP is described by the IAWQ. The ASM 1 and ASM 2 utilizes the time dimension to describe the ASWWTP process. ASM 2d describes the ASWWTP process in both time and space dimensions. By extending ASM 1 and 2, it describes the biological phosphorus removal process under anaerobic conditions in detail.

Since we only consider the DO concentration in each bioreaction tank as the control output, the mathematical model in the state-space model of the structure of ASWWTP is derived from the mass balance and rewriting the ASM 2d [182]. This mathematical model encompasses ASWWTP variables, as depicted in equations (5.4-1) - (5.4-8).

$$\frac{dX_n}{dt} = \mu_n(t)X_n(t) - D_n(t)X_n + \gamma_1 D_n(t)X_m(t) \tag{5.4-1}$$

$$\frac{dS_n}{dt} = -\frac{\mu_n(t)X_n(t)}{Y_n} - D_n(t)(1+r)S_n(t) + D_n(t)S_k(t) \tag{5.4-2}$$

$$\begin{aligned}\frac{dDO_n}{dt} = &-\frac{K_{0.n}\mu_n(t)X_n(t)}{Y_n} \\ &- D_n(t)(1+\gamma_1)DO_n(t) + D_n(t)DO_k(t) \\ &+ a_n Q_{air.n}(t)(DO_{\max.n} - DO_n(t))\end{aligned} \tag{5.4-3}$$

$$\frac{dX_r}{dt} = D_3(t)(1+\gamma_1)X_3(t) - D_3(t)(\beta+\gamma_1)X_r(t) \tag{5.4-4}$$

$$\mu_n(t) = \mu_{\max.n} \frac{s_n(t)}{K_{s.n} + S_n(t)} \frac{DO_n(t)}{K_{DO.n} + DO_n(t)} \tag{5.4-5}$$

where

$$D_n(t) = \frac{Q_{in}}{V_{a.n}},\ V_n = \frac{V_{a.n}}{V_{S.n}},\ \gamma_1 = \frac{Q_r}{Q_{in}},\ \beta = \frac{Q_w}{Q_{in}} \tag{5.4-6}$$

And $n = 1, 2, 3$, $m = r, 1, 2$, $k = in, 1, 2$.

Where: n, m, and k denote the sequence of sewage intake and discharge for each bioreactor.

$X_n(t)$, $S_n(t)$, $DO_{\max.n}$, $X_{r.n}(t)$, $D_n(t)$, $S_{in.n}(t)$, $DO_{in.n}(t)$, Y_n, $\mu_n(t)$, $\mu_{\max.n}$, $K_{s.n}$, $K_{DO.n}$, $Q_{air.n}(t)$, $K_{0.n}$, r_n, β_n, $Q_{in.n}(t)$, $Q_{out.n}(t)$, $Q_{r.n}(t)$, $Q_{w.n}(t)$, $V_{a.n}$ are biomass concentration, substrate concentration, maximum dissolved oxygen concentration, recycled biomass concentration, dilution rate, substrate concentration in the influent, dissolved oxygen concentration in the influent, biomass yield factor, biomass growth rate, maximum specific growth rate, affinity constant, saturation constant, aeration rate, model constant, recycled sludge rate, removed sludge rate, influent flow rate, effluent flow rate, recycled flow rate, waste flow rate and aerator volume.

In [170], it is demonstrated that the oxygen transfer function is dependent on the airflow from the blower actuator and the sludge concentration measurement by the DO controller. The respiration rate and sludge condition determine oxygen transfer, with

function $K_{L.a.i}(Q_{air.k}(t))$ representing the oxygen transfer. The OTF can be estimated using time-varying respiration rates [83]. If the OTF has been estimated, there is no need to calculate the respiration rate from the airflow rate during the biochemical reaction. [105] demonstrated the following representation of the oxygen transfer function.

$$K_{La.i}(t) = \alpha_j Q_{air.k}(t) + \delta_m \tag{5.4-7}$$

Where: α_j and δ_m represents known constants for oxygen transfer. The i, j, k, and m corresponds to the number of bioreactors, where $i = 1, 2, 3$, $j = 1, 2, 3$, $k = 1, 2, 3$, and $m = 1, 2, 3$.

$$Q_{air.\max}(t) \le Q_{air.1}(t) + Q_{air.2}(t) + Q_{air.3}(t) \tag{5.4-8}$$

Where: $Q_{air.\max}(t) \neq Q_{air.n}(t)$, and $n = 1, 2,$ and 3, where n represents the number of bioreactors,

The architecture of ASWWTP utilizes a single blower to serve as the three bioreaction tanks. The amount of anoxic and aerobic zones in the wastewater within each bioreaction tank fluctuates during ASWWTP operation. Therefore, using equations (5.4-1) to (5.4-6), the dissolved oxygen concentration in each bioreactor is analysed from a two-dimensional perspective. The dissolved oxygen is supported by the blower actuator, as it is highly nonlinear dynamic. As discussed in [125], a two-layer control system for the DO concentration trajectory tracks reference DO concentration trajectory.

The output of the upper layer control system is reference DO centration trajectory, determined by the input reference airflow, which is provided by a per-setpoint. By optimized the airflow, the DO concentration trajectory tracks the reference DO concentration trajectory. As discussed in [112], the lower layer control system utilizes Fuzzy-MPI to ensure that the blower actuator output airflow equals the reference airflow, thereby enabling the DO concentration trajectory to track the reference DO concentration trajectory.

In this study, only the lower control system is considered. by optimizing the airflow in each bioreaction tank, to ensure that the DO concentration trajectory in each bioreaction tank tracks the reference DO concentration trajectory, and that each airflow matches the corresponding reference airflow. Additionally, as demonstrated in [83], the airflow equals the reference airflow. In our study, we assume that the blower actuator control system has been designed, ensuring that the sum of the three airflows equals that total reference airflow ($\sum_{i=1}^{3} Q_{air.i}(t) = total.Q_{air}^{ref}(t)$).

As discussed in [97], internal and external disturbances during ASWWTP operation can influence microorganism growth, leading to system collapse. In our ASWWTP system, the unknown disturbance inputs with time varying in each bioreaction tank include the influent flow rate ($Q_{in,1,2}(t)$), the substrate concentration in the influent ($S_{in,1,2}(t)$) and the dissolved oxygen concentration in the fluent ($DO_{in,1,2}(t)$). One of

the goals in designing the control system is to ensure its robustness against these unknown disturbance inputs.

The [25] demonstrated that the control system of the blower actuator ensures the airflow is equal to the reference airflow. Consequently, it can be inferred that each airflow in ASWWTP equals its respective reference airflow under the assumption that the blower actuator control system has been designed. The supervised fuzzy logic – DDMRAC control system is designed and implemented in the architecture of ASWWTP for nutrient removal. Additionally, an ideal DO concentration hard sensor is assumed to exist in Figure 5-3. Therefore, it can use the adaptive control law to estimate the DO concentration without the need to estimate 'respiration' to determine the DO concentration.

As previously mentioned, the blower controller has been designed according to [113] and [36] to obtain $Q_{air.n}^{ref}(t) = Q_{air.n}(t)$. We assume that the $Q_{air.\max}(t) = Q_{air}^{ref}(t)$ controller is already in place, as illustrated in Figure 5-3.

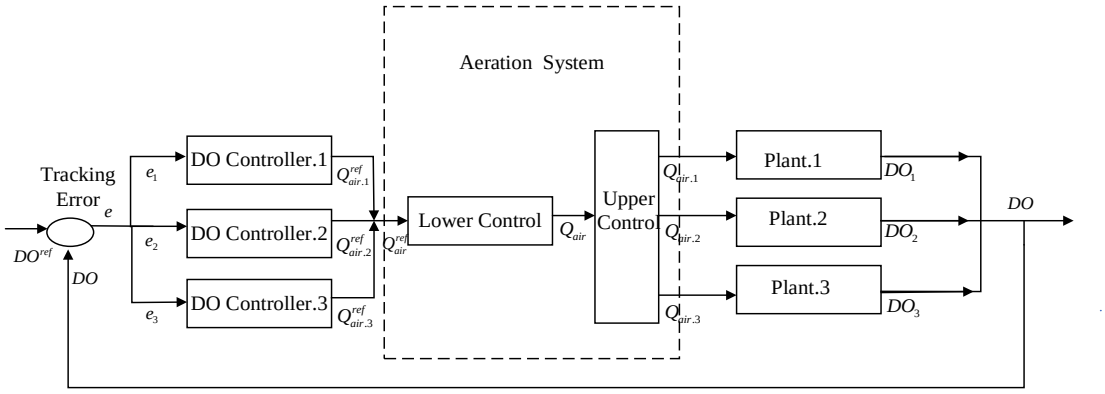

Figure 5- 3 Structure of an Overall Control System with a Blower and Three Bioreactors

In Chapter 5, the two-layer dynamic control is employed for the $DO_n(t)$ trajectory. In the sub-layer, the fuzzy supervised method addresses the distribution of air quantity to each of the bioreactors, while in the lower layer, the decentralized DMRAC method solves the DO_n trajectory tracking problem at each of the bioreactors.

5.5 Two-layers controller design

In the ASWWTP, multiple input-outputs, disturbance inputs, and uncertain state variables exist. Due to the complexity of the plant system, the designed controller must be capable of simultaneously rejecting disturbance inputs and ensuring stability and achieving highly efficient DO_n trajectory tracking performance for each of the bioreactors.

The DO_n controller is a hierarchical, two-layer control system. The lower-layer controller utilizes decentralized direct model reference adaptive control (DDMRAC),

while the upper-layer controller employs supervised fuzzy logical control. It exhibits strong robustness to the uncertainty of the controlled object through GA optimization. Additionally, decentralized DMRAC can adjust adaptive rates and enables automatic updating of control parameters for each individual bioreactor, leading to enhanced system robustness and performance.

5.5.1 Decentralized DMRAC design

The dynamic of DO_n in an input-output model is determined by rearranging the state space model equations (5.4-1) to (5.4-6). The state variables $X_{r.n}$, $X_{r.n}$, and S_n are not directly measurable online by a hard sensor due to the operational characteristics of the ASWWTP. The model reference adaptive controller estimates the respiration rate using an adaptive control law that is automatically updated online. This respiration rate is integrated into a single term in the state variable input-output model. Therefore, the oxygen transfer function is defined as shown in equation (5.4-7).

The $Q_{air.n}(t)$, $Q_{w.n}(t)$, $Q_{in.n}(t)$, and $DO_n(t)$ are variables of the dynamic equation (5.4.-3) for $DO_n(t)$, and these variables are unmeasurable online. They require an online update through decentralized DMRA control. The first-order dynamics of $DO_n(t)$ an input-output model is determined by both disturbance input and the state variable.

By substituting equations (5.4-5) and (5.4-7) into equation (5.4-3), the term $D_n(t)DO_{in.n}(t)$ is considerably smaller than other plant parameters; it can be neglected [134]. Finally, the dynamic of $DO_n(t)$, as a first-order model of a single input-output, and the design of the multiple DMRAC controller is based on equation (5.5.1-1), which can be rewritten as follows:

$$\begin{aligned}\frac{dDO_n}{dt} &= -a_{p.n}(t)\cdot DO_n(t) - c_{p.n}(t)\cdot f(DO_n(t) \\ &\quad + b_{p.n}(t)Q_{air.n}(t) + d_{p.n}\end{aligned} \tag{5.5.1-1}$$

Where: $a_{p.n}(t)$, $c_{p.n}(t)$, $b_{p.n}(t)$, and $d_{p.n}$ represents the plant model parameters and

$$\begin{aligned}a_{p.n}(t) &= \frac{Q_w(1+r)}{\beta V_{a.n}} \\ c_{p.n}(t) &= \frac{K_{0.n}X_n(t)}{Y_n}\frac{\mu_{\max.n}S_n(t)}{K_{s.n}+S_n(t)} \\ f(DO_n(t)) &= \frac{DO_n(t)}{K_{DO.n}+DO_n(t)} \\ b_{p.n}(t) &= \alpha_n(DO_{\max.n} - DO_n(t)) \\ d_{p.n} &= \beta DO_{\max.n}\end{aligned} \tag{5.5.1-2}$$

Where: $n = 1, 2, 3$, and n represents the number of bioreactors.

The parameter $d_{p.n}$ is known and varies slowly over time. The dynamics of DO are fast compared to the dynamics of biological state variables $X_n(t)$ and $S_n(t)$ [115, 171]. Conversely, the dynamics of the state variables $X_n(t)$ and $S_n(t)$ are slow variations

during biological response processes. Therefore, the parameter $c_{p.n}(t)$ is known to vary slowly over time.

The parameters of ASWWTP operations at various time scales were presented in [19]. The time scale of plant variables Q_r and Q_w are determined by the sub-layer control system, and their dynamics are slower compared to the time scale of $DO_n(t)$. The time scales of $Q_{in.n}(t)$, $S_{in.n}(t)$, and $X_{r.n}(t)$ are slower in comparison to $DO_n(t)$. Therefore, the plant parameter $a_{p.n}(t)$ is identified as having slower variation and remains unknown, as presented in [169]. The time scale of parameter $b_{p.n}(t)$ corresponds to the control time scale of $DO_n(t)$, resulting in rapid changes. Since the oxygen transfer constant $K_{La.i}(t)$ in equation (5.4-7) is known, the parameter $b_{p.n}(t)$ is also determined.

The model reference dynamics in each of the bioreactors are obtained through closed-loop control. This can be guaranteed that the control output ($DO_n(t)$) trajectory effectively tracks the dynamic ($DO_{m.ref.j}(t)$) trajectory, and therefore, the MRD equation reads:

$$\frac{dDO_{m.ref.j}}{dt} = -a_{m.j} DO_{m.ref.j}(t) + b_{m.j} DO_j^{ref}(t) \qquad (5.5.1\text{-}3)$$

Where: $j = 1, 2, 3$, and j represents the number of bioreactors. $DO_{m.ref.j}(t)$ denotes the number of model reference outputs. The model reference adaptive control parameters $a_{m.j}$ and $b_{m.j}$ are constants, and they can be selected by the designer. We selected $a_{m.j}$ and $b_{m.j}$ to be equal.

The model reference adaptive control law for each of the bioreactors can be chosen as following:

$$Q_{air.n}(t) = a_{DO.n}(t)DO_n(t) + a_{f.n}(t)\,f(DO_n(t)) + a_{DO_n^{ref}}(t)DO_n^{ref}(t) - \frac{\delta_k DO_{\max.n}}{b_{p.n}(t)} \tag{5.5.1-4}$$

Where: $n = 1, 2, 3$, and n is the number of bioreactors and $Q_{air.n}(t) \le Q_{\max.n}$.

The MRD is a linear dynamic (5.5.1-3) that can cancel the second and fourth terms of equation (5.5.1-1) in closed-loop, which can reduce the impact of the nonlinear and additive terms in equation (5.5.1-1).

The adaptive control law parameters consist of $a_{DO.n}(t)$, $a_{f.n}(t)$, and $a_{DO^{ref}.n}(t)$. We assume the existence of ideal adaptive control law parameters. Therefore, the MRD closed-loop system is expressed as follows:

$$\frac{dDO_n}{dt} = -(a_{p.n}(t) - b_{p.n}(t)a_{DO.n}(t)) - (c_{p.n}(t) - b_{p.n}a_{f.n}(t))\,f(DO_n(t)) + b_{p.n}(t)a_{DO^{ref}.n}(t)DO_n^{ref}(t) \tag{5.5.1-5}$$

Where: $n = 1, 2, 3$, and n represents the number of bioreactors.

$$-(a_{p.n}(t) - b_{p.n}(t))\hat{a}_{DO.n}(t) = -a_{m.n} \tag{5.5.1-6}$$

$$-(c_{p.n}(t) - b_{p.n}(t)\hat{a}_{f.n}(t)) = 0 \tag{5.5.1-7}$$

$$b_{p.n}(t)\hat{a}_{DO^{ref}.n}(t) = b_{m.n} \tag{5.5.1-8}$$

Where: $\hat{a}_{DO.n}(t)$, $\hat{a}_{f.n}(t)$ and $\hat{a}_{DO^{ref}.n}(t)$ are the ideal parameters. They can be achieved by rewriting equations (5.5.1-6), (5.5.1-7), and (5.5.1-8) as follows:

$$\hat{a}_{DO.n}(t) = \frac{-a_{m.n} + a_{p.n}(t)}{b_{p.n}(t)} \tag{5.5.1-9}$$

$$\hat{a}_{f.n}(t) = \frac{c_{p.n}(t)}{b_{p.n}(t)} \tag{5.5.1-10}$$

$$\hat{a}_{DO^{ref}.n}(t) = \frac{b_{m.n}}{b_{p.n}(t)} \tag{5.5.1-11}$$

where: $n = 1, 2, 3$, and n represents the number of bioreactors.

The parameter $b_{m.n}$ and $b_{p.n}(t)$ are known, while $b_{m.n}$ being designer selected and $b_{p.n}(t)$ updated according to equation (5.5.1-2). Therefore, the parameter $\hat{a}_{DO^{ref}.n}(t)$ is suitable for updating online from available data. Finally, the adaptive control law is expressed as:

$$\begin{aligned} Q_{air.n}(t) = {} & a_{DO.n}(t) DO_n(t) + a_{f.n}(t) f(DO_n(t)) \\ & + \frac{b_{m.n} DO_n^{ref}(t)}{b_{p.n}(t)} - \frac{\delta_i DO_{\max.n}}{b_{p.n}(t)} \end{aligned} \tag{5.5.1-12}$$

Where: $i = 1, 2, 3$, $n = 1, 2, 3$ and i, n are the numbers of bioreactors. The adaptive control law design is different from [15], it does not consider the parameter $a_{DO^{ref}.n}(t)$. The corresponding closed-loop dynamic is:

$$\begin{aligned}\frac{dDO_n}{dt} &= -(a_{p.n}(t) - b_{p.n}(t)a_{DO.n}(t))DO_n(t) \\ &\quad -(c_{p.n}(t) - b_{p.n}(t)a_{f.n}(t))\,f(DO_n(t)) \\ &\quad + b_{p.n}(t)\frac{b_{m.n}}{b_{p.n}(t)}DO_n^{ref}(t)\end{aligned} \tag{5.5.1-13}$$

Where: $n = 1, 2, 3$. n is the number of bioreactors.

The parameters $a_{p.n}(t)$ and $c_{p.n}(t)$ are unknown, while $b_{p.n}(t)$ is updated online based on corresponding parameters adaptive law. Additionally, the $a_{DO.n}(t)$ and $a_{f.n}(t)$ are updated by using available online data. These variables are relevant to both $DO_n(t)$ and $e_n(t)$. The error dynamics can be written as follows:

$$e_n(t) = DO_n(t) - DO_{m.ref.j} \tag{5.5.1-14}$$

Where: $n = 1, 2, 3$, $j = 1, 2, 3$, n and j represents the number of bioreactors.

The SISO $DO_n(t)$ first-order equation can be utilized to establish parameter adaptive control laws, contributing to the stability of the DDMRAC controller. The SISO $DO_n(t)$ includes the linear constants of uncertain state parameters. These parameters are not time-varying, and $d_{p.n}$ in the last term of equation (5.5.1-1) is linear and known. The parameter adaptive rates are derived by the parameter adaptive laws in equation (5.5.1-1), which read:

$$\frac{da_{DO_n}}{dt} = -\gamma_{zone.z.1}e_n(t)DO_n(t) \tag{5.5.1-15}$$

$$\frac{da_{f_n}}{dt} = -\gamma_{zone.z.2} e_n(t) f(DO(t)) \qquad (5.5.1\text{-}16)$$

Where: $n = 1, 2, 3$ and $z = 1, 2, 3$, n and z are the number of bioreactors.

The adaptive gain parameters $\gamma_{zone.z.1}$ and $\gamma_{zone.z.2}$ are sufficiently small and positive constants. These gains are subsequently utilized to control the parameters of decentralized adaptive rates (PDAS). The stability of the closed-loop system is guaranteed by the PDAS, which adjusts the adaptive rate to rapidly respond to the variable with time-varying responses during the ASWWTP process. The DDMRAC structure for each of the aeration stations is depicted in Figure 5-4.

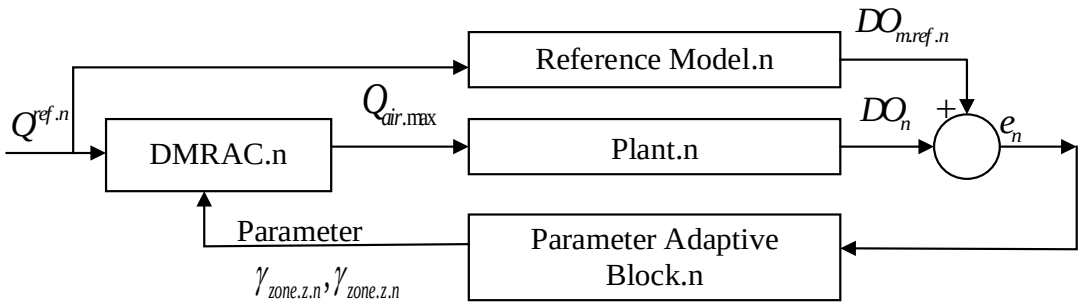

Figure 5- 4 The DDMRAC Structure for Each of the Three Bioreactors

5.5.2 Supervised fuzzy logic controller design

The supervised fuzzy logic control design (SFLC) ensures that constraints of aeration tank air capacity requirements are met (5.5.1-1), the structure of the SFLC is illustrated in Figure 5-5. The supervised fuzzy controller allocates airflow to each of the

bioreactors based on the magnitude of errors between $DO_n(t)$ and $DO_{m.ref.n}(t)$. If a large error is detected during online updates, a substantial quantity of air should be delivered to its bioreactor, otherwise, a minimal amount of air should be supplied. In the operational state condition of the ASWWTP, it is assumed that the sum of inputs from the three bioreactors must not exceed the quantity of air produced by the blower ($Q_{air.i}^{\text{supervisor}}(t) \neq Q_{air}^{\text{generate.blower.max}}(t)$). The sum of fuzzy control outputs ($Q_{air}^{\text{generate.blower.max}}(t)$) generated by the blower remains constant, where $Q_{air}^{\text{generate.blower.max}}(t) = \sum_{i=1}^{q} Q_{air.i}^{\text{supervisor}}(t)$. The soft switching method depends on fuzzy logic rules outlined in equations (5.5.2-1), (5.5.2-2), (5.5.2-3), and (5.5.2-4), (5.5.2-5).

$$\sum_{i=1}^{q} Q_{air.i}^{\text{supervisor}}(t) \leq Q_{air}^{\text{generate.blower.max}}(t) \qquad (5.5.2\text{-}1)$$

Where: $Q_{air.i}^{\text{supervisor}}$ is generated by a supervised fuzzy logical control output signal and $q = 1, 2, 3$. q is the number of bioreactors. $Q_{air}^{\text{generate.blower.max}}(t)$ is the amount of air produced by the blower.

The fuzzy logic inputs $W_j(DO_{air.real.i}(t))$ are updated online based on adjustments to DMRAC control law parameters, which represent multiple DMRAC real output DO concentrations. The membership function is defined utilizing the real inflow air of multiple DMRAC. In this case, both the sigmoid function and Gauss condition function are used to limit boundaries, and they can be expressed as follows:

$$\varphi(Q_{air.input.i}(t)) = \frac{1}{1+\exp(-a(Q_{air.input.i}(t)-c)} \tag{5.5.2-2}$$

$$\varphi(Q_{air.input.i}(t)) = \begin{cases} \exp(-Q_{air.input.i}(t)-c_1)^2 / d_1^2); \text{ left cure} \\ 1 \qquad\qquad\qquad\qquad \text{whenever } c_1 < c_2 \\ \exp(-Q_{air.input.i}(t)-c_2)^2 / d_2^2); \text{ right cure} \end{cases} \tag{5.5.2-3}$$

Where: a, c, and d are the parameters of the membership function used to define its shape.

The input air to each bioreactor is determined based on the error between the actual input of each DMRAC and the ideal input and the proportion of each error in the total error.

The fuzzy logic rules are defined as follows:

1. If $\frac{1}{2} < V(t) < 1$ and $\sum_{i=1}^{q} Q_{air.input.i}(t) \le Q_{air}^{\text{generate.blower.max}}(t)$;

Then $Q_{air.i.1}^{\text{superviosr}}(t) = Q_{air.input.i}(t)$. (5.5.2-4)

2. If $\frac{1}{2} < V(t) < 1$ and $\sum_{i=1}^{q} Q_{air.input.i}(t) > Q_{air}^{\text{generate.blower.max}}(t)$;

Then $Q_{air.i.2}^{\text{superviosr}}(t) = \frac{1}{2} \cdot \frac{Q_{air}^{\text{generate.blower.max}}(t)}{\sum_{i=1}^{q} Q_{air.input.i}(t)} Q_{air.input.i}(t)$. (5.5.2-5)

3. If $0 < V(t) < 1$ and $\sum_{i=1}^{q} Q_{air.input.i}(t) \le Q_{air}^{\text{generate.blower.max}}(t)$;

Then $Q_{air.i.1}^{\text{superviosr}}(t) = Q_{air.input.i}(t)$ (5.5.2-6)

4. If $0 < V(t) < 1$ and $\sum_{i=1}^{q} Q_{air.input.i}(t) > Q_{air}^{\text{generate.blower.max}}(t)$:

$$\text{Then } Q_{air.i.2}^{\text{superviosr}}(t) = \frac{1}{2} \cdot \frac{Q_{air}^{\text{generate.blower.max}}(t)}{\sum_{i=1}^{q} Q_{air.input.i}(t)} Q_{air.input.i}(t) \qquad (5.5.2\text{-}7)$$

Where: $q = 1, 2, 3$, q is number of bioreactors. $\sum_{i=3}^{q} e_{air.k}(t)$ is the sum of errors between each fuzzy logic output ($Q_{air.i}^{\text{superviosr}}(t)$) and each DMRAC input ($Q_{air.input.i}(t)$). $Q_{air}^{\text{generate.blower.max}}(t)$ is the amount of air produced by a blower and $Q_{air}^{\text{generate.blower.max}}(t) = \sum_{i=1}^{q} Q_{air.i.n}^{\text{supervisor}}(t)$.

The difference between each fuzzy logic output and each bioreactor input is represented as follows:

$$e_k^{\text{supervioser.}air}(t) = Q_{air.i.n}^{\text{superviosr}}(t) - Q_{air.input.i}(t) \qquad (5.5.2\text{-}8)$$

Where: $Q_{air.i.n}^{\text{superviosr}}(t)$ is the fuzzy logic output, $i = 1, 2, 3$, i is the number of bioreactors, $n = 1, 2$, n is the number of outputs with fuzzy rules. $Q_{air.total}^{\text{superviosr}}(t) = \sum_{i=3}^{q} Q_{air.i.n}^{\text{superviosr}}(t)$ is the desired optimal allocation state. $Q_{air.input.i}(t)$ represents each DMRAC input, $i = 1, 2, 3$, i is the number of bioreactors.

$$V_k(t) = e_k^{\text{superviosr.}air}(t) \cdot (\sum_{i=3}^{q} e_k^{\text{superviosr.}air}(t))^{-1} \qquad (5.5.2\text{-}9)$$

Where: $k = 1, 2, 3$, k is the number of bioreactors. $V_k(t)$ is never equal to zero. Fuzzy control output:

$$Fuzzy_{output}(t) = \sum_{i=3}^{q} Q_{air.i.n}^{\text{supervioser}}(t) = Q_{air}^{\text{generate.blower.max}}(t) \qquad (5.5.2\text{-}10)$$

Where: $i = 1, 2, 3$, i is the number of bioreactors. $n = 1, 2, 3, 4$, n represents the number of fuzzy controller outputs.

The supervised controller can guarantee that the constraint in equation (5.5.2-1) is never violated. It possesses the capability to enable the trajectory of $DO_n(t)$ to track the trajectory of $DO_{m.ref.n}(t)$ and accommodate minor fluctuations. Therefore, the performance of the fuzzy controller perfectly meets our expectations. However, at the specific operational state of the ASWWTP, it may not always be the case that all the air produced by the blower will be fully distributed to the input of multiple DDMRAC in the lower layer control system, as the designed fuzzy control rules. Hence, the optimization of the fuzzy logic controller is necessary to improve and refine the logic of air distribution. Further details on the optimization of the fuzzy logic control are described in the following section.

5.5.3 Supervise fuzzy logic control optimization by GA

The optimization of the supervised fuzzy logic control system facilitates the implementation of more reasonable airflow quantities into each of the bioreactors. Therefore, this two-layer control system can achieve an optimal state. On the other hand, the upper layer supervised fuzzy logic control system guarantees a more equitable distribution of airflow quantities for the lower layer MDMRAC control system. Various optimization methods for the fuzzy logic control have been reviewed in [134]. In this section, the genetic algorithm method is employed to optimize SFLC. This optimization aims to achieve satisfactory performance, ensure stability of the control system, and enhance anti-disturbance capabilities.

The process of the GA optimization is as follows: 1) Defining one chromosome group based on the condition of fuzzy logic rules (fitness function); 2) coding individuals, 3) Initializing the population with one chromosome; 4) Performing individual selection using the Rank Selection method; 5) Conducting crossover operation; 6) Implementing mutation operations; 7) Utilising the fitness function to assess individual performance in the group; 8) Selecting the fittest individuals; 9) Repeating steps 4 through 8; 10) Finally, establishing the optimal air quantity distribution logic, which is utilized as the output of the fuzzy logic control.

Fitness function

Defined one chromosome group entails not only incorporating the condition of fuzzy logic rules but also ensuring control system stability and minimizing the error between each DMRAC real output DO and ideal output DO. The fitness function can be defined as follows:

$$\text{fitness function}=\mu_1 \cdot \text{S}+\mu_2 \cdot \text{E}+\mu_3 \cdot \text{RT}+\mu_4 \text{FR} \tag{5.5.3-1}$$

Where: $\mu_1, \mu_2, \mu_3, \mu_4$ are the weight corresponding to each component.

The variable S represents the stability of the fuzzy logic control system, which is employed to ensure the stability of the SFLC and two-layer control system. It can be expressed as follows:

$$S = \frac{1}{M}\sum_{i=1}^{M}(DO_{M.\,real\,out}(t) - DO_{M.\,ideal\,out}(t))^2 \tag{5.5.3-2}$$

Where: $M = 1, 2, 3$, M represents the number of DMRAC controllers in the lower layer control system. $DO_{M.\,real\,out}(t)$ represents the lower layer DDMRAC real output DO. $DO_{M.\,ideal\,out}(t)$ represents the lower layer DDMRAC ideal output DO.

The variable E represents the ratio of the error to the total error between each DMRAC output DO and the ideal output DO. This error is utilized to achieve a reasonable oscillation; the error in each DMRAC's real output tracking the ideal output trajectory is denoted as $DO_{M.\,real\,out}(t) - DO_{M.\,ideal\,out}(t)$. Therefore, the variable E can be expressed as follows:

$$\text{Error}=\frac{1}{M}\sum_{i=1}^{M}\left|DO_{M.\,real\,out}(t) - DO_{M.\,ideal\,out}(t)\right| \tag{5.5.3-3}$$

Where: $M = 1, 2, 3$, M is the number of DMRAC controllers in the lower layer control system.

The variable RT represents the response speed of the fuzzy logic control system. This can be expressed as follows:

$$\text{Response Speed} = \frac{1}{R_{\text{RegulateOscillation}}(t) \bullet T_{AdjustmentTime}(t)} \tag{5.5.3-4}$$

Where: $R_{\text{RegulateOscillation}}(t)$ represents the percentage of the expected fuzzy logic control system output before stabilization. $T_{AdjustmentTime}(t)$ represents the time between the set error of the control system output and the end of the control system output stabilization. The regulated oscillation ($R_{\text{RegulateOscillation}}(t)$) depends on the FLCS system's maximum output ($Q_{air}^{\text{generate.blower.max}}(t)$) and the expected output (sum of MDDMRAC inputs) ($\sum_{i=1}^{q} Q_{air.input.i}(t)$), which can be expressed as follows:

$$R_{\text{RegulateOscillation}}(t) = \frac{(Q_{air}^{\text{generate.blower.max}}(t) - \sum_{i=1}^{q} Q_{air.input.i}(t))}{(\sum_{i=1}^{q} Q_{air.input.i}(t))} 100\% \tag{5.5.3-5}$$

The response speed depends on the regulation oscillation and settling time; if both decrease, it means a faster response speed. Typically, in a control system, a faster response time is desired for enhanced tracking performance and robustness. However, it is essential to consider the comprehensive oscillation frequency of the control system, as excessive oscillation can lead to instability and reduced reliability.

Fuzzy rules

The fuzzy rules represent four rules of fuzzy logic control. They can be written as follows:

$$R_i(t) = \alpha_1\left(\frac{1}{1+\left(\sum_{i=1}^{q} Q_{air.input.i}(t) - Q_{air}^{\text{generate.blower.max}}(t)\right)}\right) + \alpha_2\left(\frac{1}{1+\left|\sum_{k=3}^{q}\left(V_k(t) - e_k^{\text{supervioser}}(t)\right)\right|}\right)$$
$$+ \alpha_3\left(\frac{1}{1+\left|\left(V_k(t) - \frac{1}{2}\sum_{k=3}^{q} e_k^{\text{supervioser}}(t)\right)\right|}\right) + \alpha_4\left(\frac{1}{1+\left|\left(V_k(t) - 0\right)\right|}\right) \quad (5.5.3\text{-}6)$$

Where: $\alpha_1, \alpha_2, \alpha_3$, and α_4 represent the weight of each rule condition.

1) The first part of equation (5.5.3-6) considers a constraint. When $\sum_{i=1}^{q} Q_{air.input.i}(t)$ is close to $Q_{air}^{\text{generate.blower.max}}(t)$, the value of first part one tends to 1; otherwise, it tends to 0. Therefore, $\sum_{i=1}^{q} Q_{air.input.i}(t) = Q_{air}^{\text{generate.blower.max}}(t) = \sum_{i=3}^{q} Q_{air.i}^{\text{supervioser}}(t)$.

2) The second part of equation (5.5.3-6) calculates the proportion between $e_k^{\text{supervioser}}(t)$ and $\sum_{i=3}^{q} e_k^{\text{supervioser}}(t)$. if the difference between them is greater, the contribution is greater, with a contribution value of 1; otherwise, it is 0. Furthermore, a larger difference between them is expected. The $e_k^{\text{supervioser}}(t)$ is indicated in the equation (5.5.2-8).

3) The third part of equation (5.5.3-6) calculates the difference between each $e_k^{\text{supervioser.air}}(t)$ and half of $\sum_{k=3}^{q} e_k^{\text{supervioser}}(t)$. A bigger difference between them is more expected. Which $e_k^{\text{supervioser.}air}(t)$ represents the difference between each supervisor

output and decentralized DMRAC input. If $e_k^{\text{supervioser}.air}(t)$ is close to half of $\sum_{k=3}^{q} e_k^{\text{supervioser}}(t)$, the contribution is 1; otherwise, it is 0.

4) The last part of the equation (5.5.3-6) calculates the difference between each $e_k^{\text{supervioser}.air}(t)$ and 0, the smaller the difference between them, the batter.

The initial population is established using the initial parameters of each DMRAC in the lower layer control system, with each bioreactor deployed with a DMRAC to adjust the air inflow.

Individual selection

The Rank Selection method is utilized for individual selection. This method depends on the ranking individuals to make decisions, without direct dependence on the fitness function. In addition, it facilitates population diversity and offers greater stability compared to other methods such as handicap selection and hill-climbing selection. 1) Each individual ($Q_{air.i}^{\text{supervioser}}(t)$) is arranged from the first, ensuring that each individual ($Q_{air.i}^{\text{supervioser}}(t)$) is greater than one ($Q_{air.i}^{\text{supervioser}}(t)+1$). 2) The cumulative probability of each individual is calculated, which is the sum of from the first individual ($Q_{air.i}^{\text{supervioser}}(t)$) to the current individual ($\sum_{i=1}^{q} Q_{air.i}^{\text{supervioser}}(t)$, q is cumulative added quantity) in the chromosome group. This ensures that the current individual has a higher cumulative probability, while the individuals ranked behind have lower cumulative probabilities.

Therefore, the cumulative probability is utilized to calculate the probability of each individual selection (IS), and it can be expressed as follows:

$$IS(i) = \frac{1}{N} + \frac{2(i-1)}{N(N-1)} \qquad (5.5.3\text{-}7)$$

Where: i represents the number of individuals. N represents the size of the population. The purpose of calculating individuals' selection is to ensure the ranking order of individuals in the population, as required by the selection operation in the GA optimization.

Crossover operation and mutation operation

According to the selection operation, a pair of individuals ($Q_{air.i}^{\text{supervioser}}(t)$) is chosen. The crossover position in the gene sequence (fitness function) is then utilized to generate a new generation of individuals ($Q_{air.i}^{\text{supervioser}}(t)$). The crossover operation utilizes uniform crossover (UC) randomly generating 0 or 1 for each location of individual $Q_{air.i}^{\text{supervioser}}(t)$. It compares parent 1 or 2 ($Q_{air.i}^{\text{supervioser}}(t)-1$ or $Q_{air.i}^{\text{supervioser}}(t)-2$) with the random individual $Q_{air.i}^{\text{supervioser}}(t)$ and then establishes the appropriate mutation probability to maintain population diversity. Combined crossover and mutation operations to adjust the location position of individuals according to cumulative probability. Finally, the new generation of individuals ($Q_{air.i}^{\text{supervioser}}(t)$) is produced and placed into the new

generation population, waiting for the selection operation. Therefore, crossover and choose operations are repeated until the desired individuals ($Q_{air.i}^{supervioser}(t)$) are found. The supervised fuzzy logic control is optimized by the GA, which involves adjusting the parameter of the SFLC to achieve better global searching and decision-marking. Furthermore, it can simultaneously optimize stability, response speed, and anti-disturbance capability.

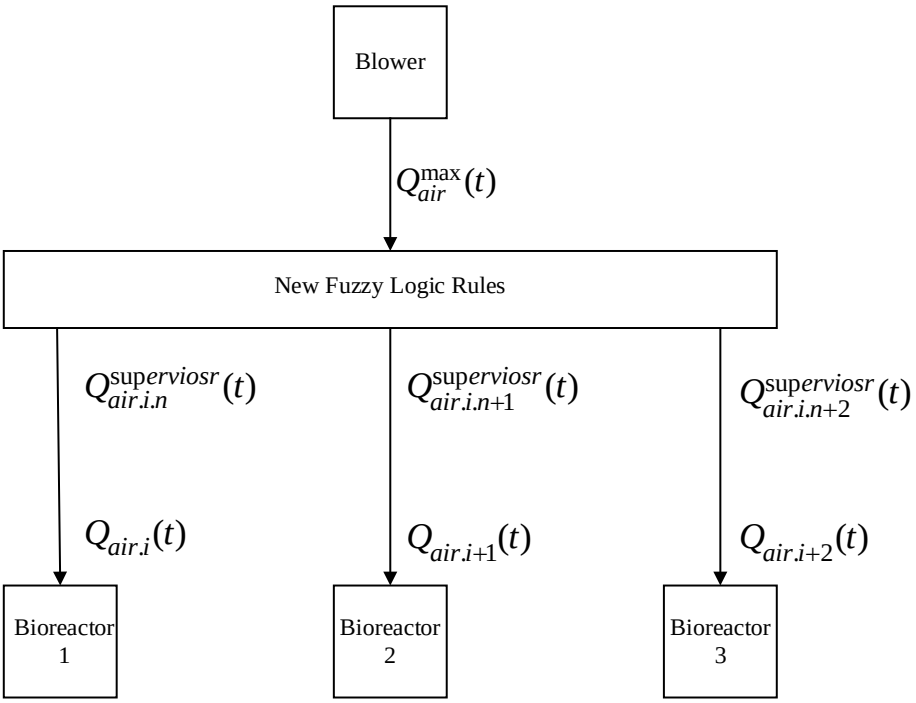

Figure 5- 5 The Structure of Airflow Distribute to Each Bioreactor

5.6 Stability Analysis of Supervised Fuzzy Logic Decentralized DMRAC System

5.6.1 Stability analysis of supervised fuzzy logic control

The air generated by the blower is distributed to the three bioreactors connected in series on the lower layer using a supervised fuzzy logic controller functioning as a soft distributor. It can determine the operation efficiency of each bioreactor. Therefore, the stability of the upper layer supervised fuzzy logic control system is crucial, as it directly impacts the stability of the lower layer control system and the overall control system.

The parameters of the supervised fuzzy logic control system may change over time due to internal and external disturbances. In addition, even with an optimized control system, there may be an accumulation of errors during long-term operation. Therefore, conducting stability analysis of the SFLC is necessary.

The online updates of SFLC outputs, represented by $\sum_{i=1}^{q} Q_{air.i}^{\text{supervioser}}(t)$, are provided by the fuzzy logic rules as shown equations from (5.5.2-2) to (5.5.2-5). Additionally, the values $DO_n(t)$ are updated online by parameter adaptive laws adjustments, which are represented in equations from (5.5.1-9) to (5.5.1-11). The error between the SFLC real

outputs $\sum_{i=1}^{q} Q_{air.i}^{\text{supervioser}}(t)$ and the ideal outputs $\sum_{i=1}^{q} Q_{air.ideal.i}^{\text{supervioser}}(t)$ is equal to $Q_{sum.error.air.output}^{\text{supervised}}(t)$, and it can be expressed as follows:

$$Q_{sum.error.air.output}^{\text{supervised}}(t) = \sum_{i=1}^{q} Q_{air.i}^{\text{supervioser}}(t) - \sum_{i=1}^{q} Q_{air.ideal.i}^{\text{supervioser}}(t) \qquad (5.6.1\text{-}1)$$

The error between MDDMRAC real outputs $\sum_{n=1}^{q} DO_n(t)$ and the MDDMRAC ideal output $\sum_{n=1}^{q} DO_{ideal.n}(t)$ is equal to $DO_{sum.error.n}(t)$, it can be written as follows:

$$DO_{sum.error.n}(t) = \sum_{n=1}^{q} DO_n(t) - \sum_{n=1}^{q} DO_{ideal.n}(t) \qquad (5.6.1\text{-}2)$$

The stability analysis for the SFLC is conducted using the Lyapunov function. The Lyapunov function is considered as follows:

$$V(t) = (Q_{sum.error.air.output}^{\text{supervised}}(t))^2 + (DO_{sum.error.n}(t))^2 \qquad (5.6.1\text{-}3)$$

The equation (5.6.1-3) can be expressed as follows:

$$V(t) = \left[\sum_{i=1}^{q} Q_{air.i}^{\text{supervioser}}(t) - \sum_{i=1}^{q} Q_{air.ideal.i}^{\text{supervioser}}(t)\right]^2 + \left[\sum_{n=1}^{q} DO_n(t) - \sum_{n=1}^{q} DO_{ideal.n}(t)\right]^2 \qquad (5.6.1\text{-}4)$$

Where: $q = 1, 2, 3$, and q represents the number of bioreactors.

The derivative of $V(t)$ (5.6.1-4) with respect to time can be rewritten as follows:

$$\frac{dV}{dt} = \frac{\partial V}{\partial(\sum_{i=1}^{q} Q_{air.i}^{\text{supervioser}}(t))} \frac{d(\sum_{i=1}^{q} Q_{air.i}^{\text{supervioser}}(t))}{dt} + \frac{\partial V}{\partial(DO_{sum.error.n}(t))} \frac{d(DO_{sum.error.n}(t))}{dt}$$

(5.6.1-5)

Where: $\frac{d(\sum_{i=1}^{q} Q_{air.i}^{\text{supervioser}}(t))}{dt}$ represents the rate of change of the fuzzy logic control system state $\sum_{i=1}^{q} Q_{air.i}^{\text{supervioser}}(t))$ over time. $\frac{d(DO_{sum.error.n}(t))}{dt}$ represents the rate of change of the MDDMRAC control system state $DO_{sum.error.n}(t)$ over time.

According to the operation condition of the two-layer control system, the upper layer fuzzy logic control output directs all the air quantity to become inputs for lower layer MDDMRAC controllers, as indicated in equation (5.5.2-1). Therefore, the $\frac{d(\sum_{i=1}^{q} Q_{air.i}^{\text{supervioser}}(t))}{dt}$ is equal to 0.

The equation (5.6.1-5) can be simplified as follows:

$$\frac{dV}{dt} = \frac{\partial V}{\partial(DO_{sum.error.n}(t))} \frac{d(DO_{sum.error.n}(t))}{dt} \qquad (5.6.1\text{-}6)$$

The equation (5.6.1-6) represents the difference between the ideal outputs and the real outputs of the lower layer MDDMRAC controllers.

The first part of the equation (5.6.1-6), $\frac{\partial V}{\partial(DO_{sum.error.n}(t))}$ represents the partial derivative of the Lyapunov function $V(t)$ with respect to the sum error of lower layer MDDMRAC output $DO_{sum.error.n}(t)$. Additionally, this partial derivative describes the rate of change of the Lyapunov function $V(t)$ under the $DO_{sum.error.n}(t)$ direction.

The second part of the equation (5.6.1-6), $\frac{d(DO_{sum.error.n}(t))}{dt}$ represents the rate of change of $DO_{sum.error.n}(t)$ over time, and it also directly indicates the proximity of the fuzzy logic control system to a stable state. Hence, let us consider the effects of $DO_{sum.error.n}(t)$ on the rate of change $\frac{dV}{dt}$ of the Lyapunov function. From the equations (5.6.1-5) and (5.6.1-6), it can be known as follows:

$$DO_{sum.error.n}(t) = \sum_{n=1}^{q} DO_n(t) - \sum_{n=1}^{q} DO_{ideal.n}(t) \qquad (5.5.1\text{-}7)$$

Therefore,

1) when $\sum_{n=1}^{q} DO_n(t) - \sum_{n=1}^{q} DO_{ideal.n}(t) = 0$, it implies that every output of MDDMRAC is an ideal DO output; thus $\frac{d(DO_{sum.error.n}(t))}{dt} = 0$, and the derivative of the Lyapunov function $\frac{dV}{dt} = 0$. Additionally, the SFLC system is stable. Moreover, during the operation of the blower in the ASWWTP, the air quantity generated by the blower is less or equal than the requirement of the three bioreactors; therefore, the $\sum_{n=1}^{q} DO_n(t)$ is equal to $\sum_{n=1}^{q} DO_{ideal.n}(t)$. Hence, the

fuzzy logic control system is stable.

2) When $\sum_{n=1}^{q} DO_n(t) - \sum_{n=1}^{q} DO_{ideal.n}(t) > 0$, according to the fuzzy rules, at least one output of the MDDMRAC deviates from the ideal output DO, resulting in the real output DO of the adaptive controller not tracking the ideal output DO. Hence, the multiple adaptive control system tends toward an unstable direction, leading to $\frac{d(DO_{sum.error.n}(t))}{dt} > 0$, and the derivative of Lyapunov function $\frac{dV}{dt} > 0$. Based on the Lyapunov function theory, the fuzzy logic control system is unstable.

3) When $\sum_{n=1}^{q} DO_n(t) - \sum_{n=1}^{q} DO_{ideal.n}(t) < 0$, basis on the fuzzy logic rules, each output DO of the multiple adaptive controllers is smaller than the ideal output DO, resulting in the multiple adaptive control system tending toward a stable direction. This leads to $\frac{d(DO_{sum.error.n}(t))}{dt} < 0$, and the derivative of the Lyapunov function $\frac{dV}{dt} < 0$. According to the Lyapunov function theory, the parameters of the fuzzy logic control are bounded by the sum of error between $\sum_{n=1}^{q} DO_n(t)$ and $\sum_{n=1}^{q} DO_{ideal.n}(t)$. Therefore, the fuzzy logic control system is stable.

The local stability analysis of the supervised fuzzy logic control, utilizing the Lyapunov function, confirms the stability of the control system under the condition where

$\sum_{n=1}^{q} DO_n(t) - \sum_{n=1}^{q} DO_{ideal.n}(t) < 0$. However, to ensure the stability requirements of the global two-layer control system, further analysis of the stability of the lower layer control system, which is the decentralized DMRAC system, is necessary.

5.6.2 Stability analysis of decentralized DMRAC system

Due to the adjustment of DO concentration in the ASWWTP operation employing a two-layer control system, the stability of this two-layer control system depends not only on the upper layer fuzzy control system but also on the lower layer adaptive control system. The stability of the supervised fuzzy logic control system has been proven as previously. Therefore, the stability of the lower layer DO decentralized DMRAC control system will be analysed using the Lyapunov function.

Let us consider the Lyapunov function in the following equation:

$$V_i(t) = \frac{1}{2} {e_k}^2(t) + \frac{1}{2} \Delta {a_{DO.n}}^2(t) + \frac{1}{2} \Delta {a_{f.n}}^2(t) \qquad (5.6.2\text{-}1)$$

Where: $i = 1, 2, 3$, $k = 1, 2, 3$, $n = 1, 2, 3$, i, k and n represent the numbers of bioreactors.

The error dynamic $e_k(t)$ is represented as the disparity between the dissolved oxygen dynamic $DO_n(t)$ and dissolved oxygen reference dynamic $DO_{m.ref.n}(t)$, as illustrated in equations (5.5.1-4). The ideal parameters $\Delta a_{DO.n}(t)$ and $\Delta a_{f.n}(t)$ are estimated by the

direct model reference adaptive control laws on-line and updated in equations (5.6.2-2) and (5.6.2-3).

$$\Delta a_{DO.n}(t) = a_{DO.n}(t) - \hat{a}_{DO.n}(t) \tag{5.6.2-2}$$

$$\Delta a_{f.n}(t) = a_{f.n}(t) - \hat{a}_{f.n}(t) \tag{5.6.2-3}$$

Where: $n = 1, 2, 3$, and n is the number of bioreactors.

Therefore, the derivative of the Lyapunov function is given by the equation:

$$\begin{aligned}\frac{dV_i(t)}{dt} = e_k(t)\dot{e}_k(t) + (a_{DO.n}(t) - \hat{a}_{DO.n}(t))(\dot{a}_{DO.n}(t) - \dot{\hat{a}}_{DO.n}(t))\frac{1}{\gamma_{zone.z.1}} \\ + (a_{f.n}(t) - \hat{a}_{f.n}(t))(\dot{a}_{f.n}(t) - \dot{\hat{a}}_{f.n}(t))\frac{1}{\gamma_{zone.z.2}}\end{aligned} \tag{5.6.2-4}$$

Where: $i = 1, 2, 3$, $k = 1, 2, 3$, $n = 1, 2, 3$, and $z = 1, 2$. i, k and n are the numbers of bioreactors. z represents the numbers of gains.

It follows from (5.5.1-14), (5.5.1-3) and (5.5.1-5) that:

$$\begin{aligned}\dot{e}_k(t) = &-(a_{p.n}(t) - b_{p.n}(t)a_{DO.n}(t))DO_n(t) \\ &-(c_{p.n}(t) - b_{p.n}(t)a_{f.n}(t))\,f(DO_n(t)) \\ &+ a_{m.n}DO_{m.ref.j}(t)\end{aligned} \tag{5.6.2-5}$$

Where: $k = 1, 2, 3$, $n = 1, 2, 3$, $j = 1, 2, 3$ and k, n, j are the numbers of bioreactors.

Now, add and subtract the term $a_{m.n}DO_n(t)$ on the right-hand side of equation (5.6.2-5) as follows:

$$\dot{e}_k(t) = -a_{m.n}e(t) - ((a_{p.n}(t) - b_{p.n}(t)a_{DO.n}(t)) - a_{m.n})DO_i(t) - (c_{p.n}(t) - b_{p.n}(t)a_{f.n}(t))f(DO_i(t)) \quad (5.6.2\text{-}6)$$

By substituting equations (5.5.1-6) and (5.5.1-7) into equation (5.6.2-6) yields:

$$\dot{e}_k(t) = -a_{m.n}e(t) + (a_{DO.n}(t) - \hat{a}_{DO.n}(t))b_{p.n}(t)DO_i(t) + (a_{f.n}(t) - \hat{a}_{f.n}(t))b_{p.n}(t)f(DO_i(t)) \quad (5.6.2\text{-}7)$$

Applying equations (5.6.2-6), (5.5.1-15), and (5.5.1-16) into equation (5.6.2-1) yields:

$$\begin{aligned}\frac{dV_i(t)}{dt} &= -a_{m.n}e_k^{\,2}(t) \\ &+(a_{DO.n}(t) - \hat{a}_{DO.n}(t))(e_k(t)b_{p.n}(t)DO_n(t) - e_k(t)DO_n(t) - \hat{a}_{DO.n}(t)\frac{1}{\gamma_{zone.z.1}}) \\ &+(a_{f.n}(t) - \hat{a}_{f.n}(t))(e_k(t)b_{p.n}(t)f(DO_n(t)) - e_k(t)f(DO_n(t)) - \hat{a}_{f.n}(t)\frac{1}{\gamma_{zone.z.2}})\end{aligned} \quad (5.6.2\text{-}8)$$

Where: $i = 1, 2, 3$, $n = 1, 2, 3$ and $k = 1, 2, 3$, $z = 1, 2$. i, n and k are the numbers of bioreactors. z represents the number of adaptive gains.

The right-hand side of equation (5.6.2-8) involves a quadratic function of $e_k(t)$. If $-a_{m.n} < 0$, then the condition of the right-hand side equation (5.6.2-8) is smaller than zero. The condition for $\frac{dV_i(t)}{dt} < 0$ to hold is proven in Appendix C. Therefore, equation (5.6.2-8) can be considered as $(\frac{dV_i(t)}{dt})^2$ being bound.

Consider the stability of the Lyapunov function result employing Barbalat's Lemma.

If $V_i(t)$ has a finite value as time goes to infinity, then $(\frac{dV_i(t)}{dt})^2$ is bounded.

Hence $\frac{dV_i(t)}{dt} < 0$, as time goes to infinity.

Barbalat's lemma can be applied to analysis the standard result of the Lyapunov function. When the ideal and real system parameters $a_{DO.n}(t), \hat{a}_{DO.n}(t), a_{f.n}(t)$, and $\hat{a}_{f.n}(t)$ are bounded, the output of the decentralized adaptive control system is capable of achieving asymptotic tracking of the model reference dissolved oxygen dynamics. The establishment of these boundaries requires three conditions to be met: 1) The initial condition in the ASWWTP dynamic must be sufficiently close to the equilibrium point. 2) The parameter adaptive laws (5.5.1-15) and (5.5.1-16) are also close enough to the equilibrium. 3) The parameter adaptive rates $\gamma_{zone.z.1}$ and $\gamma_{zone.z.2}$ are small enough. The simulation results utilizing real data will be employed to validate these three requirements.

Under the rules of supervised fuzzy logic control, each bioreactor receives airflow that is less than or equal to the ideal amount. Therefore, each bioreactor fails to satisfy the saturation input condition. However, each bioreactor satisfies the three conditions listed in Barbalat's lemma results. Finally, although each bioreactor may not always achieve perfect DO tracking performance during ASWWTP processes, it attains a balance

between control system efficiency and energy consumption. Thus, ensuring the stable operation of the purification system.

5.6.3 Analysis of the stability impact of feedback on two-layer control system

The two control systems can continue to operate only when the upper fuzzy logic control system receives fast DO feedback from the lower DDMRAC control system. In addition, if the lower control system cannot quickly adjust the output DO to track the ideal output DO trajectory, or there is a large deviation, it may affect the stability of the upper control system and even the stability of the global two-layer control system.

The two-layer control system is employed to regulate DO concentration during bioreactor operation. The stability of both the lower-layer and upper-layer control systems has been proven. The structure of this two-layer control system operates as a closed-loop feedback control system. Let us now consider the impact of feedback on the stability of this two-layer control system. The closed-loop transfer functions, as defined by equations (5.6.1-1) and (5.6.2-1), are expressed as follows:

$$H(DO)=\frac{(Q_{sum.error.air.output}^{supervised}(t))^2+(DO_{sum.error.n}(t))^2}{\frac{1}{2}{e_k}^2(t)+\frac{1}{2}{\Delta a_{DO.n}}^2(t)+\frac{1}{2}{\Delta a_{f.n}}^2(t)} \qquad (5.6.3\text{-}1)$$

The numerator is the upper layer SFLC control output, influenced by the lower layer MDDMRAC controller. The denominator is the lower layer MDDMRAC control input, which is influenced by the upper layer SFLC controller. Under the operational condition of the SFLC control system, all air generated by the blower is provided to the input of the lower layer MDDMRAC controller. Therefore, this closed-loop transfer function (5.6.3-1) is an equality transfer function. Additionally, the relationship between inputs and outputs is one-to-one, implying no amplification or reduction in the quantity of air. Finally, this closed-loop feedback system produces an output of consistent amplitude for all frequency input air quantities, without changing its phase.

The closed-loop feedback transfer function (5.6.3-1) can be rewritten as follows:

$$H(DO(t)) = \frac{(Q^{\sup ervised}_{sum.error.air.output}(t))^2 + (DO_{sum.error.n}(t))^2}{(Q^{\sup ervised}_{sum.error.air.output}(t))^2 + (DO_{sum.error.n}(t))^2} = 1 \qquad (5.6.3\text{-}2)$$

The gain of this closed-loop transfer function is equal to 1, and it does not have poles. The stability of the feedback cycle ensures that the system is stable and enhances the robust stability of the two-layer control system against external disturbances.

5.6.4 Global stability analysis of a two-layer control system

As mentioned before, in the stability analysis of a two-layer control system, the output of the upper layer control system has a direct impact on the stability of the lower layer control system because the input of the MDDMRAC control system depends on the output of SFLC control system. In addition, the output of the lower-layer controller is fed back to the input of the upper layer fuzzy control system. Therefore, the stability of the upper layer control system is also affected by the output of the lower layer control system.

The upper layer SFLC control system is stable at $\sum_{n=1}^{q} DO_n(t) - \sum_{n=1}^{q} DO_{ideal.n}(t) \le 0$, as indicated by the Lyapunov function $(\frac{dV}{dt})^2 \le 0$. Moreover, the lower layer DDMRAC control system is stable, as evidenced by the Lyapunov function $\frac{dV}{dt} \le 0$, with the adaptive control parameters bounded by $(\frac{dV}{dt})^2 \le 0$. Additionally, the feedback cycle between the two-layer controller is stable. Therefore, this two-layer DO concentration control system is stable when all the above conditions are met simultaneously. The MATLAB simulation utilized real data based on the University of Poland [161].

5.7 Simulation results and discussion

In this chapter, the MATLAB simulation utilizes the supervised fuzzy logic - DDMRAC applied to the ASWWTP with global parameters to prove stability and robustness. The controller is designed based on the limited ASWWTP parameters. Subsequently, real data from a single blower and a single bioreactor provided by [161] were used simulate the operational efficiency of the ASWWTP under various unknown disturbances. The three bioreaction tank initially contained equal amount of wastewater. The initial ASWWTP operation condition used in the simulation are $X_n(0)=15mg/l$, $S_n(0)=200mg/l$, $DO_n(0)=3mg/l$, $X_{r.n}(0)=18mg/l$, $DO_{\max.n}=7mg/l$, $S_{in.n}(0)=600mg/l$, $D_n(0)=3$, $DO_{in.n}(0)=0.5mg/l$. The process parameters are listed as follows: $Y_n=0.65$, $r_n=0.6$, $\beta_n=0.2$, $a_n=3.34m^{-3}$, $\delta_n=3.45h^{-1}$, $K_{0.n}=0.5$. The kinetic parameters are $\mu_{\max.n}=0.15mg/l$, $K_{s.n}=100mg/l$, $K_{DO.n}=2mg/l$. The disturbance inputs $S_{in.n}(t)$, $D_n(t)$, and $DO_{in.n}(t)$ change over time, as depicted in Figures 5-6, 5-7, and 5-8.

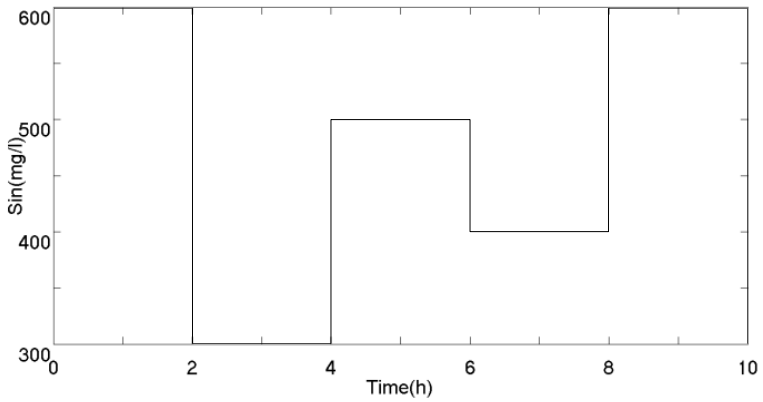

Figure 5- 6 Influent Substrate $S_{in.n}(t)$

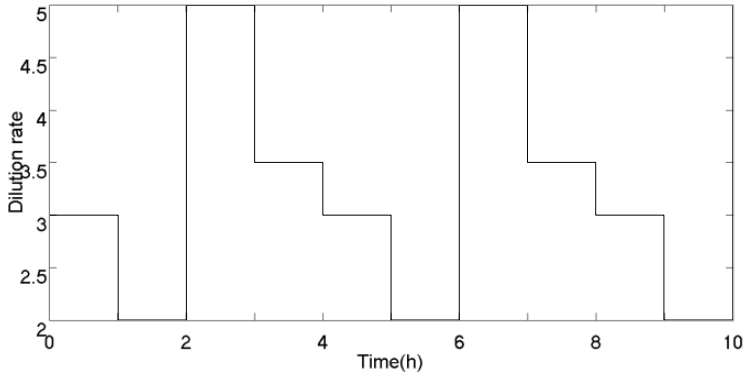

Figure 5- 7 Dilution Rate $D_n(t)$

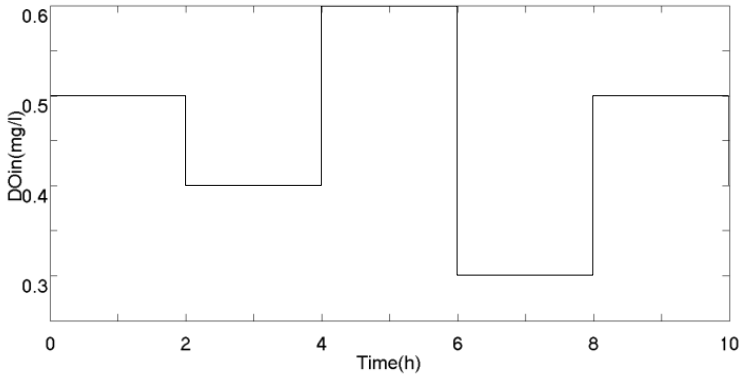

Figure 5- 8 Influent Dissolved Oxygen $DO_{in.n}(t)$

The reference model adaptive control parameters for each biological reaction station were determined using parameters $a_{m.n} = 2$ and $b_{m.n} = 2$. The parameter $DO_{m.ref.j}(t)$ was assumed to be piecewise constant. Figure 5-9 demonstrates that this two layer control system output $DO_n(t)$ can rapidly and stably track $DO_{m.n}(t)$, indicating good tracking performance and stability. Figure 5-10 demonstrate that this two layer control system can reject disturbance inputs while maintaining good tracking performance of output $DO_n(t)$ for $DO_{m.ref.j}(t)$, further demonstrating the stability of the control system.

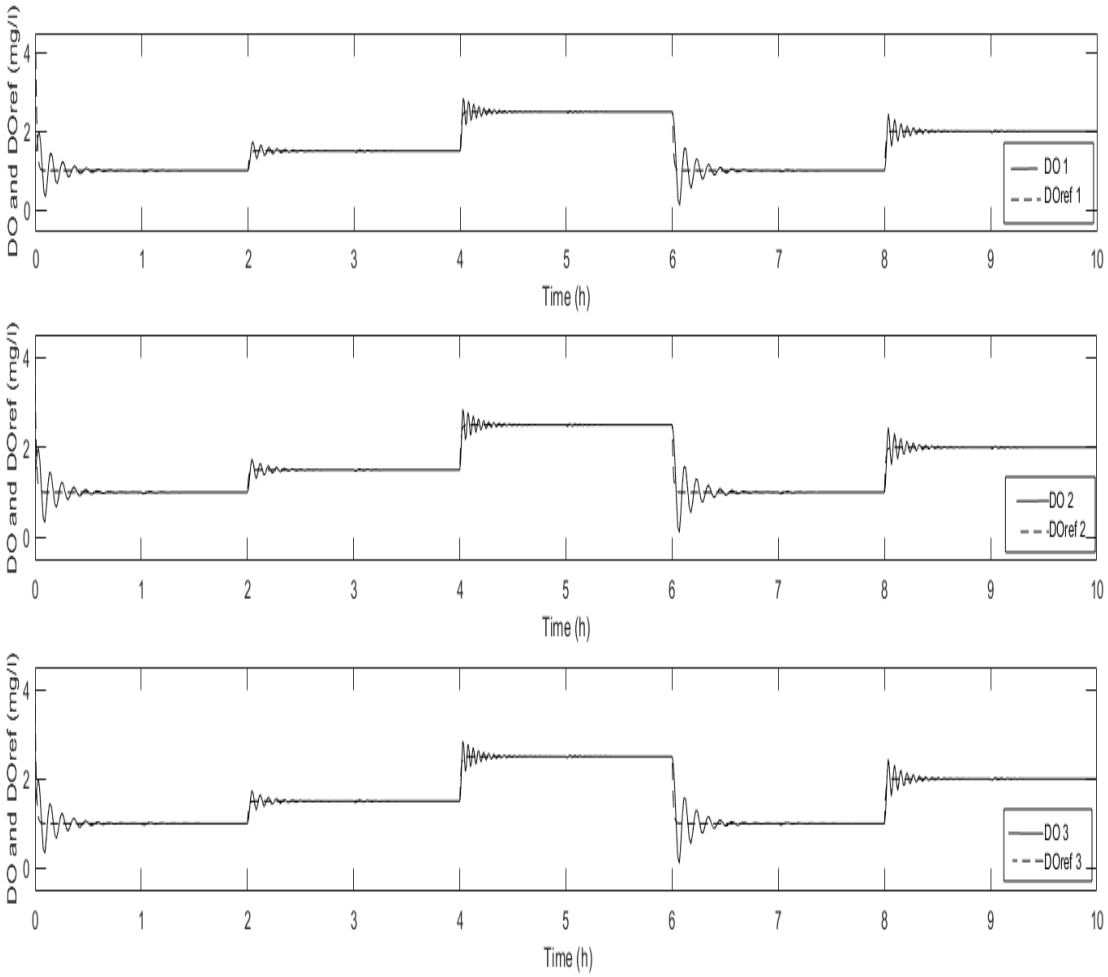

Figure 5- 9 The trajectories of $DO_n(t)$ and $DO_{m.ref.j}(t)$ under conditions of no disturbance inputs and slow adaptive rates ($\gamma_{z.1} = 0.5$, $\gamma_{z.2} = 0.5$), under Supervised Fuzzy DDMRAC

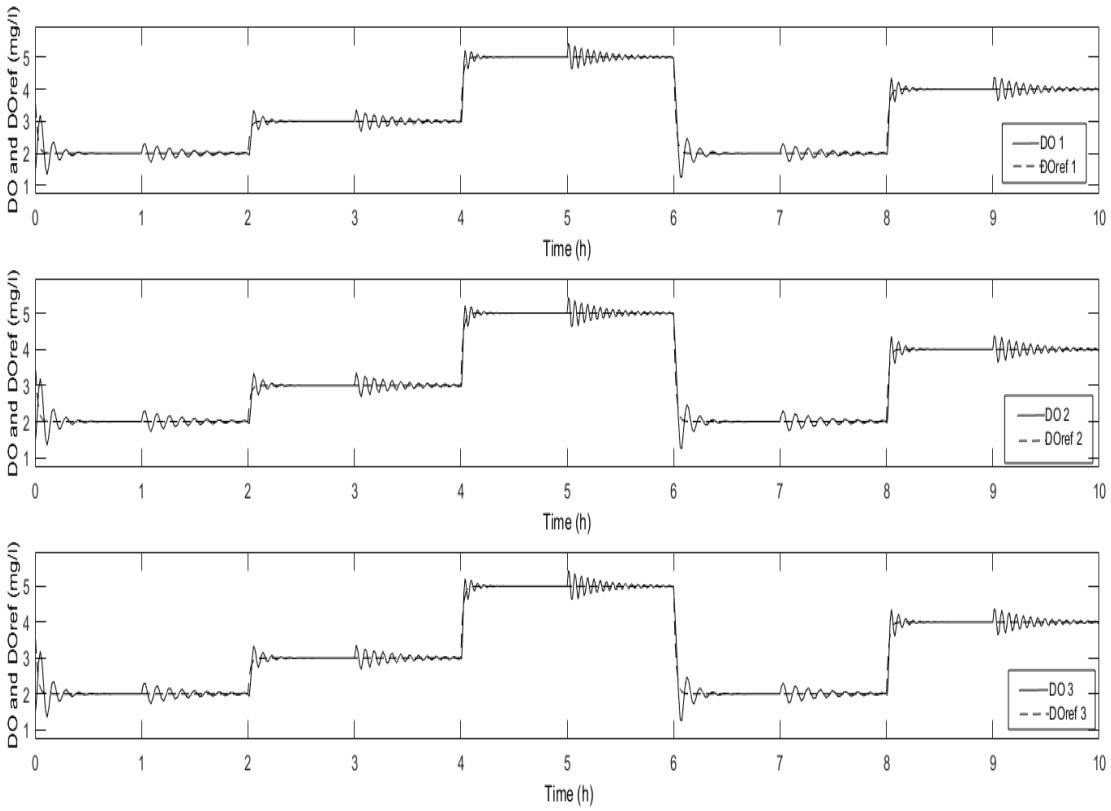

Figure 5- 10 The trajectories of $DO_n(t)$ and $DO_{m.ref.j}(t)$ under conditions of disturbance inputs and slow adaptive rates ($\gamma_{z.1} = 0.5$, $\gamma_{z.2} = 0.5$), under Supervised Fuzzy DDMRAC

Comparing the results shown in Figures 5-9 and 5-10 with those in Figures 5-11 and 5-12 demonstrates that the $DO_n(t)$ trajectory can be rapidly tracked to the $DO_{m.ref.j}(t)$ trajectory under the supervised fuzzy logic control of GA optimization. In addition, Figure 5-12 also shows that the $DO_n(t)$ trajectory has good tracking performance, and in the presence of input disturbances. The trajectory of DO concentration further confirms the stability of the two-layer control system. Therefore, we can conclude that this two-layer control system is stable. Moreover, it can be ensured that the feedback

loop in this two-layer control system is stable. These results demonstrate the feasibility of a single blower supplying air to three bioreactors and the effectiveness of optimization through GA in reducing energy consumption in the two-layer control system for ASWWTP operation.

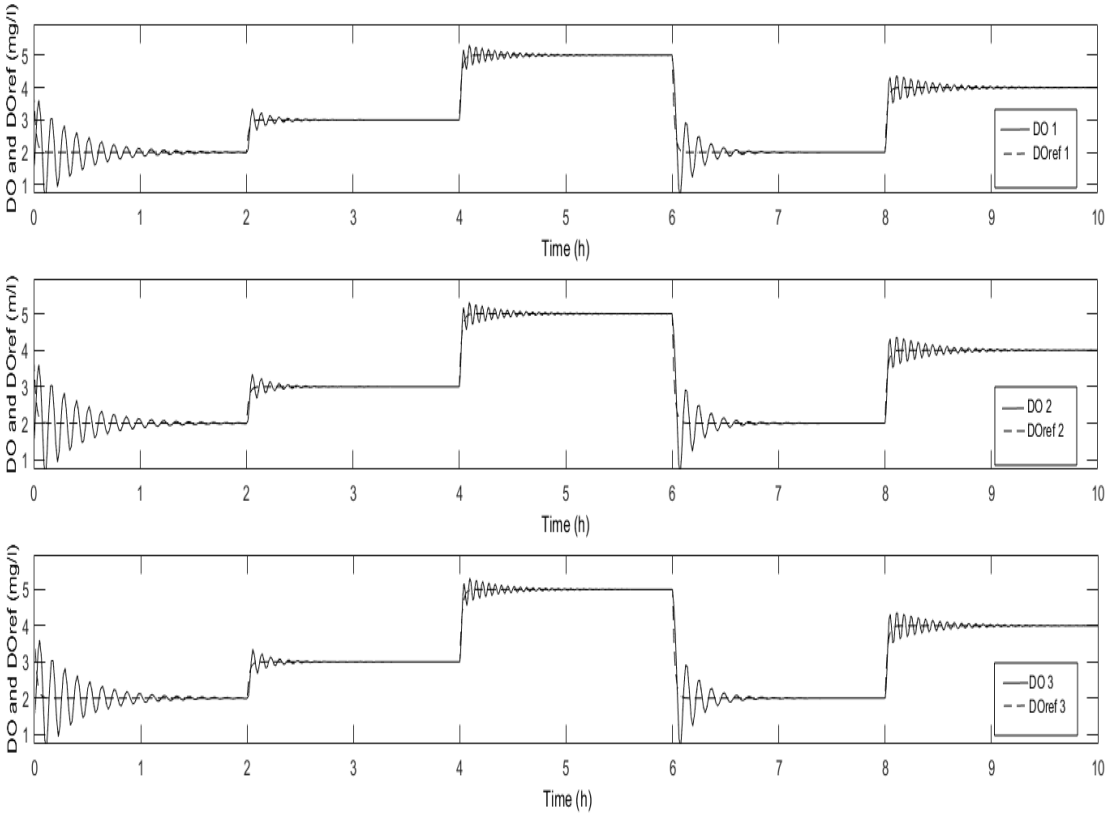

Figure 5- 11 The trajectories of $DO_n(t)$ and $DO_{m.ref.j}(t)$ under conditions of no disturbance inputs and slow adaptive rates ($\gamma_{z.1} = 0.5$, $\gamma_{z.2} = 0.5$), under Supervised Fuzzy DDMRAC Optimized by GA

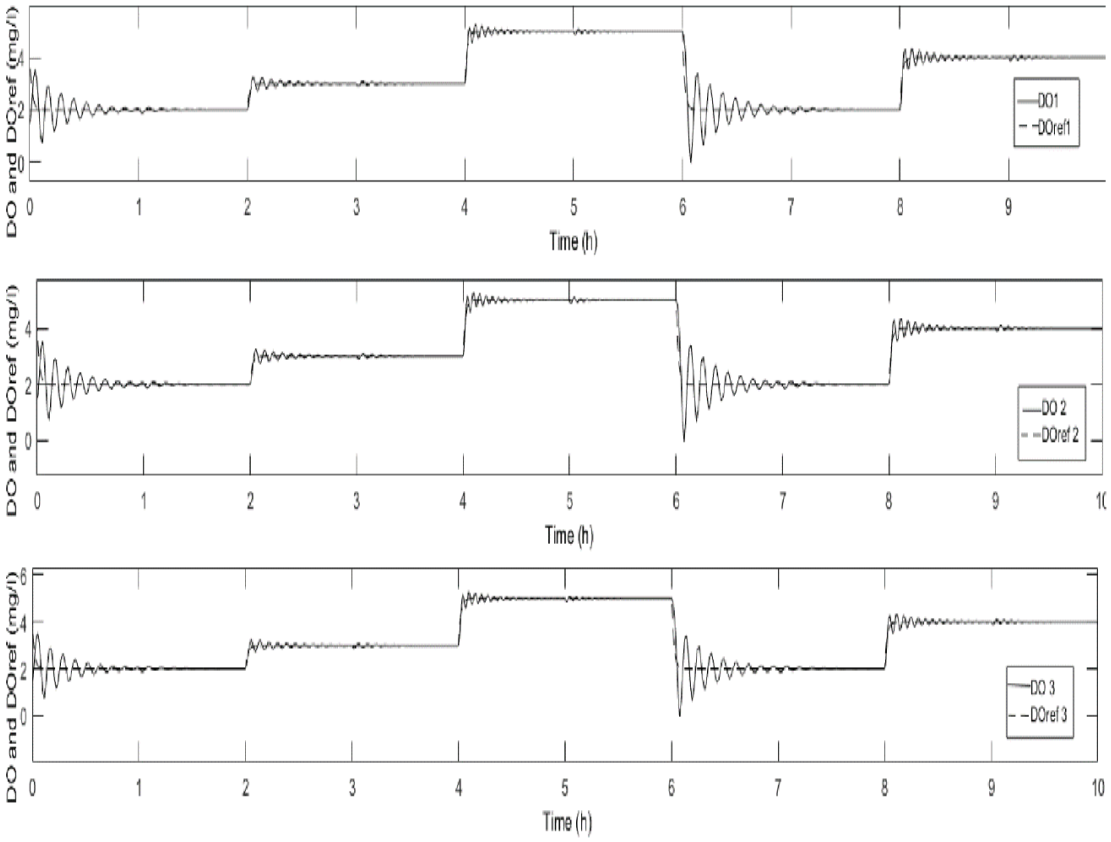

Figure 5- 12 The trajectories $DO_n(t)$ and $DO_{m.ref.j}(t)$ under conditions of disturbance inputs and slow adaptive rates ($\gamma_{z.1}=0.5$, $\gamma_{z.2}=0.5$), under Supervised Fuzzy DDMRAC Optimized by GA

Subsequently, the initial operating conditions of Figure 5-13 are consistent with those of Figure 5-12. Furthermore, using fast adaptive gain, $DO_{m.ref.j}(t)$ remains piecewise constant. The response trajectory of $DO_n(t)$ is shown in Figure 5-13, indicating that the closed-loop two-layer control system becomes unstable. This instability arises because of long-term oscillations, causing the adaptive control system to exceed the expected output trajectory $DO_n(t)$ of the underlying control system before reaching stability. In

addition, due to the unstable output of the lower layer, the upper layer feedback fuzzy control system becomes unstable, so that the global two-layer control system is unstable. This validates the stability analysis presented in Chapter 5.6.

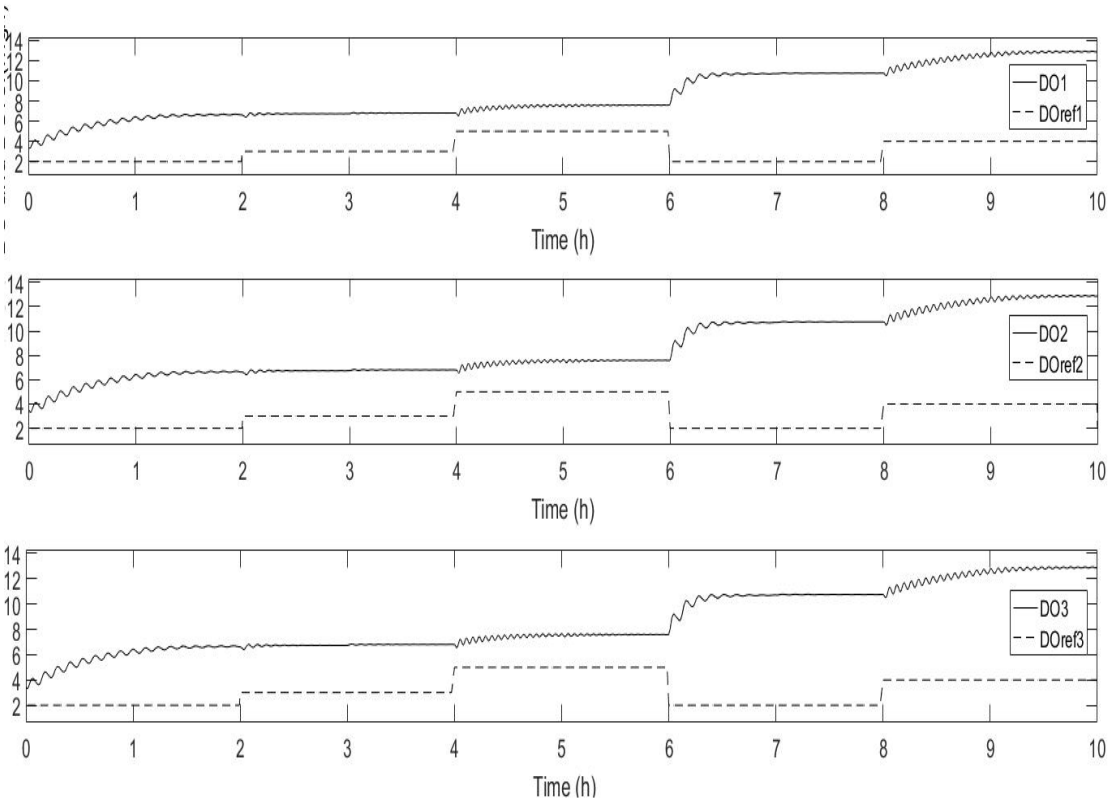

Figure 5- 13 The response of $DO_n(t)$ becomes unstable under the conditions of no disturbance inputs and fast adaptive rates ($\gamma_{z.1} = 5,\ \gamma_{z.2} = 5$), under Supervised Fuzzy DDMRAC optimized by GA

In the next experiment, the same initial system condition as before was utilized, but plant operation involved a large input disturbance. Figure 5-14 demonstrates that the

output $DO_n(t)$ trajectory of the two-layer control system is unstable to track the reference model $DO_{m.ref.j}(t)$ trajectory due to large input disturbance. This occurs because the large disturbance input exceeds the robust boundary of the adaptive control, causing the adaptive control law parameters to be unable to update online in a timely manner. In this specific two-layer feedback control system, the output of the adaptive control impacts the stability of the fuzzy logic control system. Therefore, the lower layer adaptive control becomes unstable, leading to instability in the upper layer fuzzy logic control. Finally, the two-layer control system becomes unstable during ASWWTP operation when subjected to a large enough input disturbance.

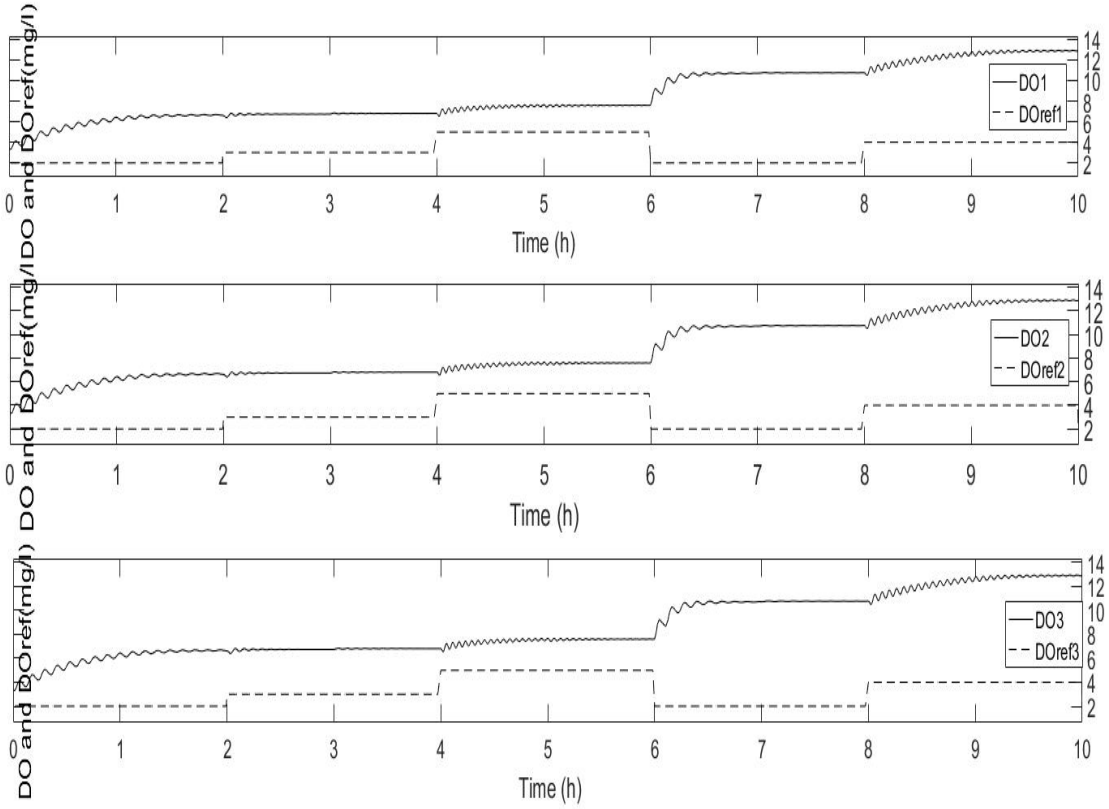

Figure 5- 14 The response of $DO_n(t)$ becomes unstable with large disturbance inputs and slow adaptive rates ($\gamma_{z.1}=0.5$, $\gamma_{z.2}=0.5$), under Supervised Fuzzy DDMRAC Optimized by GA

At the initial conditions of ASWWTP, it was far from the predicted equilibrium point $X_n(0)=30mg/l$, $S_n(0)=860mg/l$, $X_{r.n}(t)=35mg/l$, $DO_n(0)=7mg/l$. The corresponding $DO_n(t)$ response is illustrated in Figure 5-15, indicating that the two-layer control system is unstable. Due to the starting point of ASWWTP operation being far from the predicted equilibrium point of the adaptive controller, the response of the adaptive control system exhibits excessive oscillations, resulting in instability. Furthermore, due to this two-layer feedback control system, if the lower layer DDMRAC control system

is unstable, the upper layer fuzzy logic control system is also considered unstable. Therefore, the output $DO_n(t)$ trajectory of the two-layer control system confirms the stability analysis results presented in Chapter 5.6.

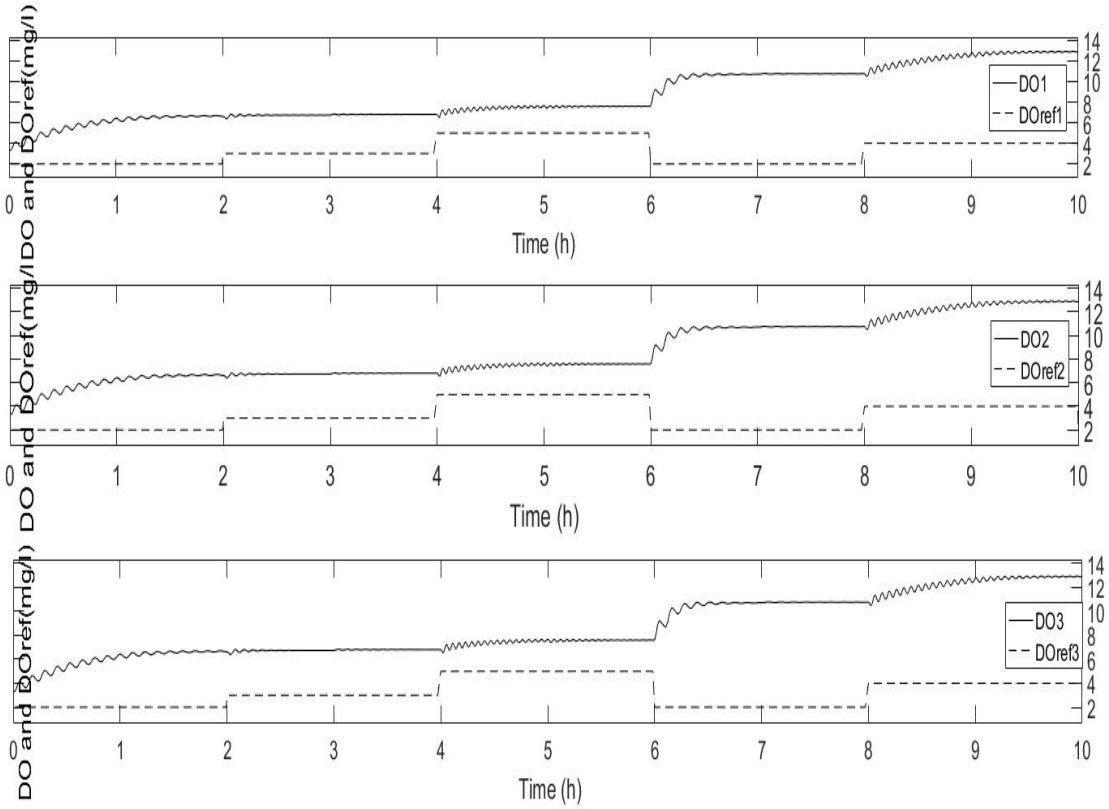

Figure 5- 15 The initial operation state of the ASWWTP exhibits significant deviation from the predicted equilibrium point. The dynamic of $DO_n(t)$ fail to track the trajectory of $DO_{m.ref.j}(t)$, rendering the system unstable under conditions characterized by the absence of disturbance inputs and slow adaption rates ($\gamma_{z.1} = 0.5$, $\gamma_{z.2} = 0.5$), utilizing Supervised Fuzzy DDMRAC optimized by GA

5.8 Conclusions

This chapter addresses nutrient removal at the ASWWTP by solving the dissolved oxygen concentration trajectory tracking issue. Considering the large volume of wastewater, minimal construction, and minimal energy consumption, a new structure of the ASWWTP is proposed. This structure is composed of three bioreactors with a single blower and a single sedimental unit. The blower operates under the specific conditions. The mathematical model of ASWWTP is formed by rewriting the ASM 2d model based on the principles of mass balance and ion kinetic energy conservation.

A dissolved oxygen concentration supervised fuzzy logic DMRAC system is designed based on limited ASWWTP parameters and applied to the mathematical model of global ASWWTP parameters. The control parameters are adjusted through MATLAB simulations to meet design requirements, with the fuzzy logic optimized by a GA. The MATLAB simulation results demonstrate ASWWTP's ability to process large volumes of wastewater efficiently, its stability, and its capability to resist disturbances. The stability of the supervised fuzzy logic DMRAC system is further ensured using the Lyapunov function.

CHAPTER 6 CONCLUSION AND FUTURE RESEARCH WORK

6.1 Conclusions

In this thesis, we address the nutrient removal in ASWWTP by solving the trajectory tracking issue of dissolved oxygen concentration. We construct various ASWWTP architectures tailored to specific wastewater volume treatment requirements and design distinct types of adaptive control systems for different operational conditions of ASWWTP. The objective is to achieve stability and efficiency in ASWWTP operation, along with the ability to withstand disturbances. Each ASWWTP architecture's mathematical model is developed by rewriting the ASM 2d model, adhering to the principles of mass balance and ion conservation of kinetic energy. According to different wastewater treatment requirements, from the architecture, mathematical model, and control system, it is classified as follows:

Firstly, we established an ASWWTP architecture consisting of a single bioreactor unit with a single blower and a single settlement unit, with the blower operating under ideal conditions. This configuration addresses the requirements for small wastewater volume and minimized construction space. The mathematical model of the ASWWTP is

developed by rewriting the ASM 2d model, based on the principles of mass balance and ion kinetic energy conservation.

Nutrient removal in ASWWTP is achieved by solving the trajectory tracking problem. Designing this control system relies on limited ASWWTP parameters and is implemented to global ASWWTP parameters. The adaptive control parameters are adjusted using MATLAB simulations, ensuring the stability and high efficiency of the ASWWTP, as well as its ability to resist disturbances. The stability of the DMRAC system is further validated using the Lyapunov function.

Secondly, based on the existing ASWWTP architecture, we address the issue of the blower overproducing and delivering excess air volume. A DO concentration DMRAC system with a filter function is designed using limited ASWWTP parameters and applied to the mathematical model of global ASWWTP parameters. The adaptive control parameters are adjusted through MATLAB simulation to obtain the expected control system requirements. The MATLAB simulation results show that the adaptive control system can filter out excess air volume while maintaining the stability and good efficiency of the ASWWTP and has anti-interference ability. The stability of the DMRAC system with the filter function is further validated using the Lyapunov function.

Finally, a new architecture of ASWWTP has been established to handle the large wastewater volumes while minimizing construction requirements. This architecture is composed of three bioreactors with a single blower unit and a single sedimental unit. The mathematical model of ASWWTP was developed by rewriting the ASM 2d model, adhering to the principle of mass balance and conservation of ion kinetic energy.

The supervised fuzzy logic direct model reference adaptive control system was designed using limited ASWWTP parameters and applied to the mathematical model of global ASSWTP parameters to ensure stability and high efficiency operational. The adaptive control parameters were adjusted through MATLAB simulation, and the fuzzy logic control system was further optimized using genetic algorithm to achieve the optimal regulation of dissolved oxygen concentration.

The MATLAB simulation results proved the stability and efficiency of ASWWTP, as well as its anti-interference ability. Additionally, the stability of the fuzzy logic DMRAC system is further proven by analysing both global and local control system using the Lyapunov function

6.2 Future research work

Based on the several valuable experiments conducted in this thesis, further research on activated sludge wastewater treatment plants can be summarized as bellows:

In Chapter 3, we studied the ideal state of the blower. But in further discussion, we will consider the time delay of the blower in different switching cycles. This characteristic is used to adjust the DO concentration in the bioreactor to solve the nutrient removal problem of wastewater containing specific chemical elements in ASWWTP.

In Chapter 4, we focused on how to use a blower actuator to solve the problem of nutrient removal in the ASWWTP by eliminating excess air. In the future we should consider increasing the amount of wastewater to solve the excess air problem.

In chapter 5, we demonstrated the use of a single blower supplying oxygen to multiple bioreactors arranged in series, confirming its high efficiency for nutrient removal. Further investigation could consider the utilization of multiple blowers in series to provide oxygen to the activated sludge across multiple bioreactors, thus enhancing the efficacy of wastewater purification in the ASWWTP.

LIST OF PUBLICATIONS

Conference Paper

[1] Li, M. and M.A. Brdys*, *Direct model reference adaptive control of nutrient removal at activated sludge wastewater treatment plant.* 2015 20th International Conference on Methods and Models in Automation and Robotics (MMAR), 2015: p. 608-613.

Book Chapter

[1] Li, M., *Design and Stability Analysis of Fuzzy-Based Adaptive Controller for Wastewater Treatment Plant*, in *Modern Fuzzy Control Systems and Its Applications*. 2017, IntechOpen.

APPENDIX A Mathematic Model of ASWWTP, Derivation of The DMRAC Controller and Stability Analysis

A mathematical model of the wastewater treatment plant.

$$\frac{dX}{dt} = \mu(\mathrm{t})X(t) - D(\mathrm{t})(1+r)\ X + rD(t)X_r(t) \tag{1}$$

$$\frac{dS}{dt} = -\frac{\mu(t)X(t)}{Y} - D(t)(1+r)S(t) + D(t)S_{in}(t) \tag{2}$$

$$\frac{dDO}{dt} = -\frac{K_0\mu(t)X(t)}{Y} - D(t)(1+r)DO(t) + k_{La}(Q_{air}(t))(DO_{\max} - DO(t)) + D(t)DO_{in}(t) \tag{3}$$

$$\frac{dX_r}{dt} = D(t)(1+r)X(t) - D(t)(\beta + r)X_r(t) \tag{4}$$

$$\mu(t) = \mu_{\max}\frac{S(t)}{K_s + S(t)} \cdot \frac{DO(t)}{K_{DO} + DO(t)} \tag{5}$$

Where:

$$D(t) = \frac{Q_{in}}{V_a}\ ;\quad r = \frac{Q_r}{Q_{in}}\ ;\quad \beta = \frac{Q_w}{Q_{in}} \tag{6}$$

The function $k_{La}(Q_{air}(t))$ is the oxygen transfer and depends on the aeration actuating system and sludge conditions. It is assumed as:

$$k_{La}(t) = \alpha Q_{air}(t) + \delta$$

Input-output model:

$$\frac{dDO}{dt} = -\frac{K_0\mu(t)X(t)}{Y} - D(t)(1+r)DO(t) + (\alpha Q_{air}(t)+\delta)(DO_{\max} - DO(t)) + D(t)DO_{in}(t) \tag{3}$$

$$\frac{dDO}{dt} = -D(t)(1+r)DO(t) - \frac{K_0X(t)}{Y}\mu(t) + (\alpha Q_{air}(t)+\delta)(DO_{\max} - DO(t)) + D(t)DO_{in}(t) \tag{7}$$

$$\frac{dDO}{dt} = -D(t)(1+r)DO(t) - \frac{K_0 X(t)}{Y}\mu(t) + (\alpha Q_{air}(t)+\delta)(DO_{\max} - DO(t)) + D(t)DO_{in}(t) \quad (8)$$

$$\frac{dDO}{dt} = -D(t)(1+r)DO(t) - \frac{K_0 X(t)}{Y}\mu(t) + (\alpha Q_{air}(t)+\delta)(DO_{\max} - DO(t)) + D(t)DO_{in}(t) \quad (9)$$

$$\frac{dDO}{dt} = -D(t)(1+r)DO(t) - \frac{K_0 X(t)}{Y}\mu(t) + (\alpha Q_{air}(t)(DO_{\max} - DO(t))) + (\delta(DO_{\max} - DO(t))) + D(t)DO_{in}(t) \quad (10)$$

$$\frac{dDO}{dt} = -D(t)(1+r)DO(t) - \frac{K_0 X(t)}{Y}\mu(t) + \alpha Q_{air}(t)(DO_{\max} - DO(t)) + \delta DO_{\max} - \delta DO(t) + D(t)DO_{in}(t) \quad (11)$$

$$\frac{dDO}{dt} = -D(t)(1+r)DO(t) - \delta DO(t) - \frac{K_0 X(t)}{Y}\mu(t) + \alpha Q_{air}(t)(DO_{\max} - DO(t)) + \delta DO_{\max} + D(t)DO_{in}(t) \quad (12)$$

$$\frac{dDO}{dt} = -(D(t)(1+r)+\delta)DO(t) - \frac{K_0 X(t)}{Y}\mu(t) + \alpha Q_{air}(t)(DO_{\max} - DO(t)) + \delta DO_{\max} + D(t)DO_{in}(t) \quad (13)$$

$$D(t) = \frac{Q_{in}}{V_a} \quad (14), \qquad \mu(t) = \mu_{\max}\frac{S(t)}{K_s + S(t)} \cdot \frac{DO(t)}{K_{DO} + DO(t)} \quad (15)$$

Apply (14), (15) into (13)

$$\frac{dDO}{dt} = -(\frac{Q_{in}}{V_a}(1+r)+\delta)DO(t) - \frac{K_0 X(t)}{Y}\frac{\mu_{\max} S(t)}{K_s + S(t)}\frac{DO(t)}{K_{DO} + DO(t)} + \alpha Q_{air}(t)(DO_{\max} - DO(t)) + \delta DO_{\max} + D(t)DO_{in}(t) \quad (16)$$

The term $D(t)DO_{in}(t)$ is small it is neglected.

$$\frac{dDO}{dt} = -(\frac{Q_{in}}{V_a}(1+r)+\delta)DO(t) - \frac{K_0 X(t)}{Y}\frac{\mu_{\max} S(t)}{K_s + S(t)}\frac{DO(t)}{K_{DO} + DO(t)} + \alpha Q_{air}(t)(DO_{\max} - DO(t)) + \delta DO_{\max} \quad (17)$$

The resulting input –output model reads:

$$\frac{dDO}{dt} = -a_p(t)DO(t) - c_p(t)\,f(DO(t)) + b_p(t)Q_{air}(t) + \delta DO_{\max} \tag{18}$$

where $a_p(t), c_p(t), b_p(t), d_p$ are the model parameters and

$$\begin{aligned} a_p(t) &= \frac{Q_{in}(1+r)}{V_a} + \delta \\ c_p(t) &= \frac{K_0 X(t)}{Y}\frac{\mu_{\max} S(t)}{(K_s + S(t))} \\ f(DO(t)) &= \frac{DO(t)}{(K_{DO} + DO(t))} \\ b_p(t) &= \alpha(DO_{\max} - DO(t)) \\ d_p &= \delta DO_{\max} \end{aligned} \tag{19}$$

The model reference dynamics equation as:

$$\frac{dDO_{m,ref}}{dt} = -a_m DO_{m.ref}(t) + b_m DO^{ref}(t) \tag{20}$$

The affine model reference adaptive control law is applied as:

$$Q_{air}(t) = a_{DO}(t)DO(t) + a_f(t)\,f(DO(t)) + a_{DO^{ref}}(t)DO^{ref}(t) - \frac{\delta DO_{\max}}{b_p(t)} \tag{21}$$

Closed-loop:

$$\begin{aligned} \frac{dDO}{dt} = &-a_p(t)DO(t) - c_p(t)\,f(DO(t)) \\ &+ b_p(t)\{a_{DO}(t)DO(t) + a_f(t)\,f(DO(t)) \\ &+ a_{DO^{ref}}(t)DO^{ref}(t) - \frac{\delta DO_{\max}}{b_p(t)}\} + \delta DO_{\max} \end{aligned} \tag{22}$$

Rewriting (22)

$$\frac{dDO}{dt} = -a_p(t)DO(t) - c_p(t)f(DO(t)) + b_p(t)a_{DO}(t)DO(t) + b_p(t)a_f(t)f(DO(t)) + b_p(t)a_{DO^{ref}}(t)DO^{ref}(t) - b_p(t)\frac{\delta DO_{\max}}{b_p(t)} + \delta DO_{\max} \tag{23}$$

Rewriting (23)

$$\frac{dDO}{dt} = -a_p(t)DO(t) + b_p(t)a_{DO}(t)DO(t) - c_p(t)f(DO(t)) + b_p(t)a_f(t)f(DO(t)) + b_p(t)a_{DO^{ref}}(t)DO^{ref}(t) - b_p(t)\frac{\delta DO_{\max}}{b_p(t)} + \delta DO_{\max} \tag{24}$$

Rewriting (24)

$$\frac{dDO}{dt} = -(a_p(t) - b_p(t)a_{DO}(t))DO(t) - (c_p(t) - b_p(t)a_f(t))f(DO(t)) + b_p(t)a_{DO^{ref}}(t)DO^{ref}(t) \tag{25}$$

$$-(a_p(t) - b_p(t)\hat{a}_{DO}(t)) = -a_m \tag{26}$$

$$-(c_p(t) - b_p(t)\hat{a}_f(t)) = 0 \tag{27}$$

$$b_p(t)\hat{a}_{DO^{ref}}(t) = b_m \tag{28}$$

The ideal parameters can be obtained as

$$\hat{a}_{DO}(t) = \frac{-a_m + a_p(t)}{b_p(t)} \tag{29}$$

$$\hat{a}_f(t) = \frac{c_p(t)}{b_p(t)} \tag{30}$$

$$\hat{a}_{DO^{ref}}(t) = \frac{b_m}{b_p(t)} \tag{31}$$

The resulting control law reads:

$$Q_{air}(t) = a_{DO}(t)DO(t) + a_f(t)f(DO(t)) + \frac{b_m}{b_p(t)}DO^{ref}(t) - \frac{\delta DO_{\max}}{b_p(t)} \tag{32}$$

The corresponding closed-loop dynamics reads:

$$\frac{dDO}{dt} = -(a_p(t) - b_p(t)a_{DO}(t))DO(t) - (c_p(t) - b_p(t)a_f(t))f(DO(t)) + b_p(t)\frac{b_m}{b_p(t)}(t)DO^{ref}(t) \tag{33}$$

The sufficient data are DO(t) and e(t) where:

$$e(t)=DO(t) - DO_{m,ref}(t) \tag{34}$$

The adaptive control laws:

$$\frac{da_{DO}}{dt} = -\gamma_1 e(t)DO(t) \tag{35}$$

$$\frac{da_f}{dt} = -\gamma_2 e(t)f(DO(t)) \tag{36}$$

Stability analysis for the DMRAC

$$\dot{V} = e(t)[-a_m e(t) + (a_{DO}(t) - \hat{a}_{DO}(t))b_p(t)DO(t) + (a_f(t) - \hat{a}_f(t))b_p(t)f(DO(t)) + (a_{DO^{ref}}(t) - \hat{a}_{DO^{ref}}(t))b_p(t)DO^{ref}(t)] + (a_{DO}(t) - \hat{a}_{DO}(t))((-\gamma_1 eDO(t)) - \dot{\hat{a}}_{DO}(t))\frac{1}{\gamma_1} + (a_f(t) - \hat{a}_f(t))((-\gamma_2 ef(DO(t))) - \dot{\hat{a}}_f(t))\frac{1}{\gamma_2} + (a_{DO^{ref}}(t) - \hat{a}_{DO^{ref}}(t))((-\gamma_3 eDO^{ref}(t)) - \dot{\hat{a}}_{DO^{ref}}(t))\frac{1}{\gamma_3} \quad (1)$$

$$\dot{V} = -a_m e^2(t) + (a_{DO}(t) - \hat{a}_{DO}(t))b_p(t)DO(t)e(t) + (a_f(t) - \hat{a}_f(t))b_p(t)f(DO(t))e(t) + (a_{DO^{ref}}(t) - \hat{a}_{DO^{ref}}(t))b_p(t)DO^{ref}(t)e(t) + (a_{DO}(t) - \hat{a}_{DO}(t))((-\gamma_1 eDO(t)) - \dot{\hat{a}}_{DO}(t))\frac{1}{\gamma_1} + (a_f(t) - \hat{a}_f(t))((-\gamma_2 ef(DO(t))) - \dot{\hat{a}}_f(t))\frac{1}{\gamma_2} + (a_{DO^{ref}}(t) - \hat{a}_{DO^{ref}}(t))((-\gamma_3 eDO^{ref}(t)) - \dot{\hat{a}}_{DO^{ref}}(t))\frac{1}{\gamma_3} \quad (2)$$

$$\dot{V} = -a_m e^2(t) + (a_{DO}(t) - \hat{a}_{DO}(t))\{b_p(t)DO(t)e(t) + ((-\gamma_1 eDO(t)) - \dot{\hat{a}}_{DO}(t))\frac{1}{\gamma_1}\} + (a_f(t) - \hat{a}_f(t))\{b_p(t)f(DO(t))e(t) + ((-\gamma_2 ef(DO(t))) - \dot{\hat{a}}_f(t))\frac{1}{\gamma_2}\} + (a_{DO^{ref}}(t) - \hat{a}_{DO^{ref}}(t))\{b_p(t)DO^{ref}(t)e(t) + ((-\gamma_3 eDO^{ref}(t)) - \dot{\hat{a}}_{DO^{ref}}(t))\frac{1}{\gamma_3}\} \quad (3)$$

1. $\begin{Bmatrix} a_{DO}(t) - \hat{a}_{DO}(t) \\ a_f(t) - \hat{a}_f(t) \\ a_{DO^{ref}}(t) - \hat{a}_{DO^{ref}}(t) \end{Bmatrix}$ are bounded by $\dot{e}$
2. b_p is bounded by $\dot{e}$

3. $\gamma_1, \gamma_2, \gamma_3$ are bounded by adaptive law

APPENDIX B Mathematic Model of ASWWTP, Derivation of The DMRAC Controller with limited Control Input and Stability Analysis

The DO dynamics described by following equation (1)

$$\begin{aligned}\frac{dDO}{dt} &= -\frac{Q_w(1+r)}{\beta V_a}\cdot DO(t) - \frac{K_0 X(t)}{Y}\cdot\frac{\mu_{\max} S(t)}{(\mathrm{K}_s + S(t))}\cdot\frac{DO(t)}{(K_{DO}+DO(t))} \\ &+\alpha(DO_{\max} - DO(t))\,\mathrm{Q}_{air}(t) + \beta DO_{\max}\end{aligned} \tag{1}$$

Rewriting equation (1)

$$\frac{dDO}{dt} = -a_p \cdot DO(t) - c_p \cdot f(\mathrm{DO(t)}) + \mathrm{b}_p \cdot Q_{air}(t) + d_p \tag{2}$$

Where

$$\begin{aligned} a_p &= \frac{Q_w(1+r)}{\beta V_a} \\ c_p &= \frac{K_0 X(t)}{Y}\cdot\frac{\mu_{\max}\cdot S(t)}{(K_s + S(t))} \\ f(DO(t)) &= \frac{DO(t)}{(K_{DO}+DO(t))} \\ b_p &= \alpha(DO_{\max} - DO(t) \\ d_p &= \beta DO_{\max} \end{aligned} \tag{3}$$

Assume V is saturation controller with constraint.

$$V = Saturation(\mathrm{Q}_{air}) \tag{4}$$

$$V = \begin{cases} Q_{air}^{+}, Q_{air} > Q_{air}^{+} \\ Q_{air} \\ Q_{air}^{-}, Q_{air} < Q_{air}^{-} \end{cases}$$

The DO dynamic with input saturation is described by applying (4) into (2).

$$\frac{dDO}{dt} = -a_p \cdot DO(t) - c_p \cdot f(\mathrm{DO(t)}) + b_p \cdot V + d_p \tag{5}$$

The ΔQ_{air} is the different between saturation limit and real signal. It is showing in equation (6)

$$\Delta Q_{air} = \mathrm{V} - Q_{air} \tag{6}$$

Set up the auxiliary signal is showing equation (7)

$$\dot{\lambda} = b_p \cdot \Delta Q_{air}(t) - \Phi \cdot \lambda(t) \tag{7}$$

Where Φ is position constant.

The model reference is taken as:

$$\dot{DO}_m = -a_m \cdot DO_m + b_m \cdot DO^{ref} \tag{7.1}$$

Error dynamic

$$\dot{e} = \dot{DO} - \dot{DO}_m \tag{8}$$

Filtered tracking error with input saturation constraint.

$$n = e - \lambda \tag{8.1}$$

Differentiating (8.1) with respect to time

$$\dot{n} = \dot{e} - \dot{\lambda} \tag{8.2}$$

Applying $\dot{DO}, \dot{DO}_m, \dot{\lambda}$ input equation (8.2)

$$\begin{aligned} &\dot{n} = \dot{e} - \dot{\lambda} \\ &= \dot{DO} - \dot{DO}_m - \dot{\lambda} \\ &= -a_p \cdot DO(t) - c_p \cdot f(\mathrm{DO(t)}) + b_p \cdot V + d_p \\ &-(-a_m \cdot DO_m(t) + b_m \cdot DO^{ref}(t)) \\ &-b_p \cdot \Delta Q_{air}(t) + \Phi \cdot \lambda(t) \end{aligned} \tag{9}$$

Rewriting equation (9)

$$\begin{aligned} &\dot{n} = \dot{e} - \dot{\lambda} \\ &= \dot{DO} - \dot{DO}_m - \dot{\lambda} \\ &= -a_p \cdot DO(t) - c_p \cdot f(\mathrm{DO(t)}) + d_p \\ &+a_m \cdot DO_m(t) - b_m \cdot DO^{ref}(t)) \\ &+b_p \cdot V - b_p \cdot \Delta Q_{air}(t) + \Phi \cdot \lambda(t) \end{aligned} \tag{10}$$

Rewriting equation (10)

$$
\begin{aligned}
&\dot{n} = \dot{e} - \dot{\lambda} \\
&= \dot{DO} - \dot{DO}_m - \dot{\lambda} \\
&= -a_p \cdot DO(t) - c_p \cdot f(\mathrm{DO(t)}) + d_p \\
&+ a_m \cdot DO_m(t) - b_m \cdot DO^{ref}(t)) \\
&+ (V - \Delta Q_{air}(t)) \cdot b_p \cdot + \ \Phi \cdot \lambda(t)
\end{aligned}
\tag{11}
$$

Rewriting equation (11)

$$
\begin{aligned}
&\dot{n} = \dot{e} - \dot{\lambda} \\
&= \dot{DO} - \dot{DO}_m - \dot{\lambda} \\
&= -a_p \cdot DO(t) - c_p \cdot f(\mathrm{DO(t)}) + d_p \\
&+ a_m \cdot DO_m(t) - b_m \cdot DO^{ref}(t)) \\
&+ (V - \Delta Q_{air}(t)) \cdot b_p \cdot + \ \Phi \cdot \lambda(t)
\end{aligned}
\tag{12}
$$

The term $V - \Delta Q_{air}(t)$ is equal to $Q_{air}(t)$, from equation (6)

Rewriting equation (12)

$$
\begin{aligned}
&\dot{n} = \dot{e} - \dot{\lambda} \\
&= \dot{DO} - \dot{DO}_m - \dot{\lambda} \\
&= -a_p \cdot DO(t) - c_p \cdot f(\mathrm{DO(t)}) + d_p \\
&+ a_m \cdot DO_m(t) - b_m \cdot DO^{ref}(t)) \\
&+ Q_{air}(t) \cdot b_p \cdot + \ \Phi \cdot \lambda(t)
\end{aligned}
\tag{13}
$$

Design control law

The control law is parameterised as

$$
Q_{air} = \frac{1}{b_p}[a_{DO} \cdot DO(\mathrm{t}) + a_f \cdot f\left(DO(\mathrm{t})\right) + a_{DO^{ref}} \cdot DO^{ref}(\mathrm{t}) - d_p - \Phi(DO(\mathrm{t}) - DO_m(\mathrm{t}))] \tag{15}
$$

We shall now that values of parameters $a_{DO}, a_f, a_{DO^{ref}}$ exist so that closed-loop system dynamics under the control law (15) with such indeed, apply (15) into to (5)

$$\begin{aligned}&\frac{dDO}{dt} = -a_p \cdot DO(t) - c_p \cdot f(\mathrm{DO(t)}) + b_p \cdot \frac{1}{b_p} \\ &[a_{DO} \cdot DO(\mathrm{t}) + a_f \cdot f\left(DO(\mathrm{t})\right) + a_{DO^{ref}} \cdot DO^{ref}(\mathrm{t}) \\ &-d_p - \Phi(DO(\mathrm{t}) - DO_m(\mathrm{t}))] + d_p\end{aligned} \tag{15.1}$$

$$\begin{aligned}&\frac{dDO}{dt} = -(a_p - a_{DO}) \cdot DO(t) - (c_p - a_f) \cdot f(\mathrm{DO(t)}) + a_{DO^{ref}} \cdot DO^{ref}(\mathrm{t}) \\ &-\Phi \cdot e\end{aligned} \tag{15.2}$$

Assuming term $(c_p - a_f)$ equal to zero by (15.2) gives $c_p = a_f$ (15.a), from $a_p - a_{DO} = a_m$ we have $a_{DO} = a_p - a_m$ (15.b), the term $a_{DO^{ref}}$ is a known parameter and equal to model reference parameter b_m.

For constant or slowly varying parameters in (2), the parameter adaptive laws can be derived as in (Brdy.2005) and (Slotine and Li (1992)) to produce:

$$\begin{aligned}&\frac{\mathrm{d}\, a_{\mathrm{DO}}}{\mathrm{dt}} = -\gamma_1 \cdot e \cdot DO \\ &\frac{\mathrm{d}\, a_{\mathrm{f}}}{\mathrm{dt}} = -\gamma_2 \cdot e \cdot f(DO) \\ &\frac{\mathrm{d}\, a_{\mathrm{DO^{ref}}}}{\mathrm{dt}} = -\gamma_3 \cdot e \cdot DO^{ref}\end{aligned} \tag{16}$$

where

$$f(DO(t)) = \frac{DO(t)}{(K_{DO} + DO(t))} \tag{17}$$

Stability Analyses

For the stability analyses we used lyapunov function

$$V\left[(t),\Delta a_{DO}(t),\Delta a_f\left(t\right),\Delta a_{DO^{ref}}\left(t\right)\right] = \frac{n^2}{2}+\frac{\Delta a_{DO}{}^2}{2\cdot\gamma_1}+\frac{\Delta a_f{}^2}{2\cdot\gamma_2}+\frac{\Delta a_{DO^{ref}}{}^2}{2\cdot\gamma_3} \tag{18}$$

Time-derivative of Lyapunov function

$$\begin{aligned}&\dot{V}\left[e(t),\Delta a_{DO}(t),\Delta a_f\left(t\right),\Delta a_{DO^{ref}}\left(t\right)\right]\\&=n\cdot\dot{n}+\frac{1}{\gamma_1}\cdot\Delta a_{DO}\cdot\dot{\Delta a}_{DO}+\frac{1}{\gamma_2}\cdot\Delta a_f\cdot\dot{\Delta a}_f+\frac{1}{\gamma_3}\cdot\Delta a_{DO^{ref}}\cdot\dot{\Delta a}_{DO^{ref}}\\&=n\cdot\dot{n}+\frac{1}{\gamma_1}\cdot\left(a_{DO}-\hat{a}_{DO}\right)\cdot\left(\dot{a}_{DO}-\dot{\hat{a}}_{DO}\right)+\frac{1}{\gamma_2}\cdot\left(a_f-\hat{a}_f\right)\cdot\left(\dot{a}_f-\dot{\hat{a}}_f\right)\\&+\frac{1}{\gamma_3}\cdot\left(a_{DO^{ref}}-\hat{a}_{DO^{ref}}\right)\cdot\left(\dot{a}_{DO^{ref}}-\dot{\hat{a}}_{DO^{ref}}\right)\end{aligned} \tag{19}$$

The $\left[\Delta a_{DO}(t),\Delta a_f\left(t\right),\Delta a_{DO^{ref}}\left(t\right)\right]$ are the error between ideal parameter and update parameter. The $\hat{a}_{DO},\hat{a}_f,\hat{a}_{DO^{ref}}$ represent the ideal parameter. The $a_{DO},a_f,a_{DO^{ref}}$ represent update parameter. by rewriting the equation (15.a) (15.b)

$$\hat{a}_{DO}=a_p-a_m \text{ (19.a) } \hat{a}_f=c_p \text{ (19.b), } \hat{a}_{DO^{ref}}=b_m \tag{19.c}$$

The ideal parameters are constant. Therefore time-derivative of ideal parameters are equal to 0. Substitute parameter adaptive control law into update parameters.

$$\begin{aligned}
&\dot{V}\left[e(t),\Delta a_{DO}(t),\Delta a_f(t),\Delta a_{DO^{ref}}\right] \\
&= n\cdot\dot{n}+\frac{1}{\gamma_1}\cdot\Delta a_{DO}\cdot\dot{\Delta a}_{DO}+\frac{1}{\gamma_2}\cdot\Delta a_f\cdot\dot{\Delta a}_f+\frac{1}{\gamma_3}\cdot\Delta a_{DO^{ref}}\cdot\dot{\Delta a}_{DO^{ref}} \\
&= n\cdot\dot{n}+\frac{1}{\gamma_1}\cdot\left(a_{DO}-\hat{a}_{DO}\right)\cdot\left(\left(-\gamma_1\cdot e\cdot DO\right)-0\right)+\frac{1}{\gamma_2}\cdot\left(a_f-\hat{a}_f\right)\cdot\left(\left(-\gamma_2\cdot e\cdot f\left(DO\right)-0\right)\right. \\
&+\frac{1}{\gamma_3}\cdot\left(a_{DO^{ref}}-\hat{a}_{DO^{ref}}\right)\cdot\left(\left(-\gamma_2\cdot e\cdot DO^{ref}\right)-0\right)
\end{aligned} \tag{20}$$

The close-loop DO dynamic system filtered tracking error dynamic is with input saturation system. The filtered tracking error dynamic is applying the control law (15) into filtered tracking error dynamic (13).

$$\begin{aligned}
&\dot{n}=\dot{e}-\dot{\lambda} \\
&=\dot{DO}-\dot{DO}_m-\dot{\lambda} \\
&=-a_p\cdot\cdot DO(t)-c_p\cdot f(\mathrm{DO(t)})+d_p \\
&+a_m\cdot DO_m(t)-b_m DO^{ref}(t)) \\
&+(\frac{1}{b_p}[a_{DO}\cdot DO(\mathrm{t})+a_f\cdot f\left(DO\right)(\mathrm{t})+a_{DO^{ref}}\cdot DO^{ref}(\mathrm{t}) \\
&-d_p-\Phi(DO-DO_m)])\cdot b_p\cdot+\ \Phi\cdot\lambda(t)
\end{aligned} \tag{21}$$

$$
\begin{aligned}
&\dot{n} = \dot{e} - \dot{\lambda} \\
&= \dot{DO} - \dot{DO}_m - \dot{\lambda} \\
&= -a_p \cdot DO(t) - c_p \cdot f(\mathrm{DO(t)}) + d_p \\
&+ a_m \cdot DO_m(t) - b_m \cdot DO^{ref}(t)) \\
&+ [a_{DO} \cdot DO(\mathrm{t}) + a_f \cdot f\left(DO(\mathrm{t})\right) + a_{DO^{ref}} \cdot DO^{ref}(\mathrm{t}) \\
&- d_p - \Phi(DO(\mathrm{t}) - DO_m(\mathrm{t}))] \cdot + \ \Phi \cdot \lambda(t)
\end{aligned}
\tag{21.1}
$$

Rewriting equation (21.1)

$$
\begin{aligned}
&\dot{n} = \dot{e} - \dot{\lambda} \\
&= \dot{DO} - \dot{DO}_m - \dot{\lambda} \\
&= -a_p \cdot DO(t) + a_{DO} \cdot DO(\mathrm{t}) - c_p \cdot f(\mathrm{DO(t)}) + a_f \cdot f\left(DO(\mathrm{t})\right) \\
&+ d_p \\
&+ a_m \cdot DO_m(t) - b_m \cdot DO^{ref}(t) + a_{DO^{ref}} \cdot DO^{ref} \\
&- d_p - \Phi(DO - DO_m)] \cdot + \ \Phi \cdot \lambda(t)
\end{aligned}
\tag{22}
$$

Rewriting equation (22)

$$
\begin{aligned}
&\dot{n} = \dot{e} - \dot{\lambda} \\
&= \dot{DO} - \dot{DO}_m - \dot{\lambda} \\
&= -a_p \cdot DO(t) + a_{DO} \cdot DO - c_p \cdot f(\mathrm{DO(t)}) + a_f \cdot f\left(DO(\mathrm{t})\right) \\
&+ a_m \cdot DO_m(t) - b_m \cdot DO^{ref}(t) + a_{DO^{ref}} \cdot DO^{ref}(\mathrm{t}) \\
&- [DO(\mathrm{t}) - DO_m(\mathrm{t}) - \lambda(t)] \cdot \Phi
\end{aligned}
\tag{22}
$$

The term $(DO(t) - DO^{ref}(t) - \lambda(t))$ is equal the analyses control system error.

Rewriting equation (22)

$$
\begin{aligned}
&\dot{n} = \dot{e} - \dot{\lambda} \\
&= \dot{DO} - \dot{DO}_m - \dot{\lambda} \\
&= -a_p \cdot DO(t) + a_{DO} \cdot DO - c_p \cdot f(\mathrm{DO(t)}) + a_f \cdot f\left(DO(\mathrm{t})\right) \\
&+ a_m \cdot DO_m(t) - b_m \cdot DO^{ref}(t) + a_{DO^{ref}} \cdot DO^{ref}(\mathrm{t}) \\
&- n \cdot \Phi
\end{aligned}
\tag{23}
$$

Apply equations $\hat{a_{DO}} = a_p - a_m$ (19.a) $\hat{a_f} = c_p$ (19.b), $\hat{a_{DO^{ref}}} = b_m$ (19.c) into equation (23)

$$
\begin{aligned}
&\dot{n} = \dot{e} - \dot{\lambda} \\
&= \dot{DO} - \dot{DO}_m - \dot{\lambda} \\
&= (a_{DO} - \hat{a_{DO}}) \cdot DO + (a_f - \hat{a_f}) \cdot f\left(DO(\mathrm{t})\right) \\
&+ (a_{DO^{ref}} - \hat{a_{DO^{ref}}}) \cdot DO^{ref}(\mathrm{t}) \\
&- n \cdot \Phi
\end{aligned}
\tag{23.1}
$$

For the close-loop dynamic system with input saturation, apply error dynamic (23.1) to the lyapunve function (20).

$$
\begin{aligned}
&\dot{V}\left[\mathrm{n}(t), \Delta a_{DO}(t), \Delta a_f(t), \Delta a_{DO^{ref}}\right] \\
&= n \cdot \dot{n} + \frac{1}{\gamma_1} \cdot \Delta a_{DO} \cdot \dot{\Delta a_{DO}} + \frac{1}{\gamma_2} \cdot \Delta a_f \cdot \dot{\Delta a_f} + \frac{1}{\gamma_3} \cdot \Delta a_{DO^{ref}} \cdot \dot{\Delta a_{DO^{ref}}} \\
&= n \cdot \left((a_{DO} - \hat{a_{DO}}) \cdot DO(t) + (a_f - \hat{a_f}) \cdot f\left(DO(t)\right) \right. \\
&\left. + (a_{DO^{ref}} - \hat{a_{DO^{ref}}}) \cdot DO^{ref}(t) - e \cdot \Phi \right) \\
&+ \frac{1}{\gamma_1} \cdot \left(a_{DO} - \hat{a_{DO}} \right) \cdot \left(\left(-\gamma_1 \cdot e \cdot DO \right) - 0 \right) + \frac{1}{\gamma_2} \cdot \left(a_f - \hat{a_f} \right) \cdot \left(\left(-\gamma_2 \cdot e \cdot f\left(DO\right) - 0 \right) \right. \\
&+ \frac{1}{\gamma_3} \cdot \left(a_{DO^{ref}} - \hat{a_{DO^{ref}}} \right) \cdot \left(\left(-\gamma_2 \cdot e \cdot DO^{ref} \right) - 0 \right)
\end{aligned}
\tag{24}
$$

Rewriting equation (24)

$$
\begin{aligned}
&\dot{V}\left[\mathrm{n}(t), \Delta a_{DO}(t), \Delta a_f(t), \Delta a_{DO^{ref}}\right] \\
&= n \cdot \dot{n} + \frac{1}{\gamma_1} \cdot \Delta a_{DO} \cdot \Delta \dot{a}_{DO} + \frac{1}{\gamma_2} \cdot \Delta a_f \cdot \Delta \dot{a}_f + \frac{1}{\gamma_3} \cdot \Delta a_{DO^{ref}} \cdot \Delta \dot{a}_{DO^{ref}} \\
&= (a_{DO} - \hat{a}_{DO}) \cdot e \cdot DO(t) + (a_f - \hat{a}_f) \cdot e \cdot f\left(DO(t)\right) \\
&+ (a_{DO^{ref}} - \hat{a}_{DO^{ref}}) \cdot e \cdot DO^{ref}(t) - e \cdot e \cdot \Phi \\
&+ \left(a_{DO} - \hat{a}_{DO}\right) \cdot \left(-e \cdot DO(t)\right) \left(a_f - \hat{a}_f\right) \cdot \left(-e \cdot f\left(DO(t)\right)\right) \\
&+ \left(a_{DO^{ref}} - \hat{a}_{DO^{ref}}\right) \cdot \left(-e \cdot DO^{ref}(t)\right)
\end{aligned}
\tag{25}
$$

Rewriting equation (25)

$$
\begin{aligned}
&\dot{V}\left[\mathrm{n}(t), \Delta a_{DO}(t), \Delta a_f(t), \Delta a_{DO^{ref}}\right] \\
&= n \cdot \dot{n} + \frac{1}{\gamma_1} \cdot \Delta a_{DO} \cdot \Delta \dot{a}_{DO} + \frac{1}{\gamma_2} \cdot \Delta a_f \cdot \Delta \dot{a}_f + \frac{1}{\gamma_3} \cdot \Delta a_{DO^{ref}} \cdot \Delta \dot{a}_{DO^{ref}} \\
&= -\Phi \cdot n^2
\end{aligned}
\tag{26}
$$

Summary result of lyapunov function with input saturation close-loop DO dynamic system.

1. The result of lyapunov function is $\dot{V} = -\Phi \cdot n^2$. It is showing that $\dot{V}$ progressive tend to zero. So the system is stability.

$$\dot{V} = -\Phi \cdot n^2 \to 0 \Rightarrow n \to 0, t \to \infty$$

2. The close-loop DO dynamic system with input saturation is need to find the bounded of saturation for the system.
   The Φ is positive constant value, and the n^2 is positive value. We can limit the error square to find the bounded of saturation. To find what limit of bounded of saturation affect control system stability.

$$\text{Limit}\left\{DO(t) - DO^{ref}(t) - \lambda\right\} \le 0,$$

   The term $\left\{DO(t) - DO^{ref}(t)\right\} \le 0$, if it is have enough time.

$$\left(DO(t) - DO^{ref}(t)\right) \to 0, \quad t \to \infty$$

So we need consider term $-\lambda$, it is going to negative or positive value.
We used the lyapunov function to consider the value of term $-\lambda$.
The lyapunov function is showing below.

$$V_\lambda = \frac{1}{2} \cdot \lambda^2 \tag{27}$$

The time-derivation of the lyapunve function.

$$\dot{V}_\lambda = \lambda \cdot \dot{\lambda} \tag{28}$$

Apply the equation (7) into the equation (28)

$$\dot{V}_\lambda = \lambda \cdot (b_p \cdot \Delta Q_{air}(t) — \Phi \cdot \lambda(t)) \tag{29}$$

Rewriting the equation (29)

$$\dot{V}_\lambda = \lambda \cdot b_p \cdot \Delta Q_{air}(t) — \lambda(t) \cdot \lambda(t) \cdot \Phi \tag{30}$$

We assume term $b_p \cdot \Delta Q_{air}(t)$ is equal to $\Delta Q_{air}{}^*(t)$, rewriting the equation （30）

$$\dot{V}_\lambda = \lambda \cdot \Delta Q_{air}{}^*(t) — \lambda^2(t) \cdot \Phi \tag{31}$$

Rewriting the equation by using formula

$$\begin{aligned} &(a-b)^2 \le 0 \\ &a^2 - 2ab + b^2 \le 0 \\ &ab \ge \frac{a^2 + b^2}{2} \\ &ab \ge \frac{1}{2} \cdot a^2 + \frac{1}{2} \cdot b^2 \end{aligned}$$

It is showing

$$\begin{aligned} \dot{V}_\lambda &= \lambda \cdot \Delta Q_{air}{}^*(t) — \lambda^2(t) \cdot \Phi \\ &\le —\lambda^2(t) \cdot \Phi + \frac{1}{2} \cdot \lambda^2 + \frac{1}{2} \cdot \Delta Q_{air}{}^{*2}(t) \end{aligned} \tag{32}$$

The Φ is positive constant value, we assume $\Phi=\frac{1}{2}+a_0$, $a_0>0$ (33). The a_0 is positive constant value.

Apply the equation (33) into the equation (32)

$$\begin{aligned}\dot{V}_\lambda &= \lambda\cdot\Delta Q_{air}^{*}(t) - \lambda^2(t)\cdot\Phi \\ &\le -\lambda^2(t)\cdot\left(\frac{1}{2}+a_0\right)+\frac{1}{2}\cdot\lambda^2+\frac{1}{2}\cdot\Delta Q_{air}^{*2}(t) \\ &\le -\frac{1}{2}\cdot\lambda^2(t)-\lambda^2(t)\cdot a_0+\frac{1}{2}\cdot\lambda^2+\frac{1}{2}\cdot\Delta Q_{air}^{*2}(t)\end{aligned} \tag{34}$$

Rewriting the equation (34)

$$\begin{aligned}\dot{V}_\lambda &= \lambda\cdot\Delta Q_{air}^{*}(t) - \lambda^2(t)\cdot\Phi \\ &\le -\lambda^2(t)\cdot\left(\frac{1}{2}+a_0\right)+\frac{1}{2}\cdot\lambda^2(t)+\frac{1}{2}\cdot\Delta Q_{air}^{*2}(t) \\ &\le -\frac{1}{2}\cdot\lambda^2(t)-a_0\cdot\lambda^2(t)+\frac{1}{2}\cdot\lambda^2(t)+\frac{1}{2}\cdot\Delta Q_{air}^{*2}(t) \\ &\le -2\cdot V_\lambda\cdot a_0+\frac{1}{2}\cdot\Delta Q_{air}^{*2}(t)\end{aligned} \tag{36}$$

Integral the V_λ

$$V_\lambda=\frac{\frac{1}{2}\cdot\Delta Q_{air}^{*2}(t)}{2\cdot a_0}\cdot\left(1-e^{-2\cdot a_0}\right)+V_{\lambda.0}\cdot e^{-2\cdot a_0} \tag{37}$$

Rewriting equation (37)

$$V_\lambda=\frac{\Delta Q_{air}^{*2}(t)}{4\cdot a_0}+\left(V_{\lambda.0}+\frac{\Delta Q_{air}^{*2}(t)}{4\cdot a_0}\right)\cdot e^{-2\cdot a_0} \tag{38}$$

If time going to infinity and a_0 big enough, then term $\left(V_{\lambda.0}+\frac{\Delta Q_{air}^{*2}(t)}{4\cdot a_0}\right)\cdot e^{-2\cdot a_0}$ is equal to zero.

Rewriting equation (38)

$$V_\lambda = \frac{\Delta Q_{air}^{*2}(t)}{4\cdot a_0} \tag{39}$$

Now limit the V_λ is negative or zero.

$$\frac{1}{2}\cdot\lambda^2 = \frac{\Delta Q_{air}^{*2}(t)}{4\cdot a_0} \tag{39.1}$$

Rewriting equation (39)

$$\lambda = \sqrt{\frac{\Delta Q_{air}^{*2}(t)}{2\cdot a_0}} \tag{40}$$

Apply equation (10) into the Limit $\left\{DO(t)-DO^{ref}(t)-\lambda\right\}\le 0$.

$$\begin{aligned} &\left|DO(t)-DO^{ref}(t)-\lambda\right|\le 0\\ &\left|DO(t)-DO^{ref}(t)\right|\le \lambda\\ &\left|DO(t)-DO^{ref}(t)\right|\le \sqrt{\frac{\Delta Q_{air}^{*2}(t)}{2\cdot a_0}} \end{aligned} \tag{41}$$

Comment if a_0 bigger enough, the term $\left|DO(t)-DO^{ref}(t)\right|$ more going to zero. And more stable.

APPENDIX C Mathematic Model of The ASWWTP and Derivation of The DDMRAC Controller

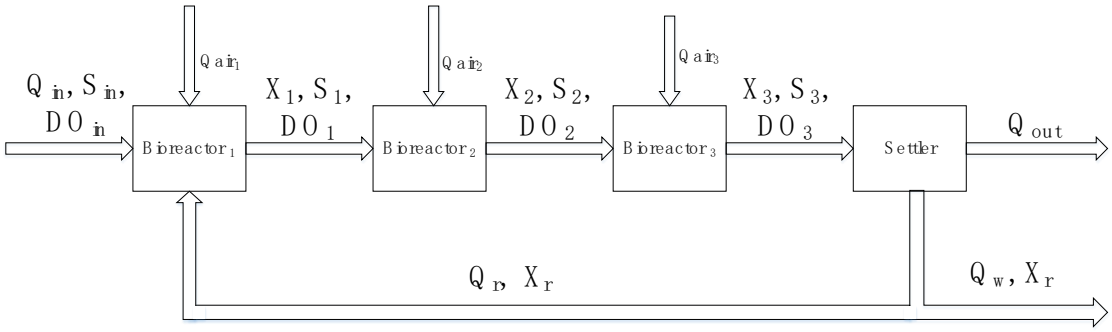

$$\frac{dX_1}{dt} = \mu_1(t)\cdot X_1(t) - D_1(t)\cdot(1+r_1)\cdot X_1 + r_1\cdot D_1(t)\cdot X_{r.1}(t) \tag{1}$$

$$\frac{dS_1}{dt} = -\frac{\mu_1(t)\cdot X_1(t)}{Y_1} - D_1(t)\cdot(1+r_1)\cdot S_1(t) + D_1(t)\cdot S_{in}(t) \tag{2}$$

$$\frac{dDO_1}{dt} = -\frac{K_{0.1}\cdot\mu_1(t)\cdot X_1(t)}{Y_1} - D_1(t)\cdot(1+r_1)\cdot DO_1(t) + D_1(t)\cdot DO_{in}(t) + k_{La.1}(Q_{air.1}(t))\cdot(DO_{\max.1} - DO_1(t)) \tag{3}$$

$$\frac{dX_{r.1}}{dt} = D_3(t)\cdot(1+r_1)\cdot X_3(t) - D_3(t)\cdot r_1\cdot X_{r.3}(t) \tag{4}$$

$$\mu_1(t) = \mu_{\max.1}\cdot\frac{S_1(t)}{K_{s.1}+S_1(t)}\cdot\frac{DO_1(t)}{K_{DO.1}+DO_1(t)} \tag{5}$$

With:

$$D_1(t)=\frac{Q_{in}}{V_{a.1}}\ ,\quad r_1=\frac{Q_r}{Q_{in}}\ ,\quad V_1=\frac{V_{a.1}}{V_{s.1}}$$

The function $k_{La}(Q_{air}(t))$ is the oxygen transfer and depends on the aeration actuating system and sludge conditions. It is assumed as:

$$k_{La.1}(t)=\alpha_1 Q_{air.1}(t)+\delta_1 \tag{6}$$

The resulting input-output model

$$\begin{aligned}&\frac{dDO_1}{dt}=-\frac{K_{0.1}\cdot\mu_1(t)\cdot X_1(t)}{Y_1}-D_1(t)\cdot(1+r_1)\cdot DO_1(t)+D_1(t)\cdot DO_{in}(t)\\&+(\alpha_1 Q_{air.1}(t)+\delta_1)\cdot(DO_{\max.1}-DO_1(t))\end{aligned} \tag{7}$$

Substitute $D_1(t)$ and $\mu_1(t)$ into (7)

$$D_1(t)=\frac{Q_{in}}{V_{a.1}}\ ,\quad \mu_1(t)=\mu_{\max.1}\cdot\frac{S_1(t)}{K_{s.1}+S_1(t)}\cdot\frac{DO_1(t)}{K_{DO.1}+DO_1(t)}$$

Rewriting (7)

$$\begin{aligned}&\frac{dDO_1}{dt}=-(\frac{Q_{in}}{V_{a.1}}\cdot(1+r_1)+\delta_1)\cdot DO_1(t)-\frac{K_{0.1}\cdot X_1(t)}{Y_1}\cdot\mu_{\max.1}\cdot\frac{S_1(t)}{K_{s.1}+S_1(t)}\cdot\frac{DO_1(t)}{K_{DO.1}+DO_1(t)}\\&+D_1(t)\cdot DO_{in}(t)+(\alpha_1\cdot(DO_{\max.1}-DO_1(t)\cdot Q_{air.1}(t))+\delta_1\cdot DO_{\max.1}\end{aligned} \tag{8}$$

As the term $D_1(t)\cdot DO_{in}(t)$ is small it is neglected.

$$\begin{aligned}&\frac{dDO_1}{dt}=-(\frac{Q_{in}}{V_{a.1}}\cdot(1+r_1)+\delta_1)\cdot DO_1(t)-\frac{K_{0.1}\cdot X_1(t)}{Y_1}\cdot\mu_{\max.1}\cdot\frac{S_1(t)}{K_{s.1}+S_1(t)}\cdot\frac{DO_1(t)}{K_{DO.1}+DO_1(t)}\\&+(\alpha_1\cdot(DO_{\max.1}-DO_1(t)\cdot Q_{air.1}(t))+\delta_1\cdot DO_{\max.1}\end{aligned} \tag{9}$$

Rewriting (9)

$$\frac{dDO_1}{dt} = -a_{p.1}(t)DO_1(t) - c_{p.1}(t)\,f\,(DO_1(t)) + b_{p.1}(t)Q_{air.1}(t) + d_{p.1} \qquad (10)$$

$$a_{p.1} = \frac{Q_{in}(1+r_1)}{V_{a.1}} + \delta_1$$

$$c_{p.1} = \frac{K_{0.1}X_1(t)}{Y_1}\frac{\mu_{\max.1}S_1(t)}{K_{s.1}+S_1(t)}$$

$$b_{p.1} = \alpha_1(DO_{\max.1} - DO_1(t))$$

$$d_{p.1} = \delta_1 DO_{\max.1}$$

Model Reference Dynamics equation as

$$\frac{dDO_{m.ref.1}}{dt} = -a_{m.1}DO_{m.ref.1}(t) + b_{m.1}DO_1^{ref}(t) \qquad (11)$$

The affine model reference adaptive control law is applied as

$$Q_{air.1}(t) = a_{DO.1}(t)DO_1(t) + a_{f.1}(t)\,f\,(DO_1(t)) + a_{DO_1^{ref}}(t)DO_1^{ref}(t) - \frac{\delta_1 DO_{\max.1}}{b_{p.1}(t)} \qquad (12)$$

Closing loop by (10)

$$\frac{dDO_1}{dt} = -(a_{p.1}(t) - b_{p.1}(t)a_{DO.1}(t))DO_1(t) - (c_{p.1}(t) - b_{p.1}a_{f.1}(t))\,f\,(DO_1(t)) + b_{p.1}(t)a_{DO_1^{ref}}(t)DO_1^{ref}(t) \qquad (13)$$

and

$$-(a_{p.1}(t) - b_{p.1}(t)\,\hat{a}_{DO.1}(t)) = -a_{m.1}$$

$$-(c_{p.1}(t)-b_{p.1}\hat{a}_{f.1}(t))=0$$

$$b_{p.1}(t)\hat{a}_{DO_1^{ref}}(t)=b_{m.1}$$

where $\hat{a}_{DO.1}(t)$, $\hat{a}_{f.1}(t)$ and $\hat{a}_{DO_1^{ref}}$ are the ideal parameters.

As the values of $b_{m.1}$ and $b_{p.1}(t)$ are known the parameter $\hat{a}_{DO_1^{ref}}(t)$ can be determined on-line from available data. The resulting control law reads:

$$\begin{aligned} Q_{air.1}(t)=&a_{DO.1}(t)DO_1(t)+a_{f.1}(t)\,f(DO_1(t)) \\ &+\frac{b_{m.1}}{b_{p.1}(t)}DO_1^{ref}(t)-\frac{\delta_1 DO_{\max.1}}{b_{p.1}(t)} \end{aligned} \tag{14}$$

The corresponding closed-loop dynamics reads:

$$\begin{aligned} \frac{dDO_1}{dt}=&-(a_{p.1}(t)-b_{p.1}(t)a_{DO.1}(t))DO_1(t) \\ &-(c_{p.1}(t)-b_{p.1}a_{f.1}(t))\,f(DO_1(t)) \\ &+b_{p.1}(t)\frac{b_{m.1}}{b_{p.1}(t)}DO_1^{ref}(t) \end{aligned} \tag{15}$$

The error between DO_1 and $DOm.ref_1$

$$e_1(t)=DO_1(t)-DO_{m.ref.1}(t) \tag{16}$$

The parameter adaption laws.

$$\frac{da_{DO_1}}{dt}=-\gamma_{zone1.1}e_1(t)DO_1(t) \tag{17}$$

$$\frac{da_{f_1}}{dt}=-\gamma_{zone1.2}e_1(t)\,f(DO_1(t)) \tag{18}$$

The three bioreactors in single input and output model

$$\frac{dDO_1}{dt} = -a_{p.1}(t)DO_1(t) - c_{p.1}(t)\,f\,(DO_1(t)) + b_{p.1}(t)Q_{air.1}(t) + d_{p.1} \quad (1)$$

$$\frac{dDO_2}{dt} = -a_{p.2}(t)DO_2(t) - c_{p.2}(t)\,f\,(DO_2(t)) + b_{p.2}(t)Q_{air.2}(t) + d_{p.2} \quad (2)$$

$$\frac{dDO_3}{dt} = -a_{p.3}(t)DO_3(t) - c_{p.3}(t)\,f\,(DO_3(t)) + b_{p.3}(t)Q_{air.3}(t) + d_{p.3} \quad (3)$$

The resulting input-output model. Rewriting (1, 2, 3)

$$\frac{dDO_i}{dt} = -a_{p.i}(t)DO_i(t) - c_{p.i}(t)\,f\,(DO_i(t)) + b_{p.i}(t)Q_{air.i}(t) + d_{p.i} \quad (4)$$

$$a_{p.i} = \frac{Q_{in}(1+r_1)}{V_{a.i}} + \delta_i$$

$$c_{p.i} = \frac{K_{0.i}X_i(t)}{Y_i}\,\frac{\mu_{\max.i}S_i(t)}{K_{s.i} + S_i(t)}$$

$$b_{p.i} = \alpha_i(DO_{\max.i} - DO_i(t))$$

$$d_{p.i} = \delta_i DO_{\max.i}$$

Where

$i = 1,\ 2,\ 3$

Model Reference Dynamics equation as

$$\frac{dDO_{m.ref.j}}{dt} = -a_{m.j} DO_{m.ref.j}(t) + b_{m.j} DO_j^{ref}(t) \tag{5}$$

Where

$j = 1,\ 2,\ 3$

The affine model reference adaptive control law is applied as

$$Q_{air.k}(t) = a_{DO.k}(t) DO_k(t) + a_{f.k}(t) f(DO_k(t)) + a_{DO_k^{ref}}(t) DO_k^{ref}(t) - \frac{\delta_k DO_{\max.k}}{b_{p.k}(t)} \tag{6}$$

Where

$k = 1,\ 2,\ 3.$

Closing loop by (4)

$$\begin{aligned} \frac{dDO_n}{dt} = & -(a_{p.n}(t) - b_{p.n}(t) a_{DO.n}(t)) DO_n(t) - (c_{p.n}(t) - b_{p.n} a_{f.n}(t)) f(DO_n(t)) \\ & + b_{p.n}(t) a_{DO_n^{ref}}(t) DO_n^{ref}(t) \end{aligned} \tag{7}$$

Where

$$n = 1,\quad 2,\quad 3.$$

and

$$-(a_{p.n}(t) - b_{p.n}(t)\,\hat{a}_{DO.n}(t)) = -a_{m.n}$$

$$-(c_{p.n}(t) - b_{p.n}\,\hat{a}_{f.n}(t)) = 0$$

$$b_{p.n}(t)\,\hat{a}_{DO_n^{ref}}(t) = b_{m.n}$$

where $\hat{a}_{DO.n}(t)$, $\hat{a}_{f.n}(t)$ and $\hat{a}_{DO_n^{ref}}$ are the ideal parameters.

As the values of $b_{m.n}$ and $b_{p.n}(t)$ are known the parameter $\hat{a}_{DO_n^{ref}}(t)$ can be determined on-line from available data. The resulting control law reads:

$$Q_{air.i}(t) = a_{DO.i}(t)DO_i(t) + a_{f.i}(t)\,f(DO_i(t)) + \frac{b_{m.i}}{b_{p.i}(t)}DO_i^{ref}(t) - \frac{\delta_i DO_{\max.i}}{b_{p.i}(t)} \tag{8}$$

Where $i = 1,\ 2,\ 3$

The corresponding closed-loop dynamics reads:

$$\frac{dDO_j}{dt} = -(a_{p.j}(t) - b_{p.j}(t)a_{DO.j}(t))DO_j(t) - (c_{p.j}(t) - b_{p.j}a_{f.j}(t))f(DO_j(t)) + b_{p.j}(t)\frac{b_{m.j}}{b_{p.j}(t)}DO_j^{ref}(t) \quad (9)$$

Where $j = 1,\ 2,\ 3$

The error between DO_i and $DOm.ref_j$

$$e_k(t) = DO_i(t) - DO_{m.ref.j}(t) \quad (8)$$

Where $k = 1,\quad 2,\quad 3\ ; i = 1,\quad 2,\quad 3\ ; j = 1,\quad 2,\quad 3$.

Adaptive control Law

$$\frac{da_{DO_n}}{dt} = -\gamma_{zone.z.1}e_k(t)DO_i(t) \quad (9)$$

$$\frac{da_{f_n}}{dt} = -\gamma_{zone.z.2}e_k(t)f(DO_i(t)) \quad (10)$$

Where. $n = 1,\quad 2,\quad 3\ ; z = 1,\quad 2,\quad 3\ ; k = 1,\quad 2,\quad 3\ ; i = 1,\quad 2,\quad 3$.

The diagram of supervisor

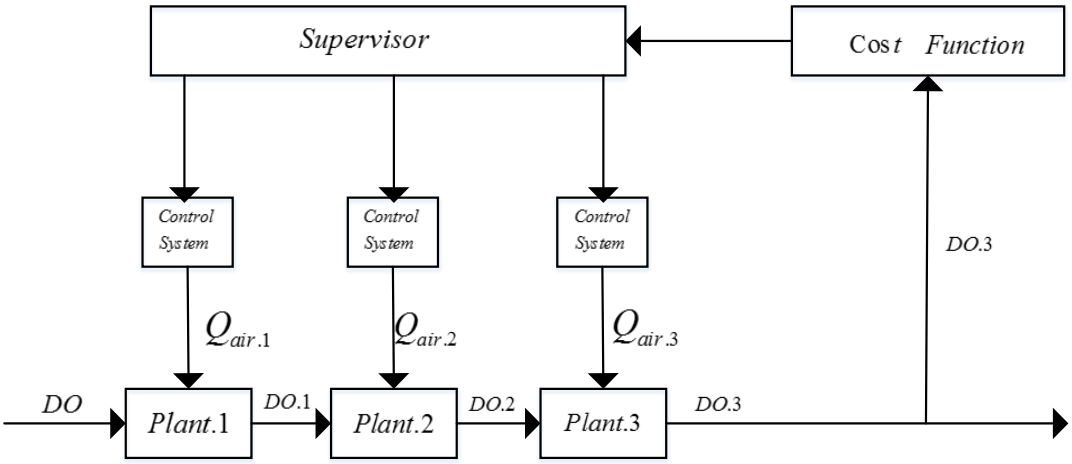

The purpose of supervisor function is to guarantee meting the constraint (12)

$$\sum_{i=1}^{q} Q_{air.i}^{supervisor}(t) \le Q_{air}^{\max}(t) \tag{12}$$

where $Q_{air.i}^{supervisor}(t)$ is generated by supervisor.

$Q_{air}^{\max}(t)$ is the current aeration system capacity limit.

(Max limit $Q_{air}(t)$ value for provide total 3 aeration zones)

i is the number of aeration zone,

Fuzzy rule：

1. If $\sum_{i=1}^{q} Q_{air.i}(t) \le Q_{air}^{\max}(t)$,

Then $Q_{air.i.1}^{superviosr}(t)=Q_{air.i}(t)$

2. If $V(t)$ is big, and $\sum_{i=1}^{q} Q_{air.i}(t) \ge Q_{air}^{\max}(t)$

Then $Q_{air.i.2}^{superviosr}(t) = \dfrac{Q_{air}^{\max}(t)}{\sum_{i=1}^{q} Q_{air.i}(t)} \cdot Q_{air.i}$

3. If $V(t)$ is small, and $\sum_{i=1}^{q} Q_{air.i}(t) \ge Q_{air}^{\max}(t)$,

Then $Q_{air.i.1}^{superviosr}(t)=Q_{air.i}(t)$

Where the variable $V(t)$ is defined as follow:

$$V(t) = e_i(t)^{-1} \bullet \sum_{i=3}^{q} e_i(t) \tag{13}$$

Fuzzy blending is described as follow:

$$Q_{air.i}^{superviosr}(t) = \frac{\sum_{s=1}^{2} w_s(v(t)) \cdot Q_{air.i.n}^{superviosr}(t)}{\sum_{s=1}^{2} w_s(v(t))} \tag{14}$$

Where $n = 1,\ 2,\ 3$

DDMRAC Stability analysis

Let us consider the Lyapunov function in the equation as follows.

$$V_i(t) = \frac{1}{2} e_k{}^2(t) + \frac{1}{2} \Delta a_{DO.n}{}^2(t) + \frac{1}{2} \Delta a_{f.n}{}^2(t) \tag{1}$$

where $i = 1,2,3$, $k = 1,2,3$, $n = 1,2,3$, i, k and n are the numbers of bioreactors.

$$\Delta a_{DO.n}(t) = a_{DO.n}(t) - \hat{a}_{DO.n}(t) \tag{2}$$

$$\Delta a_{f.n}(t) = a_{f.n}(t) - \hat{a}_{f.n}(t) \tag{3}$$

where $n = 1,2,3$, and n is the number of bioreactors.

Hence, the derivative of the Lyapunov function is given by the equation:

$$\begin{aligned} \frac{dV_i(t)}{dt} &= e_k(t)\dot{e}_k(t) + (a_{DO.n}(t) - \hat{a}_{DO.n}(t))(\dot{a}_{DO.n}(t) - \dot{\hat{a}}_{DO.n}(t)) \frac{1}{\gamma_{zone.z.1}} \\ &\quad + (a_{f.n}(t) - \hat{a}_{f.n}(t))(\dot{a}_{f.n}(t) - \dot{\hat{a}}_{f.n}(t)) \frac{1}{\gamma_{zone.z.2}} \end{aligned} \tag{4}$$

$$\begin{aligned} \dot{e}_k(t) = &-(a_{p.n}(t) - b_{p.n}(t) a_{DO.n}(t)) DO_n(t) \\ &-(c_{p.n}(t) - b_{p.n}(t) a_{f.n}(t))\, f(DO_n(t)) \\ &+a_{m.n}\, \mathrm{DO}_{m,ref.j}(t) \end{aligned} \tag{5}$$

Now add and subtract the term $a_{m.n} DO_n(t)$ on the right-hand side of equation (5.6-4) as follows:

$$\dot{V} = e(t)[-a_m e(t) + (a_{DO}(t) - \hat{a}_{DO}(t))b_p(t)DO(t) + (a_f(t) - \hat{a}_f(t))b_p(t)f(DO(t)) + (a_{DO^{ref}}(t) - \hat{a}_{DO^{ref}}(t))b_p(t)DO^{ref}(t)] + (a_{DO}(t) - \hat{a}_{DO}(t))((-\gamma_1 eDO(t)) - \dot{\hat{a}}_{DO}(t))\frac{1}{\gamma_1} + (a_f(t) - \hat{a}_f(t))((-\gamma_2 ef(DO(t))) - \dot{\hat{a}}_f(t))\frac{1}{\gamma_2} + (a_{DO^{ref}}(t) - \hat{a}_{DO^{ref}}(t))((-\gamma_3 eDO^{ref}(t)) - \dot{\hat{a}}_{DO^{ref}}(t))\frac{1}{\gamma_3} \quad (6)$$

$$\dot{V} = -a_m e^2(t) + (a_{DO}(t) - \hat{a}_{DO}(t))b_p(t)DO(t)e(t) + (a_f(t) - \hat{a}_f(t))b_p(t)f(DO(t))e(t) + (a_{DO^{ref}}(t) - \hat{a}_{DO^{ref}}(t))b_p(t)DO^{ref}(t)e(t) + (a_{DO}(t) - \hat{a}_{DO}(t))((-\gamma_1 eDO(t)) - \dot{\hat{a}}_{DO}(t))\frac{1}{\gamma_1} + (a_f(t) - \hat{a}_f(t))((-\gamma_2 ef(DO(t))) - \dot{\hat{a}}_f(t))\frac{1}{\gamma_2} + (a_{DO^{ref}}(t) - \hat{a}_{DO^{ref}}(t))((-\gamma_3 eDO^{ref}(t)) - \dot{\hat{a}}_{DO^{ref}}(t))\frac{1}{\gamma_3} \quad (7)$$

$$\dot{V} = -a_m e^2(t) + (a_{DO}(t) - \hat{a}_{DO}(t))\{b_p(t)DO(t)e(t) + ((-\gamma_1 eDO(t)) - \dot{\hat{a}}_{DO}(t))\frac{1}{\gamma_1}\} + (a_f(t) - \hat{a}_f(t))\{b_p(t)f(DO(t))e(t) + ((-\gamma_2 ef(DO(t))) - \dot{\hat{a}}_f(t))\frac{1}{\gamma_2}\} + (a_{DO^{ref}}(t) - \hat{a}_{DO^{ref}}(t))\{b_p(t)DO^{ref}(t)e(t) + ((-\gamma_3 eDO^{ref}(t)) - \dot{\hat{a}}_{DO^{ref}}(t))\frac{1}{\gamma_3}\}$$

(7)

$$\dot{e}_k(t) = -a_{m.n}e(t) - \{(a_{p.n}(t) - b_{p.n}(t)a_{DO.n}(t)) - a_{m.n}\}DO_i(t) - (c_{p.n}(t) - b_{p.n}(t)a_{f.n}(t))f(\mathrm{DO}_i(t)) \quad (8)$$

By substituting (5.5.1-6) and (5.5.1-7) into (5.5-6) yields:

$$\begin{aligned}\dot{e}_k(t) &= -a_{m.n}e(t) + (a_{DO.n}(t) - \hat{a}_{DO.n}(t))b_{p.n}(t)DO_i(t) \\ &+ (a_{f.n}(t) - \hat{a}_{f.n}(t))b_{p.n}(t)f(DO_i(t))\end{aligned} \tag{9}$$

Applying (5.6-7), (5.5.1-15) and (5.5.1-16) into (5.6-4) yields:

$$\begin{aligned}&\frac{dV_i(t)}{dt} = -a_{m.n}e_k{}^2(t) + \\ &+(a_{DO.n}(t) - \hat{a}_{DO.n}(t))\{e_k(t)b_{p.n}(t)DO_n(t) - e_k(t)DO_n(t) - \dot{\hat{a}}_{DO.n}(t)\frac{1}{\gamma_{zone.z.1}}\} \\ &+(a_{f.n}(t) - \hat{a}_{f.n}(t))\{e_k(t)b_{p.n}(t)f(DO_n(t)) - e_k(t)f(DO_n(t)) - \dot{\hat{a}}_{f.n}(t)\frac{1}{\gamma_{zone.z.2}}\}\end{aligned} \tag{10}$$

$$\frac{dV_i(t)}{dt} < 0 \tag{11}$$

$$\frac{d^2V_i(t)}{dt^2} > 0 \tag{12}$$

Consider the stability of the Lyapunov function result employing Barbalat's Lemma.

If $V_i(t)$ has a finite value, as time goes to infinity, then $\frac{d^2V_i(t)}{dt^2}$ is bounded.

Then $\frac{dV_i(t)}{dt} < 0$, as time going to infinity.

1. $\left\{\begin{array}{l} a_{DO}(t) - \hat{a_{DO}}(t) \\ a_f(t) - \hat{a_f}(t) \\ a_{DO^{ref}}(t) - \hat{a_{DO^{ref}}}(t) \end{array}\right\}$ are bounded by $\dot{e}$

2. b_p is bounded by $\dot{e}$

3. $\gamma_1, \gamma_2, \gamma_3$ are bounded by parameter adaptive law

REFERENCE

1. Fan, H., et al., *Aeration optimization through operation at low dissolved oxygen concentrations: Evaluation of oxygen mass transfer dynamics in different activated sludge systems.* Journal of environmental sciences, 2017. **55**: p. 224-235.

2. Fan, L. and K. Boshnakov. *Fuzzy logic based dissolved oxygen control for SBR wastewater treatment process*. in *2010 8th World Congress on Intelligent Control and Automation*. 2010. IEEE.

3. Akyurek, E., et al., *Comparison of control strategies for dissolved oxygen control in activated sludge wastewater treatment process*, in *Computer Aided Chemical Engineering*. 2009, Elsevier. p. 1197-1201.

4. Alasino, N., M.C. Mussati, and N. Scenna, *Wastewater treatment plant synthesis and design.* Industrial & engineering chemistry research, 2007. **46**(23): p. 7497-7512.

5. Alvarez-Ramirez, J., et al., *Feedback control design for an anaerobic digestion process.* Journal of Chemical Technology & Biotechnology, 2002. **77**(6): p. 725-734.

6. Åmand, L., *Control of aeration systems in activated sludge processes–a review*. IVL Swedish Environ. Res. Institute/Department Inf. Technol. Uppsala Univ. Uppsala, Sweden, 2011: p. 1-19.

7. Åmand, L., G. Olsson, and B. Carlsson, *Aeration control–a review.* Water Science and Technology, 2013. **67**(11): p. 2374-2398.

8. Amerlinck, Y., et al., *A realistic dynamic blower energy consumption model for wastewater applications.* Water Science and Technology, 2016. **74**(7): p. 1561-1576.

9. Astolfi, A., *Nonlinear adaptive control*, in *Encyclopedia of Systems and Control*. 2021, Springer. p. 1467-1472.

10. Ballhysa, N., S. Kim, and S. Byeon, *Wastewater treatment plant control strategies.* International journal of advanced smart convergence, 2020. **9**(4): p. 16-25.

11. Barat, R., et al., *Biological Nutrient Removal Model No. 2 (BNRM2): a general model for wastewater treatment plants.* Water Science and Technology, 2013. **67**(7): p. 1481-1489.

12. Belchior, C.A.C., R.A.M. Araújo, and J.A.C. Landeck, *Dissolved oxygen control of the activated sludge wastewater treatment process using stable adaptive fuzzy control.* Computers & Chemical Engineering, 2012. **37**: p. 152-162.

13. Barker, P. and P. Dold, *General model for biological nutrient removal activated-sludge systems: model presentation.* Water Environment Research, 1997. **69**(5): p. 969-984.

14. Bellman, R. and R. Kalaba, *On adaptive control processes.* IRE Transactions on Automatic Control, 1959. **4**(2): p. 1-9.

15. Bishop, P., *Dynamics and control of the activated sludge process*. Vol. 6. 1992: CRC Press.

16. Blomberg, K., et al., *Development of an Extended ASM3 Model for Predicting the Nitrous Oxide Emissions in a Full-Scale Wastewater Treatment Plant.* Environmental Science & Technology, 2018. **52**(10): p. 5803-5811.

17. Blyashyna, M., V. Zhukova, and L. Sabliy, *Processes of biological wastewater treatment for nitrogen, phosphorus removal by immobilized microorganisms.* Восточно-Европейский журнал передовых технологий, 2018(2 (10)): p. 30-37.

18. Brdjanovic, D., et al., *Applications of activated sludge models*. 2015: IWA publishing.

19. Brdys, M., et al., *Hierarchical predictive control of integrated wastewater treatment systems.* Control Engineering Practice, 2008. **16**(6): p. 751-767.

20. Brdys, M., et al., *Two-level dissolved oxygen control for activated sludge processes.* IFAC Proceedings Volumes, 2002. **35**(1): p. 467-472.

21. Brdys, M. and J.D. Maíquez, *Application of fuzzy model predictive control to the dissolved oxygen concentration tracking in an activated sludge process.* IFAC Proceedings Volumes, 2002. **35**(1): p. 35-40.

22. Brehar, M.-A., et al., *Influent temperature effects on the activated sludge process at a municipal wastewater treatment plant.* Studia Universitatis Babes-Bolyai Chemia, 2019. **64**.

23. Calise, F., et al., *Wastewater treatment plant: Modelling and validation of an activated sludge process.* Energies, 2020. **13**(15): p. 3925.

24. Cheng, C.-Y. and I. Ribarova, *Activated sludge system modelling and simulations for improving the effluent water quality.* Water science and technology, 1999. **39**(8): p. 93-98.

25. Chotkowski, W., M.A. Brdys *, and K. Konarczak, *Dissolved oxygen control for activated sludge processes.* International Journal of Systems Science, 2005. **36**(12): p. 727-736.

26. Chu, C., D. Lee, and J. Tay, *Gravitational sedimentation of flocculated waste activated sludge.* Water research, 2003. **37**(1): p. 155-163.

27. Comas Matas, J., *Development, implementation and evaluation of an activated sludge supervisory system for the granollers WWTP*. 2000: Universitat de Girona.

28. Cristea, S., et al., *Aeration control of a wastewater treatment plant using hybrid NMPC.* Computers & Chemical Engineering, 2011. **35**(4): p. 638-650.

29. Derco, J., et al., *Dynamic simulations of waste water treatment plant operation.* Chemical Papers, 2011. **65**(6): p. 813-821.

30. Descoins, N., et al., *Energy efficiency in waste water treatments plants: Optimization of activated sludge process coupled with anaerobic digestion.* Energy, 2012. **41**(1): p. 153-164.

31. Dick, R.I., *Role of activated sludge final settling tanks.* Journal of the Sanitary Engineering Division, 1970. **96**(2): p. 423-436.

32. Dochain, D. and P.A. Vanrolleghem, *Dynamical modelling & estimation in wastewater treatment processes*. 2001: IWA publishing.

33. Dold, P. and G. Ekama, *A general model for the activated sludge process*, in *Water pollution research and development*. 1981, Elsevier. p. 47-77.

34. Drewnowski, J., et al., *The process generation of WWTP models for optimization of activated sludge systems*, in *Environmental Engineering V*. 2018, CRC Press. p. 199-208.

35. Du, X., et al., *Dissolved oxygen control in activated sludge process using a neural network-based adaptive PID algorithm.* Applied sciences, 2018. **8**(2): p. 261.

36. Duzinkiewicz, K., et al., *Genetic hybrid predictive controller for optimized dissolved-oxygen tracking at lower control level.* IEEE Transactions on Control Systems Technology, 2009. **17**(5): p. 1183-1192.

37. Eberhardt, W.A. and J.B. Nesbitt, *Chemical precipitation of phosphorus in a high-rate activated sludge system.* Journal (Water Pollution Control Federation), 1968: p. 1239-1267.

38. Egardt, B., *Stability of adaptive controllers*. 1979: Springer.

39. Ekama, G., et al., *Secondary settling tanks.* London: International Association on Water Quality, 1997.

40. Ekama, G., M. Wentzel, and R. Loewenthal, *Integrated chemical–physical processes kinetic modelling of multiple mineral precipitation problems.* Water science and technology, 2006. **53**(12): p. 65-73.

41. Elmansour, T., et al., *Nutrients' behavior and removal in an activated sludge system receiving Olive Mill Wastewater.* Journal of Environmental Management, 2022. **305**: p. 114254.

42. Ericsson, B. and L. Eriksson, *Activated sludge characteristics in a phosphorus depleted environment.* Water Research, 1988. **22**(2): p. 151-162.

43. Fan, H., et al., *Oxygen transfer dynamics and activated sludge floc structure under different sludge retention times at low dissolved oxygen concentrations.* Chemosphere, 2017. **169**: p. 586-595.

44. Fannin, K.F., S.C. Vana, and W. Jakubowski, *Effect of an activated sludge wastewater treatment plant on ambient air densities of aerosols containing bacteria and viruses.* Applied and environmental microbiology, 1985. **49**(5): p. 1191-1196.

45. Flores, V.R., et al., *Dissolved oxygen regulation by logarithmic/antilogarithmic control to improve a wastewater treatment process.* Environmental technology, 2013. **34**(23): p. 3103-3116.

46. Foladori, P., et al., *Direct quantification of bacterial biomass in influent, effluent and activated sludge of wastewater treatment plants by using flow cytometry*. Water research, 2010. **44**(13): p. 3807-3818.

47. Gajewska, M., Ł. Kopeć, and H. Obarska-Pempkowiak, *The operation of a small wastewater treatment facilities in a scattered settlement.* OCHRONA ŚRODOWISKA, 2011. **13**: p. 207-226.

48. Galluzzo, M., et al., *Expert control of DO in the aerobic reactor of an activated sludge process.* Computers & Chemical Engineering, 2001. **25**(4-6): p. 619-625.

49. Gerardi, M.H., *Nitrification and denitrification in the activated sludge process*. 2002: John Wiley & Sons.

50. Gerkšič, S., D. Vrečko, and N. Hvala, *Improving oxygen concentration control in activated sludge process with estimation of respiration and scheduling control.* Water Science and Technology, 2006. **53**(4-5): p. 283-291.

51. Gernaey, K.V., et al., *Activated sludge wastewater treatment plant modelling and simulation: state of the art.* Environmental modelling & software, 2004. **19**(9): p. 763-783.

52. Gordon, G.T. and B.P. McCann, *Development of an operational performance indicator system for activated sludge wastewater treatment plants.* Water Practice and Technology, 2015. **10**(4): p. 860-871.

53. Guarino, R.D., et al., *Method for determining oxygen consumption rates of static cultures from microplate measurements of pericellular dissolved oxygen concentration.* Biotechnology and bioengineering, 2004. **86**(7): p. 775-787.

54. Guellil, A., et al., *Transfer of organic matter between wastewater and activated sludge flocs.* Water Research, 2001. **35**(1): p. 143-150.

55. Gujer, W., et al., *Activated sludge model no. 3.* Water science and technology, 1999. **39**(1): p. 183-193.

56. Hadj-Sadok, M.Z. and J.L. Gouzé, *Estimation of uncertain models of activated sludge processes with interval observers.* Journal of Process Control, 2001. **11**(3): p. 299-310.

57. Haggard, B.E., E.H. Stanley, and D.E. Storm, *Nutrient retention in a point-source-enriched stream.* Journal of the North American Benthological Society, 2005. **24**(1): p. 29-47.

58. Hájek, P., *Metamathematics of fuzzy logic*. Vol. 4. 2013: Springer Science & Business Media.

59. Han, Y., M. Brdys, and R. Piotrowski, *Nonlinear PI control for dissolved oxygen tracking at wastewater treatment plant.* IFAC Proceedings Volumes, 2008. **41**(2): p. 13587-13592.

60. Harja, G., et al., *Improvements in dissolved oxygen control of an activated sludge wastewater treatment process.* Circuits, Systems, and Signal Processing, 2016. **35**: p. 2259-2281.

61. Harja, G., G. Vlad, and I. Nascu. *MPC advanced control of dissolved oxygen in an activated sludge wastewater treatment plant*. in *2016 IEEE International Conference on Automation, Quality and Testing, Robotics (AQTR)*. 2016. IEEE.

62. Henze, M., et al., *Activated sludge model no. 2d, ASM2d.* Water science and technology, 1999. **39**(1): p. 165-182.

63. Holenda, B., et al., *Dissolved oxygen control of the activated sludge wastewater treatment process using model predictive control.* Computers & Chemical Engineering, 2008. **32**(6): p. 1270-1278.

64. Huang, H., J. Liu, and L. Ding, *Recovery of phosphate and ammonia nitrogen from the anaerobic digestion supernatant of activated sludge by chemical precipitation.* Journal of Cleaner Production, 2015. **102**: p. 437-446.

65. Huang, J., et al., *Modelling dissolved oxygen depression in an urban river in China.* Water, 2017. **9**(7): p. 520.

66. Huo, S., et al., *Characteristics and transformations of dissolved organic nitrogen in municipal biological nitrogen removal wastewater treatment plants.* Environmental Research Letters, 2013. **8**(4): p. 044005.

67. Ingildsen, P., U. Jeppsson, and G. Olsson, *Dissolved oxygen controller based on on-line measurements of ammonium combining feed-forward and feedback.* Water Science and Technology, 2002. **45**(4-5): p. 453-460.

68. Kandare, G. and A. Nevado Reviriego, *Adaptive predictive expert control of dissolved oxygen concentration in a wastewater treatment plant.* Water Science and Technology, 2011. **64**(5): p. 1130-1136.

69. Kappeler, J. and W. Gujer, *Estimation of kinetic parameters of heterotrophic biomass under aerobic conditions and characterization of wastewater for activated sludge modelling.* Water Science and Technology, 1992. **25**(6): p. 125-139.

70. Keller, J., et al., *Nutrient removal from industrial wastewater using single tank sequencing batch reactors.* Water Science and Technology, 1997. **35**(6): p. 137-144.

71. Kim, M., et al., *Operator decision support system for integrated wastewater management including wastewater treatment plants and receiving water bodies.* Environmental Science and Pollution Research, 2016. **23**: p. 10785-10798.

72. Kiuru, H.J. and J.A. Rautiainen, *Biological nutrient removal at a very low-loaded activated sludge plant with high biomass concentrations.* Water Science and Technology, 1998. **38**(1): p. 63-70.

73. Knudson, M.K., K.J. Williamson, and P.O. Nelson, *Influence of dissolved oxygen on substrate utilization kinetics of activated sludge.* Journal (Water Pollution Control Federation), 1982: p. 52-60.

74. Korzeniewska, E. and M. Harnisz, *Relationship between modification of activated sludge wastewater treatment and changes in antibiotic resistance of bacteria.* Science of the Total Environment, 2018. **639**: p. 304-315.

75. Kreisselmeier, G., *Adaptive control of a class of slowly time-varying plants.* Systems & Control Letters, 1986. **8**(2): p. 97-103.

76. Lamia, M. and K.M. Tarek. *Multi-Model Predictive Control strategies for an activated sludge model*. in *2014 International Conference on Control, Decision and Information Technologies (CoDIT)*. 2014. IEEE.

77. Lesouef, A., et al., *Optimizing nitrogen removal reactor configurations by on-site calibration of the IAWPRC activated sludge model.* Water Science and Technology, 1992. **25**(6): p. 105-123.

78. Leu, S.Y., et al., *Real-time aeration efficiency monitoring in the activated sludge process and methods to reduce energy consumption and operating costs.* Water Environment Research, 2009. **81**(12): p. 2471-2481.

79. Li, D., M. Zou, and L. Jiang, *Dissolved oxygen control strategies for water treatment: a review.* Water Science & Technology, 2022. **86**(6): p. 1444-1466.

80. Li, M. and M. Brdys. *Direct model reference adaptive control of nutrient removal at activated sludge wastewater treatment plant*. in *2015 20th International Conference on Methods and Models in Automation and Robotics (MMAR)*. 2015. IEEE.

81. Lin, M.-J. and F. Luo, *An adaptive control method for the dissolved oxygen concentration in wastewater treatment plants.* Neural Computing and Applications, 2015. **26**: p. 2027-2037.

82. Lindberg, C.-F., *Control and estimation strategies applied to the activated sludge process*. 1997: Uppsala University Stockholm, Sweden.

83. Lindberg, C.-F. and B. Carisson, *Estimation of the respiration rate and oxygen transfer function utilizing a slow DO sensor.* Water Science and Technology, 1996. **33**(1): p. 325-333.

84. Lindberg, C.-F. and B. Carlsson, *Nonlinear and set-point control of the dissolved oxygen concentration in an activated sludge process.* Water Science and Technology, 1996. **34**(3-4): p. 135-142.

85. Lindberg, C.F. and B. Carisson, *Estimation of the respiration rate and oxygen transfer function utilizing a slow do sensor.* Water Science and Technology, 1996. **33**(1): p. 325-333.

86. Liu, J., G. Olsson, and B. Mattiasson, *Control of an anaerobic reactor towards maximum biogas production.* Water Science and Technology, 2004. **50**(11): p. 189-198.

87. Lötter, L.H., *Combined chemical and biological removal of phosphate in activated sludge plants.* Water Science and Technology, 1991. **23**(4-6): p. 611-621.

88. Low, E.W. and H.A. Chase, *The effect of maintenance energy requirements on biomass production during wastewater treatment.* Water Research, 1999. **33**(3): p. 847-853.

89. Mahendraker, V., D.S. Mavinic, and K.J. Hall, *Comparative evaluation of mass transfer of oxygen in three activated sludge processes operating under uniform conditions.* Journal of Environmental Engineering and Science, 2005. **4**(2): p. 89-100.

90. Marais, G.v.R. and M.C. Van Loosdrechti, *Activated sludge model no. 2d, asm2d.* Water Science and Technology, 1999. **39**(1): p. 165182.

91. Aboobakar, A., et al., *Nitrous oxide emissions and dissolved oxygen profiling in a full-scale nitrifying activated sludge treatment plant.* Water Research, 2013. **47**(2): p. 524-534.

92. Massara, T.M., *Development of a novel model to quantify nitrous oxide emissions in the biological nutrient removal process of wastewater treatment plants*. 2018, Brunel University London.

93. Matyja, K., et al., *Dynamic modeling of the activated sludge microbial growth and activity under exposure to heavy metals.* Bioresource Technology, 2021. **339**: p. 125623.

94. Monclús, H., et al., *Biological nutrient removal in an MBR treating municipal wastewater with special focus on biological phosphorus removal.* Bioresource Technology, 2010. **101**(11): p. 3984-3991.

95. Park, J.Y. and Y.J. Yoo, *Biological nitrate removal in industrial wastewater treatment: which electron donor we can choose.* Applied Microbiology and Biotechnology, 2009. **82**(3): p. 415-429.

96. Abinandan, S., et al., *Nutrient removal and biomass production: advances in microalgal biotechnology for wastewater treatment.* Critical reviews in biotechnology, 2018. **38**(8): p. 1244-1260.

97. Moreno, R., et al., *Non-linear predictive control of dissolved oxygen in the activated sludge process.* IFAC Proceedings Volumes, 1992. **25**(2): p. 289-293.

98. Mulas, M., et al., *Predictive control of an activated sludge process: An application to the Viikinmäki wastewater treatment plant.* Journal of Process Control, 2015. **35**: p. 89-100.

99. Murillo, M., *Design of Aeration Tank and Clarifier. A Discussion.* A Discussion.(April 16, 2018), 2018.

100. Mussati, M., et al., *Optimal synthesis of activated sludge wastewater treatment plants for nitrogen removal.* 2nd Mercosur Congr. on Chem. Eng., 4th Mercosur Congr. on Process Syst. Eng., Rio De Janeiro, Brazil, 2005.

101. Nam, S.W., N.J. Myung, and K.S. Lee, *On-line integrated control system for an industrial activated sludge process.* Water environment research, 1996. **68**(1): p. 70-75.

102. Narendra, K.S. and L.S. Valavani, *Direct and indirect model reference adaptive control*. Automatica, 1979. **15**(6): p. 653-664.

103. Nejjari, F., et al., *Non-linear multivariable adaptive control of an activated sludge wastewater treatment process.* International Journal of Adaptive Control and Signal Processing, 1999. **13**(5): p. 347-365.

104. Nguyen, N.T. and N.T. Nguyen, *Model-reference adaptive control*. 2018: Springer.

105. Olsson, G. and B. Newell, *Wastewater treatment systems*. 1999: IWA publishing.

106. Olsson, G., et al., *Self tuning control of the dissolved oxygen concentration in activated sludge systems,* in *Instrumentation and Control of Water and Wastewater Treatment and Transport Systems*. 1985, Elsevier. p. 473-480.

107. Patziger, M., et al., *Influence of secondary settling tank performance on suspended solids mass balance in activated sludge systems.* Water research, 2012. **46**(7): p. 2415-2424.

108. Pell, M. and A. Wörman, *Biological wastewater treatment systems.* Ecosystem Ecology, 2009: p. 166-180.

109. Petre, E. and D. Selişteanu, *A multivariable robust-adaptive control strategy for a recycled wastewater treatment bioprocess.* Chemical Engineering Science, 2013. **90**: p. 40-50.

110. Piotrowski, R., *Two-Level Multivariable Control System of Dissolved Oxygen Tracking and Aeration System for Activated Sludge Processes.* Water Environment Research, 2015. **87**(1): p. 3-13.

111. Piotrowski, R., K. Błaszkiewicz, and K. Duzinkiewicz, *Analysis the parameters of the adaptive controller for quality control of dissolved oxygen concentration.* Information Technology and Control, 2016. **45**: p. 42-51.

112. Piotrowski, R. and M. Brdys, *LOWER–LEVEL CONTROLLER FOR HIERARCHICAL CONTROL OF DISSOLVED OXYGEN CONCENTRATION*

IN ACTIVATED SLUDGE PROCESSES. IFAC Proceedings Volumes, 2005. **38**(1): p. 9-14.

113. Piotrowski, R., et al., *Hierarchical dissolved oxygen control for activated sludge processes.* Control Engineering Practice, 2008. **16**(1): p. 114-131.

114. Piotrowski, R., M. Brdys, and D. Miotke, *Centralized dissolved oxygen tracking at wastewater treatment plant: Nowy Dwor Gdanski case study*. IFAC Proceedings Volumes, 2010. **43**(8): p. 292-297.

115. Piotrowski, R., et al., *Hierarchical dissolved oxygen control for activated sludge processes.* Control Engineering Practice, 2008. **16**(1): p. 114-131.

116. Piotrowski, R., M. Lewandowski, and A. Paul, *Mixed integer nonlinear optimization of biological processes in wastewater sequencing batch reactor.* Journal of Process Control, 2019. **84**: p. 89-100.

117. Piotrowski, R. and A. Skiba, *Nonlinear fuzzy control system for dissolved oxygen with aeration system in sequencing batch reactor.* Information Technology and Control, 2015. **44**(2): p. 182-195.

118. Piotrowski, R. and A. Zawadzki. *Multiregional PI control strategy for dissolved oxygen and aeration system control at biological wastewater treatment plant*. in *Proceedings of 2012 IEEE 17th International Conference on Emerging Technologies & Factory Automation (ETFA 2012)*. 2012. IEEE.

119. Pittoors, E., Y. Guo, and S. WH Van Hulle, *Modeling dissolved oxygen concentration for optimizing aeration systems and reducing oxygen consumption in activated sludge processes: a review.* Chemical Engineering Communications, 2014. **201**(8): p. 983-1002.

120. Pratt, C., et al., *Biologically and chemically mediated adsorption and precipitation of phosphorus from wastewater.* Current opinion in Biotechnology, 2012. **23**(6): p. 890-896.

121. Revollar, S., et al., *PI Dissolved Oxygen control in wastewater treatment plants for plantwide nitrogen removal efficiency*. IFAC-PapersOnLine, 2018. **51**(4): p. 450-455.

122. Rieger, L., et al., *Modelling of aeration systems at wastewater treatment plants.* Water science and technology, 2006. **53**(4-5): p. 439-447.

123. Rieger, L., et al., *Guidelines for using activated sludge models*. 2012: IWA publishing.

124. Sanchez, A. and M. Katebi. *Predictive control of dissolved oxygen in an activatedsludge wastewater treatment plant*. in *2003 European Control Conference (ECC)*. 2003. IEEE.

125. Santín, I., C. Pedret, and R. Vilanova, *Applying variable dissolved oxygen set point in a two level hierarchical control structure to a wastewater treatment process.* Journal of Process Control, 2015. **28**: p. 40-55.

126. Scattolini, R., *Architectures for distributed and hierarchical model predictive control–a review.* Journal of process control, 2009. **19**(5): p. 723-731.

127. Schraa, O., L. Rieger, and J. Alex, *Development of a model for activated sludge aeration systems: linking air supply, distribution, and demand.* Water Science and Technology, 2017. **75**(3): p. 552-560.

128. Schwarz, M., et al., *Oxygen transfer in two-stage activated sludge wastewater treatment plants.* Water, 2021. **13**(14): p. 1964.

129. Seco, A., et al., *Biological nutrient removal model No. 1 (BNRM1).* Water Science and Technology, 2004. **50**(6): p. 69-70.

130. Seviour, R.J., T. Mino, and M. Onuki, *The microbiology of biological phosphorus removal in activated sludge systems.* FEMS microbiology reviews, 2003. **27**(1): p. 99-127.

131. Shahriari, H., C. Eskicioglu, and R. Droste, *Simulating activated sludge system by simple-to-advanced models.* Journal of Environmental Engineering, 2006. **132**(1): p. 42-50.

132. Song, X.-l., et al., *Dissolved oxygen control in wastewater treatment based on robust PID controller.* International Journal of Modelling, Identification and Control, 2012. **15**(4): p. 297-303.

133. Stensel, H.D. and J. Makinia, *Activated sludge process development.* Activated Sludge-100 Years and Counting, 2014: p. 33.

134. Suchodolski, T., M. Brdys, and R. Piotrowski, *Respiration rate estimation for model predictive control of dissolved oxygen in wastewater treatment plant.* IFAC Proceedings Volumes, 2007. **40**(9): p. 286-291.

135. Suescun, J., et al., *Dissolved oxygen control and simultaneous estimation of oxygen uptake rate in activated-sludge plants.* Water environment research, 1998. **70**(3): p. 316-322.

136. Suresh, S., V.C. Srivastava, and I. Mishra, *Techniques for oxygen transfer measurement in bioreactors: a review.* Journal of Chemical Technology & Biotechnology: International Research in Process, Environmental & Clean Technology, 2009. **84**(8): p. 1091-1103.

137. Sustarsic, M. *Wastewater treatment: understanding the activated sludge process*. in *Safety in ammonia Plants and related facilities symposium*. 2009.

138. Tallec, G., et al., *Nitrous oxide emissions from denitrifying activated sludge of urban wastewater treatment plants, under anoxia and low oxygenation.* Bioresource technology, 2008. **99**(7): p. 2200-2209.

139. Tong, R., M. Beck, and A. Latten, *Fuzzy control of the activated sludge wastewater treatment process.* Automatica, 1980. **16**(6): p. 695-701.

140. Vaiopoulou, E., P. Melidis, and A. Aivasidis, *An activated sludge treatment plant for integrated removal of carbon, nitrogen and phosphorus.* Desalination, 2007. **211**(1-3): p. 192-199.

141. van der Meer, T.V., et al., *Wastewater treatment plant contaminant profiles affect macroinvertebrate sludge degradation.* Water Research, 2022. **222**: p. 118863.

142. Van Loosdrecht, M. and J. Heijnen, *Modelling of activated sludge processes with structured biomass.* Water Science and Technology, 2002. **45**(6): p. 13-23.

143. Van Loosdrecht, M.C., et al., *Modelling activated sludge processes.* Biological Wastewater Treatment. Principles, Modelling and Design, eds M. Henze, MC M. van Loosdrecht, GA Ekama, MC Wentzel, D. Brdjanovic (ondon: IWA Publishing), 2008. **361**.

144. Van Veldhuizen, H., M.C. van Loosdrecht, and J. Heijnen, *Modelling biological phosphorus and nitrogen removal in a full scale activated sludge process.* Water Research, 1999. **33**(16): p. 3459-3468.

145. Venkatapathi, K., et al., *Nutrient management control regulation and preparedness of a northern Colorado wastewater treatment plant.* 2013.

146. Villaverde, S., *Recent developments on biological nutrient removal processes for wastewater treatment.* Re/Views in Environmental Science & Bio/Technology, 2004. **3**: p. 171-183.

147. Vlad, C., et al., *Indirect control of substrate concentration for a wastewater treatment process by dissolved oxygen tracking.* Journal of control engineering and applied informatics, 2012. **14**(1): p. 38-47.

148. Wang, Y., et al., *Nutrient release, recovery and removal from waste sludge of a biological nutrient removal system.* Environmental technology, 2014. **35**(21): p. 2734-2742.

149. Tao, G., *Adaptive control design and analysis*. Vol. 37. 2003: John Wiley & Sons.

150. Tar, J.K., J.F. Bitó, and I.J. Rudas. *Replacement of Lyapunov's direct method in model reference adaptive control with robust fixed point transformations*. in *2010 IEEE 14th International Conference on Intelligent Engineering Systems*. 2010. IEEE.

151. Nemcik, J., et al., *Wastewater Treatment Modeling Methods Review.* IFAC-PapersOnLine, 2022. **55**(4): p. 195-200.

152. Travers, S. and D. Lovett, *Activated sludge treatment of abattoir wastewater—II: Influence of dissolved oxygen concentration.* Water research, 1984. **18**(4): p. 435-439.

153. Turmel, V.J., D. Williams, and K.O. Jones, *Dissolved oxygen control strategies in an activated sludge process.* IFAC Proceedings Volumes, 1997. **30**(6): p. 1569-1573.

154. Adonadaga, M.-G., *Effect of dissolved oxygen concentration on morphology and settleability of activated sludge flocs.* Journal of Applied & Environmental Microbiology, 2015. **3**(2): p. 31-37.

155. Brdys, M.A., et al., *Hierarchical predictive control of integrated wastewater treatment systems.* Control Engineering Practice, 2008. **16**(6): p. 751-767.

156. Chotkowski, W., M.A. Brdys*, and K. Konarczak, *Dissolved oxygen control for activated sludge processes.* International Journal of Systems Science, 2005. **36**(12): p. 727-736.

157. Brdys, M.A., T. Chang, and K. Konarczak, *Estimation of Wastewater Treatment Plant State For Model Predictive Control of N-premoval at Medium Time Scale*. IFAC Proceedings Volumes, 2004. **37**(11): p. 265-271.

158. Domański, P., M.A. Brdyś, and P. Tatjewski, *Design and stability of fuzzy logic multi-regional output controllers.* 1999.

159. Barros, P.R. and B. Carlsson, *Iterative design of a nitrate controller using an external carbon source in an activated sludge process.* Water science and technology, 1998. **37**(12): p. 95-102.

160. Bechmann, H., et al., *Control of sewer systems and wastewater treatment plants using pollutant concentration profiles.* Water science and technology, 1998. **37**(12): p. 87-93.

161. Zubowicz, T., A.B. Mieczyslaw, and R. Piotrowski, *Intelligent PI controller and its application to dissolved oxygen tracking problem.* Journal of Automation, Mobile Robotics and Intelligent Systems, 2010: p. 16-24.

162. Tatnall, M., *Model reference adaptive control systems: background and development.* Measurement and Control, 1977. **10**(12): p. 475-487.

163. Ławryńczuk, M., *Computationally efficient model predictive control algorithms.* A Neural Network Approach, Studies in Systems, Decision and Control, 2014. **3**.

164. Petersen, G., *Nitrification and denitrification wastewater treatment process*. 1996, Google Patents.

165. Vega, P., et al., *Integration of set point optimization techniques into nonlinear MPC for improving the operation of WWTPs.* Computers & Chemical Engineering, 2014. **68**: p. 78-95.

166. Qi, R. and M.A. Brdys, *Stable indirect adaptive control based on discrete-time T–S fuzzy model.* Fuzzy sets and systems, 2008. **159**(8): p. 900-925.

167. Garcia-Sanz, M., et al. *MIMO quantitative robust control of a wastewater treatment plant for biological removal of nitrogen and phosphorus*. in *2008 16th Mediterranean Conference on Control and Automation*. 2008. IEEE.

168. Zawadzki, A. and R. Piotrowski. *Nonlinear fuzzy control of the dissolved oxygen in activated sludge processes*. in *Proceedings of 2012 IEEE 17th*

International Conference on Emerging Technologies & Factory Automation (ETFA 2012). 2012. IEEE.

169. Yoo, C.K., H.K. Lee, and I.-B. Lee, *Comparisons of process identification methods and supervisory do control in the fullscale wastewater treatment plant.* IFAC Proceedings Volumes, 2002. **35**(1): p. 47-52.

170. Mineta, R., et al., *Oxygen transfer during aerobic biodegradation of pollutants in a dense activated sludge slurry bubble column: Actual volumetric oxygen transfer coefficient and oxygen uptake rate in p-nitrophenol degradation by acclimated waste activated sludge.* Biochemical Engineering Journal, 2011. **53**(3): p. 266-274.

171. Hadj-Sadok, M. and J. Gouzé, *Estimation of uncertain models of activated sludge processes with interval observers.* Journal of Process Control, 2001. **11**(3): p. 299-310.